TU

TECHNISCHE UNIVERSITÄT WIEN

DISSERTATION

Neutronics Analysis of the TRIGA Mark II Reactor Core and its Experimental Facilities

ausgeführt zum Zwecke der Erlangung des akademischen Grades eines

Doktors der technischen Wissenschaftenunter der Leitung von

Ao. Prof. Dipl.-Ing. Dr. Helmuth Böck

Vienna University of Technology, Atominstitute

Stadionallee 2, A-1020, Vienna, AUSTRIA

eingereicht an der Technische Universität Wien

Fakultät für Physik

von

Rustam Khan

Matrikelnummer: 0625503

nrustam@ati.ac.at

Abstract

The neutronics analysis of the current core of the TRIGA Mark II research reactor is performed at the Atominstitute (ATI) of Vienna University of Technology. The current core is a completely mixed core having three different types of fuels i.e. aluminium clad 20% enriched, stainless steel clad 20% enriched and SS clad 70% enriched (FLIP) Fuel Elements (FE(s)). The completely mixed nature and complicated irradiation history of the core makes the reactor physics calculations challenging. This PhD neutronics research is performed by employing the combination of two best and well practiced reactor simulation tools i.e. MCNP (general Monte Carlo N-particle transport code) for static analysis and ORIGEN2 (Oak Ridge Isotop Generation and depletion code) for dynamic analysis of the reactor core.

The PhD work is started to develop a MCNP model of the first core configuration (March 1962) employing fresh fuel composition. The neutrons reaction data libraries ENDF/B-VI is applied taking the missing isotope of Samarium from JEFF3.1. The MCNP model of the very first core has been confirmed by three different local experiments performed on the first core configuration. These experiments include the first criticality, reactivity distribution and the neutron flux density distribution experiment. The first criticality experiment verifies the MCNP model that core achieves its criticality on addition of the 57th FE with a reactivity difference of about 9.3 cents. The measured reactivity worths of four FE(s) and a graphite element are taken from the log book and compared with MCNP simulated results. The percent difference between calculations and measurements ranges from 4 to 22%. The neutron flux density mapping experiment confirms the model

completely exhibiting good agreement between simulated and the experimental results.

Since its first criticality, some additional 104-type and 110-type (FLIP) FE(s) have been added to keep the reactor into operation. This turns the current core into a complete mixed core. To analyse the current core, a good knowledge of burned fuel material composition is essential. Because of the complications of experimental methods for measuring each FE, the ORIGEN2 computer code is selected for burn up and relevant material composition calculation. These calculations are verified by measuring the Cesium isotope (Cs-137) for six spent FE(s). Modifying the confirmed ORIGEN2 model for 104 and 110 (FLIP) FE(s), the burn up calculations of all 83 FE(s) of the current core are completed and applied to the already developed MCNP model. The detailed MCNP model of the burned core is verified by three local consistent experiments performed in June 2009. The criticality experiment confirms the model that the current core achieves its criticality on addition of 78th FE. The five FE(s) from different ring positions are measured to confirm the theoretical results. The percent deviation between MCNP predictions and experimental observations ranges from 3 to 19 %. The radial and axial neutron flux density distribution experiment verifies the MCNP theoretical results in the core.

The theoretical and experimental perturbation study in the Central Irradiation Channel (CIR) of the core is performed. The reactivity effect of three small cylindrical samples (void, Cadmium and heavy water) are measured and compared with the MCNP predictions for verification. Applying the current core MCNP model, the void coefficient of reactivity is calculated as 11 cents per %-void.

To perform the calculation in the experimental facilities outside the reactor core, the MCNP model is extended to the thermal column, radiographic collimator, four beam tubes and biological shielding. The MCNP results are verified in the thermal column and the beam tube A region. The percent difference between the simulated and experimental neutron diffusion length is 13 %.

Kurzfassung

Die vorliegende Arbeit berechnet den neutronenphysikalischen Zustand des TRIGA Mark II Reaktors der am Atominstitut seit 1962 in Betrieb ist. Der derzeit verwendete Reaktorkern besteht aus drei verschiedenen Sorten von Brennelementen, nämlich Elemente mit einer Aluminium hülle und 20% Uran Anreicherung, weiter analoge Elemente allerdings mit eine Stahlhülle sowie Elemente mit einer 70% Uran-Anreicherung und Stahlhülle, sogenannte FLIP (= Fuel Lifetime Improvement Program) Elemente. Dieser komplizierte Kernaufbau sowie die Betriebsgeschichte von 48 Jahren machen die Berechnungen der Kernparameter sehr kompliziert. Die vorliegende Arbeit verwendet zu diesen Berechnungen zwei der besten und weit verwendeten Simulationsprogramme nämlich MCNP (Monte Carlo N-particle Code) für die statische Berechnung und ORIGEN2 für die dynamischen Berechnungen.

Die vorgelegte Dissertation berechnete zuerst mittels MCNP den ersten Kernaufbau im März 1962, der nur aus 20% angereicherten Aluminium Brennelementen aufgebaut war. Diese Berechnungen wurden durch drei Experimenten, die bei der Inbetriebnahme erfolgten bestätigt. Dabei handelt es sich um das 1. Kritikalitäts-Experiment, die Reaktivitätsverteilung im Reaktorkern und die Neutronen-Flussdichteverteileung, diese drei Experimente wurden 1962 gut dokumentiert und zur Validierung der Berechnungen herangezogen.

Beim ersten kritischen Experiment wurde der Reaktorkern mit dem 57.en Brennelement kritisch und erreichte eine Überschussreaktivität von 9,3 cents, dies wurde mit der MCNP Berechnung bestätigt. Auch die damals gemessene Neutronen-Flussverteilung konnte mit

3

MCNP sehr gut modelliert werden.

Seit der 1.Kritikalität wurden weiter Brennelemente mit Stahlhülle mit 20% bzw 70% Anreicherung dem Kern zugeladen, bis der heutige Mischkern entstand. Zusätzlich wurden im Laufe der Jahre die im Kern befindlichen Brennelemente auch umgeladen, sodass sich die in unterschiedlichen Kernpositionen befanden und damit unterschiedlichen Abbrand ausgesetzt waren.

Ein wichtiger Abschnitt war die genaue Erfassung aller Materialdaten, die aus Lieferscheinen, dem Sicherheitsbericht sowie anderen Reaktorunterlagen und direkten Kontakten mit der Reaktorlieferfirma zusammen gestellt wurden. Mit Hilfe von ORIGEN2 wurde für jedes einzelne Brennelement die Abbrandgeschichte und das Spaltproduktinventar berechnet. Die Berechnungen wurden durch Messung des Cs-137 Gehalts an sechs Aluminium Brennelementen verifiziert. Mit diesen Ergebnissen wurde dann unter Verwendung von MCNP der Abbrand aller 83 derzeit im Reaktorkern befindlichen Brennelementen per 30.6.2009 berechnet. Die Wiederholung des kritischen Experiments zeigte, dass der Reaktor zum Stichtag mit 78 Brennelementen kritisch wird. Die Abweichung von Experiment und MCNP Berechnung liegt zwischen 3 und 19%. Auch die radiale und axiale Verteilung der Neutronenflussdichte zeigt Übereinstimmung zwischen MCNP Berechnung und Experiment.

Weiters wurde auch im Rahmen dieser Arbeit die Rückwirkung von kleinen Veränderungen im zentralen Bestrahlungskanal des TRIGA Reaktors (Luftblase, Kadmium, Schweres Wasser) mittels MCNP berechnet und mit entsprechenden Experimenten verglichen.

Zuletzt wurde mittels MCNP die Neutronen-Flussverteilung in Bestrahlungseinrichtungen wie Thermische Säule, Strahlrohre und biologischen Schild berechnet, der Unterscheid zwischen Simulation und Experiment liegt bei ca 13%

Dedication

To my mother, uncle Fazal Rahman (Multani Tailor) and my teachers

Acknowledgement

Schauberger, Markus Hayden, Michael Lechermann for their helping discussions during the PhD research.

In collecting the reliable geometrical and material data of TRIGA Mark II reactor, I am extremely grateful of the support from Josef Stefan Institute (JSI) Ljubljana, Slovenia and General Atomics, USA. I appreciate the prompt responses from JSI during the PhD work, particularly from Luka Snoj, Tomaz Zagar, Bojan Zefran, Gasper Zerovnik. I owe a huge debt of gratitude to Dr. Yi Jason, the Senior Technical Advisor of General Atomics for his instrumental support in providing the dara and expert suggestions.

I am deeply gratedul of Mr. Saleem Khosa from TU Graz who remained in continuous touch with my professional as well as my personal activities. He always played a role in the refinement of my skills and ideas. I always recieved unexpected and generous support from him whenever he was called.

Last, but far from least, I want to express my deep appreciations for my wife who has suffered more for this dissertation than anyone. Remaining as house wife, she saved my lot of time by provding me well prepared food and pressed clothes etc. She took well care of me and my children. Her full support made my life easy in the duration of my PhD research.

Contents

Chapter 1

INTRODUCTION

Among numerous types of research reactors, the (Training, Research, Isotope production, General Atomics) research reactor is a distinct kind with inherent safety features. It is used for training, research, and isotope production. The first TRIGA research reactor started its operation on 9th May 1958 at General Atomic (GA) in San Diego (U.S.A), in just less than five years after the famous speech "Atoms for Peace" at United Nation General Assembly on 8th December 1953 by US president Dwight D. Eisenhower [1]. Because of its inherent safety, over the years, the TRIGA has emerged as the most widely used research reactor in the world. About 38 TRIGA research reactors are in operation in 17 countries of the world [2]. The basic TRIGA reactor has been developed and offered to users in several standard designs. The TRIGA Mark I, II and III are main designs in usage.

The TRIGA Mark II research reactor at Atominstitute (ATI) Vienna started its operation in March 1962 [3]. It is utilizing a mixed core of three different types of fuel elements FE(s) i.e. 20 % enriched aluminium (Al) clad, 20 % enriched stainless steel (SS) clad and 70 % enriched SS clad FLIP FE(s). The high enriched fuel (i.e. FLIP fuel with 70 % enrichment) is required to be replaced by LEU fuel due to non-proliferation resistant policies by fuel exporting countries. The ATI reactor is the only nuclear research facility in Austria to satisfy its research and training demands. Austri aplays an active role in nuclear educational

and training activities in Europe. The Atominstitute (ATI) of the Vienna University of Technology is an energetic member of the European Nuclear Education Network (ENEN), therefore contributing its activities in preserving, enhancing and managing nuclear knowledge. Beyond from regional level activities, the ATI co-operates with the nearby located International Atomic Energy Agency (IAEA) in international research projects, Coordinated Research Programs (CRP) and supplying expert services. In support to the IAEA, regular training courses are carried out for safeguard trainees, fellowship places are offered for scientists from developing countries and staff members carry out expert missions to research centres in Africa, Asia and South America. The efforts of this PhD studies is also directed toward the calculation of safe and reliable reactor operation when HEU (i.e. 9 FLIP FE(s)) is replaced by LEU (SS clad 20 % enriched FE(s)). So that this reactor can be kept in operation for longer time due to its local, regional and global research demands.

This PhD work was started to develop a MCNP model of the ATI reactor core. The developed MCNP model incorporates all geometric and material information, collected from various reliable sources i.e. different TRIGA users, General Atomic (GA), shipment documents and log books of the reactor. This developed model was confirmed by local consistent experiments, i.e. first criticality experiment performed on 7th March 1962, reactivity distribution experiment [3] and the flux density distribution of the first core configuration [4]. Since its first criticality, the reactor core has been loaded with additional 104-type and 110-type or FLIP FE(s), making the current core as mixed core with three different types of FE(s). Further, most of these FE(s) are reshuffled during their irradiation history. The different irradiation histories for each FE, their reshufflings and complete mixed nature makes its neutronics analysis challenging. To analyze the current burned core, ORIGEN2 was employed to calculate the accumulated burn up and relevant material composition from its irradiation history. These burn up calculations with relevant material composition are verified by gamma spectroscopic experiments of measuring the burn up indicator i.e. Cesium (Cs) isotope for six 102-type spent FE(s) [5]. The ORIGEN model of the FLIP fuel was developed and confirmed by spectrscopy of one FLIP FE. Applying

these ORIGEN2 models of the TRIGA fuel, an effective material composition of all FE(s) in the current core was calculated and incorporated into the already developed MCNP model, resulting into the complete model of the ATI research reactor.

1.1 TRIGA Mark II Vienna [3,5]

The TRIGA Mark-II research reactor, Vienna, was installed by GA (San Diego, California, U.S.A.) in the years 1959 through 1962. Its first criticality was achieved on March 7, 1962. Since its start-up, the reactor is operating on average of about 220 days per year, without any long outages. It has a maximum continuous power output of 250 kW (thermal). The heat produced is released into a channel of the river Danube via a primary coolant circuit (de-ionized, distilled water at temperature between 20 to 40 degrees Celsius) and the secondary coolant circuit (ground water at temperatures between 12 and 18 ^{o}C. The two circuits being separated by a heat exchanger.

The current reactor core consists of 83 FE(s) of three different types of fuel. The specification of each fuel type is described in the subsequent sections. All these FE(s) are arranged in an annular lattice surrounded by annular graphite reflector. Two FE(s) have thermocouples implemented in the fuel meat which allow to measure the fuel temperature during reactor operation. At nominal power (250 kW), the center fuel temperature is about 200 ^{o}C. Because of the low reactor power level, the burn-up of the fuel is very small and most of the FE(s) which were loaded into the core in 1962, are still in the reactor core.

Generally the TRIGA fuel utilizes a Zirconium Hydride (ZrH) fuel which is homogeneous mixture of uranium (U) and ZrH. The ZrH is being used as the main moderator. Since the moderator has the special property of moderating less efficiently at high temperatures, the TRIGA-reactor Vienna can also be operated in a pulse mode. It can generate a pulse of 250 MW for roughly 40 milliseconds. The power rise is accompanied by an increase in the maximum neutron flux density from 1×10^{13} $cm^{-2} . s^{-1}$ (at 250 kW) to $1 \times 10^{16} cm^{-2}.s^{-1}$ (at 250 MW). The negative temperature coefficient of reactivity brings the power level

back to approximately 250 kW after the excursion. The maximum pulse rate is 12 pulses per hour. Since the temperature of the fuel rises to about 360 ^{o}C during the pulse therefore the fuel is subjected to strong thermal stresses.

There are about 17 irradiation experimental facilities inside the reactor core. One of these 17 is a Central Irradiation Channel (CIR) which is used to irradiate the relatively larger samples in the core at the maximum flux density. The remaining 16 smaller experimental holes in each ring and on both sides of the core provide high level irradiation locations for in-core experiments. A high speed pneumatic transfer system permits to produce extremely short lived isotopes.

Three control rods (regulating, shim and transient-safety) control the power level of the TRIGA reactor. As far as safety control of reactor is concerned, it is experimentally proved that the large prompt negative temperature coefficient of the fuel-moderated material provides a high degree of self-regulation without the assistance of external control devices. These control rods are made of boron carbide as absorber material. When these rods are fully inserted into the reactor core, the neutrons continuously emitted from a start-up source (Sb-Be photo-neutron source) are absorbed by these control rods keeping the reactor in sub-critical state. The reactor core is surrounded by a graphite reflector in Aluminium cladding. In the upper part of the reflector, there is an annular groove called rotary groove or "lazy susan".

The TRIGA Mark II core can be observed through a 5 m vertical water shield. A graphite thermal column and radiographic collimator are on the opposite of the core and extends from outer face of the reflector assembly into the concrete shield structure. Horizontal access and shielding for the thermal column are provided by a track-mounted heavy concrete door. A dry irradiation facility 2.74 meters long, 2.44 meters wide and 3.66 meters deep provides a working face of radiographic collimator. Four beam ports supply neutrons for irradiation experiments (i.e. neutron activation, diffraction, interferometry, low temperature physics etc.)

The neutrons flux density, power level and its rate of change are monitored and indicated by 3 redundant instrumentation channels. The console displays the water and fuel temperature and the water conductivity at the inlet and outlet of the demineralizer. Additionally, a Sodium Iodide (NaI) scintillator is used to monitor the gamma radiation in the reactor water.

The water cooling and purification system maintains low water conductivity, removes impurities, maintains the optical clarity of the water and dissipates the reactor heat. It consists of a water surface skimmer, pump, filter, demineralizer, heat exchanger and associated piping and valving.

1.2   TRIGA Experimental Facilities [5]

This type of research reactor was particularly designed to allow the various fields of basic and applied nuclear research and education. The TRIGA Mark II of Vienna is equipped with many irradiation facilities inside and outside the reactor core. It incorporates facilities for neutron and gamma irradiation studies as well as for isotope production, sample activation and students training. The reactor and its experimental facilities are surrounded by a reinforced barite concrete structure standing 6.55 meters above the reactor room floor. The lower portion is 3.70 meters high and 6.55 meters wide and 8.2 meters long. The upper portion is octagonal 3.81 meters across the flats and 2.87 meters high. The entire structural shield except the thermal column has a nominal density 3.35 g/cm^3.

The top and side view of the reactor is shown in Figure 1.1 and 1.2 respectively where the reacor core, surrounding graphite reflector, four beam tubes, thermal column, radiographic collimator, reactor tank and biological TRIGA shielding can be seen.
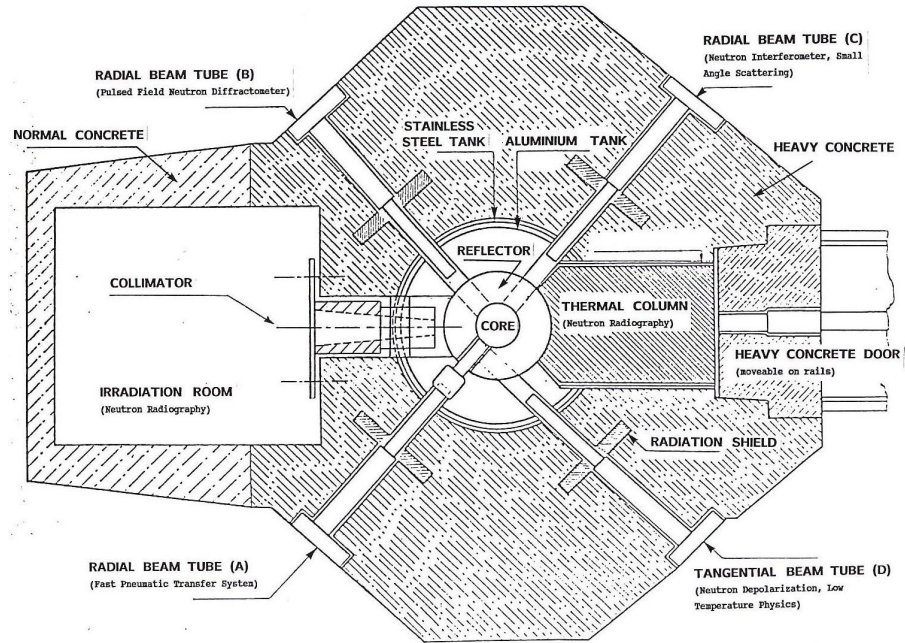
Figure 1.1: Top view of the TRIGA Mark II research reactor [5].
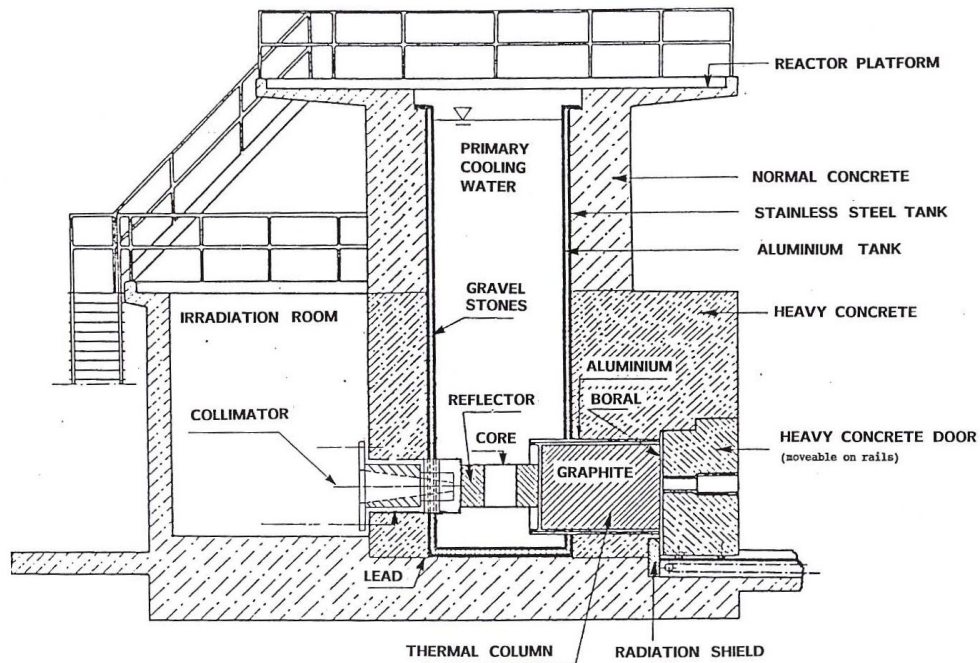
Figure 1.2: Side view of the TRIGA Mark II research reactor [5].

1.2.1   Thermal Column [6]

The thermal column of the TRIGA Mark II reactor is used to supply thermal neutrons for special irradiation experiments. It is basically a large, boral lined, graphite-filled aluminium container. Its outside dimensions are 1.2×1.2 meters in cross section by approximately 1.6 meters in depth.

The thermal column liner is a seal-welded container fabricated from a 12.7 mm thick aluminium plate. The outer portion is embedded in the concrete shield and the inner portion is welded to the aluminium tank. The exterior surfaces of the thermal column, which are in contact with concrete, are coated with plastic for corrosion protection. The portion welded to the aluminium tank extends to the graphite reflector and matches the contour of the reflector over a 100° angle. The horizontal centerline coincides with the active core lattice. In the vertical plane, the column extends approximately 33 cm above and below the reflector, with the central lines of the column and the reflector coinciding.

The aluminium container is opened toward the reactor room. Blocks of AGOT nuclear grade graphite occupy the entire void. The dimensions of each block are approximately 10.2 x 10.2 cm in cross section and 127 cm in length.

1.2.2   Beam Ports [6]

There are four beam tubes (i.e. BT-A, BT-B, BT-C and BT-D) which penetrate the concrete shield and the aluminium tank and pass through the reactor tank water to the reflector. These tubes provide neutron beams and gamma radiation for a variety of experiments. These tubes also provide the irradiation facilities for large specimen (up to 15 cm) in a region close to the core. Three of the beam tubes (i.e. BT-A, BT-B and BT-C) are oriented radially with respect to the center of the core while the fourth tube (BT-D) is tangential to the outer edge of the core. Two of the radial tubes (BT-B and BT-C) terminate at the outer edge of the reflector assembly but are aligned with the cylindrical

void in the reflector graphite. The third (i.e. BT-A) tube, specifically developed for neutron activation, penetrate into the graphite reflector and terminates at the inner surface of the reflector, just at the outer edge of the core. The fourth beam tube (i.e. tangential beam tube) terminates at the outer surface of the reflector, but is also aligned with the cylindrical void, which intersects the piercing tube in the graphite reflector. In order that the beam-tube voids in the reflector graphite pass beneath the rotary specimen rack, their horizontal centerlines are located 7 cm below the centerline of the core.

1.2.3   Graphite Reflector [6]

The annular graphite reflector surrounding the reactor core, is a ring shaped block of nuclear grade graphite. It is 30.5 cm thick radially, with an inside diameter of 45.7 cm and height of 55.9 cm. To protect its graphite from water, it is encased in leak-tight welded aluminium can. A "well" in the top of the graphite reflector (as shown in Figure 1.3), is provided for the rotatory specimen rack. This "well" is also aluminium-lined, the lining being an integral part of the aluminium reflector can. The rotatory specimen rack is self-contained unit and does not penetrate the sealed reflector assembly at any point.

The graphite and outer surface of the aluminium are pierced by an aluminium tube, which form the inner section of the piercing beam port. The reflector assembly rests upon the reflector platform and provides the support for the two grid plates. Four lugs are provided for lifting the assembly, which weights about 770 kg.
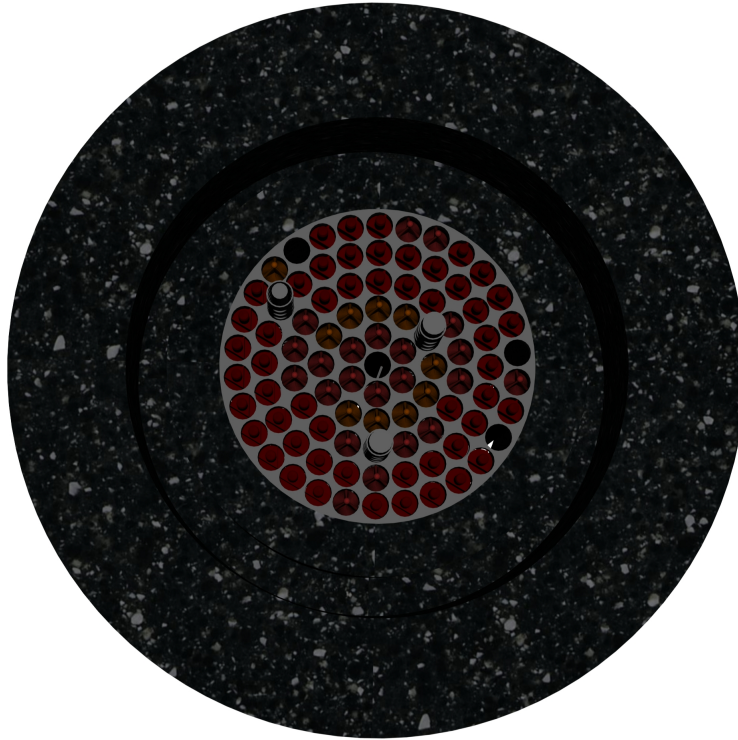
Figure 1.3: Annular graphite reflector of the TRIGA Mark II reactor.

1.2.4 Grid Plates [6]

There are two aluminium grid plates at the top and bottom of reactor core. The top grid plate, as shown in Figure 1.4, is 49.5 cm in diameter and 1.9 cm in thickness as shown in Figure 1.4. Ninety holes, each with diameter 3.82 cm, are drilled in five concentric rings to locate the core components (FE(s), source element, control rods etc.) while 91st central hole accommodates the CIR of diameter 3.81 cm. About sixteen holes, each with diameter 8 mm, at various positions permits the insertion of foils into the core to measure the flux denity data.

The bottom grid plate supports the entire weight of the core and provides the exact spacing between core components. It is an aluminium plate of 40.7 cm in diameter and 1.9 cm in thickness. The central hole of 39.9 mm diameter serves as a clearance hole for the central thimble while the other ninety holes with 7.14 mm diameter provide alignment with the

holes in the top plate.
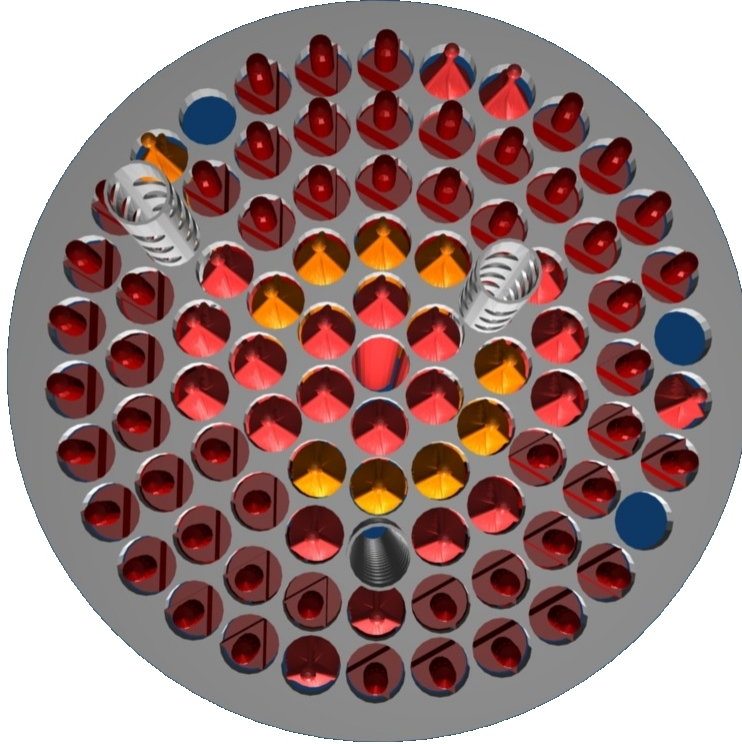
Figure 1.4: Upper grid plate of the reactor core.

1.3 Reactor Core Components [3,6]

The reactor core is a part of the reactor where the nuclear reactions take place. The reactor core is composed of 83 FE(s), 3 control rods, one neutron source element and one dummy graphite element in the F-ring. These components are explained in next section. At nominal power (250 kW), the center fuel temperature is about 200 ^0C. The current core map is described in Figure 1.5 where "ZBR" denotes CIR; "TST, RST and IST" are shim, regulating and transient-safety control rods respectively. The positions F08, F11 are occupied by two pneumatic transfer systems while F09 (i.e. no. 1941) is the only graphite element left in the current core of the reactor.
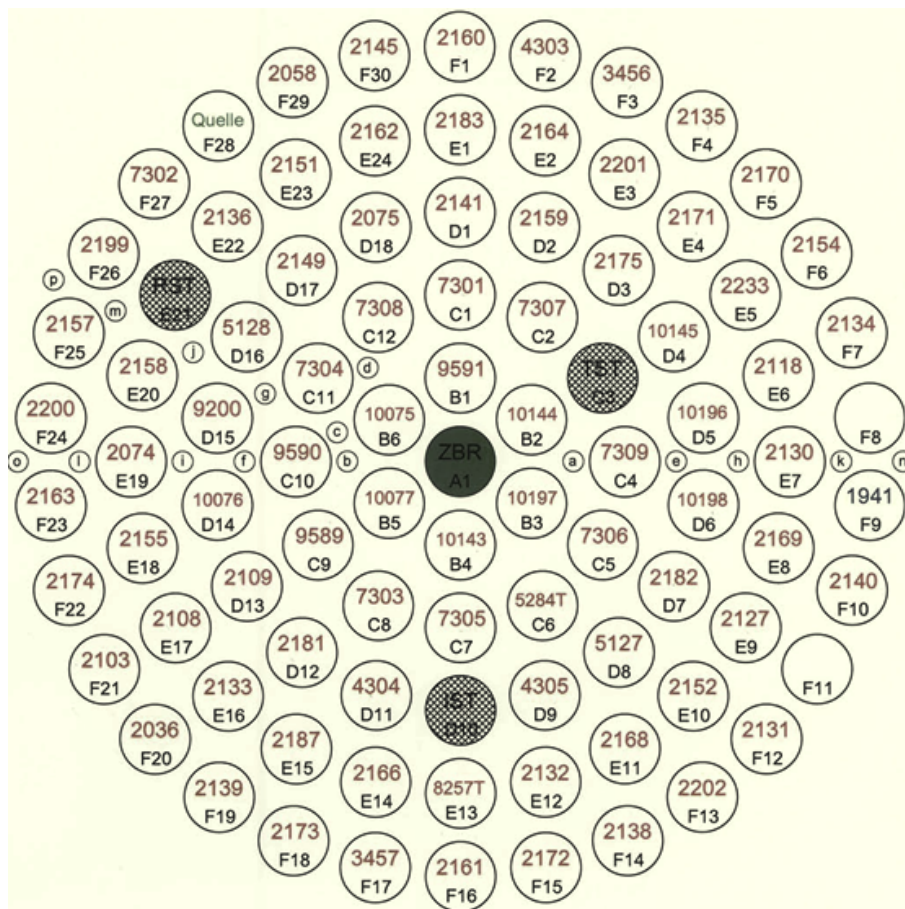
Figure 1.5: Current core configuration of the reactor core.

1.3.1   Fuel Element [3,6]

The TRIGA fuel is a metallic alloy of U and ZrH (U-ZrH) with different Hydrogen to Zirconium (H/Zr) ratios depending on the fuel type. The TRIGA fuel has cylindrical geometry as shown in Figure 1.6. Generally, the components of a TRIGA FE are enriched U-ZrH fuel meat, two axial graphite reflectors, burnable poisons (Samarium and Molybdenum disks in case of Al and SS clad fuel while homogeneously mixed erbium in case of FLIP fuel). The over all dimensions of all types of FE(s) are same i.e. 3.75 cm in diameter and 72.06 cm in length. The current reactor core is composed of the following three different types of 83 FE(s).

Aluminium Clad Fuel

The Aluminium clad or 102-type fuel is approximately 20 % enriched with 8 wt.% uranium. It has two burnable poison disks of samarium (99.18 % aluminium and 0.82 % Sm_2O_3) per FE. The Sm_2O_3 weight is 21.2 mg per disk and two disks per element which gives 5.8 mg of Sm-149 per element. The average material inventory per FE constitutes 2247.34 g of the net weight of fuel alloy, the uranium mass of 182.37 g contains 36.15 g of fissile uranium U-235 [7]. The first criticality of the TRIGA Vienna was achieved solely by aluminium clad fuel [8].

Stainless Steel Clad Fuel

The first stainless steel clad standard or 104-type FE was added to the core in October 1966 [8]. This fuel is homogeneous mixture of about 8.5 wt.% of low-enriched uranium and about 91.5 wt.% ZrH wherein the uranium enrichmnt is about 20%. This type of fuel has a central zirconium rod with one lower molybdenum disk as burnable poison. The average weight of the fuel meat alloy per FE is 2259.85 g containing 2067.02 g of ZrH, 191.27 g of uranium. The U-235 isotope per FE is 38.19 g [7].

FLIP Fuel

In 1974, the FLIP (Fuel Lifetime Improvement Program) or 110-type fuel was employed in the core [8]. This fuel is homogeneous mixture of about 8.5 wt.% uranium, 1.6 wt.% erbium and remaining zirconium hydride [5]. The Erbium is a strong contributor to the prompt negative temperature coefficient as a result of the interaction of its low energy resonances and spectrum hardening effect of ZrH [9]. The erbium also acts as poison to compensate excess reactivity supplied by high enriched uranium.

According to shipment documents [7], each FLIP FE contains 2261.78 g of net fuel alloy including 135.11 g of U-235, 59 g of U-238, 2028.44 g ZrH and 36.52 g of neutron poison

erbium. The 102-type fuel has no central zirconium rod while the 104-type and FLIP fuel, both have central zirconium rods as shown in the 1.6.

Since the employment of FLIP fuel, the reactor is operating with a completely mixed core of three different types of fuel. The current core loading is of 83 FE(s). Out of 83, 53 FE(s) are 102-type, 21 are 104-type while rest 9 FE(s) are FLIP type of fuel. All these FE are arranged in an annular lattice as shown in above Figure 1.5. The detailed geometric and material data of all three types of fuel is given in Table 1.1.
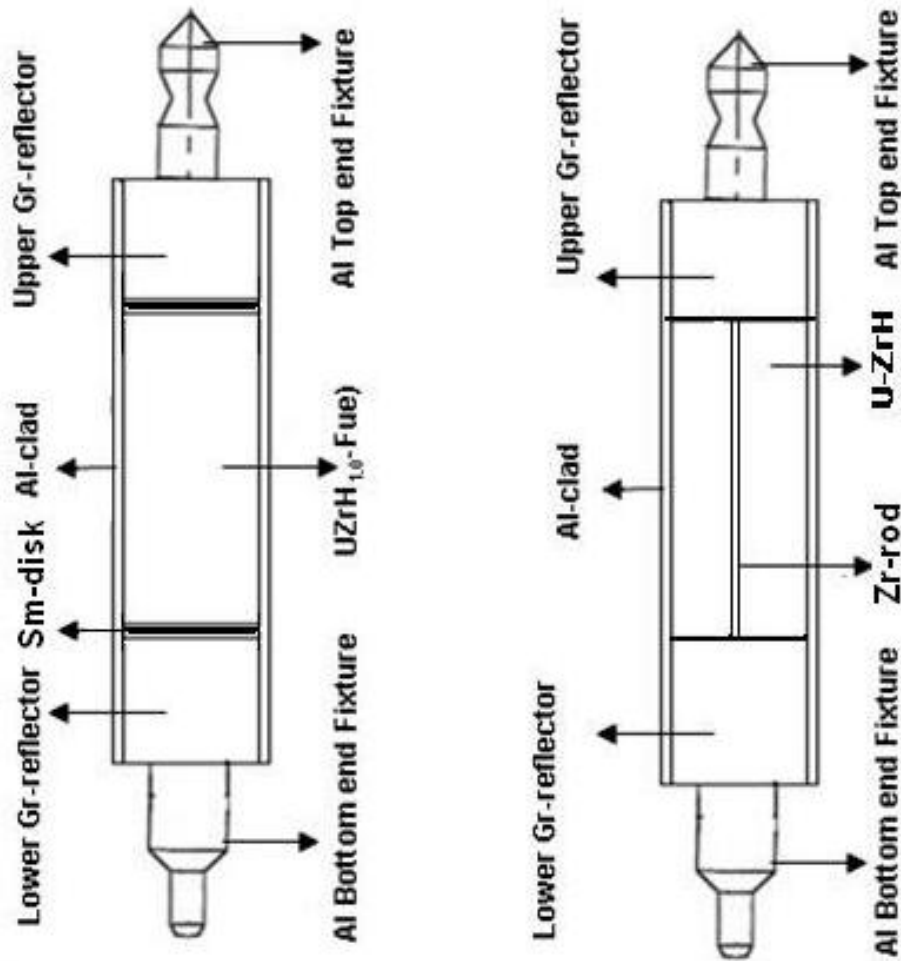
Figure 1.6: TRIGA 102-type FE (left) and 104 and 110-type FE (right).

Fuel Type	Al-clad Fuel	SS-clad	FLIP Fuel
Fuel Meat	U-ZrH	U-ZrH$_{1.6}$	U-ZrH$_{1.6}$-Er
Density (g/cm^3)	6.2134	5.8624	5.8674
Length (cm)	35.6	38.1	38.1
Diameter (m)	3.5966	3.6449	3.6449
Mass(gm/cc)	6.2134	5.8624	5.8674
Length (cm)	35.6	38.1	38.1
Burnable Poisons	2 Sm disks	1 Moly disk	1.6 wt.% Er
Density (g/cm^3)	2.80	10.28	-
Thickness (cm)	0.12192	0.02	-
Diameter(cm)	3.58	3.63	-
Axial Reflectors	Graphite	Graphite	Graphite
Density (g/cm^3)	1.6	1.6	1.6
Upper ref. length (cm)	10.21	6.8	6.8
Lower ref. length (cm)	10.21	9.31	9.31
Diameter (cm)	13.58	3.63	3.63
Central Zr-rod	No Zr-rod	Zr-rod	Zr-rod
Density (g/cm^3)	-	6.49	6.49
Length (cm)	-	38.1	38.1
Diameter (cm)	-	0.635	0.635
Fuel Cladding	Al-1100 F	SS-304	SS-304
Density (g/cm^3)	2.7	7.9	7.9
Thickness (cm)	0.076	0.051	0.051
Total length (cm)	72.06	72.06	72.06
Total Diameter	3.75	3.75	3.75

Table 1.1: Fuel specifications of the TRIGA Mark II research reactor.

1.3.2 Control Rods

The reactor is controlled by three control rods which contain boron carbide as neutron absorber material. Three control rods (i.e. safety-transient (IST), shim (TST) and regulating (RST)) are operated in perforated aluminium guide tubes. The positions of all three control rods can be seen in Figure 1.5. Each control rod is sealed in aluminium tube containing powdered boron carbide. The length of all three rods is same (i.e. 40 cm) while the diameter of each rod is different as described in Table 1.2 [6].

When these rods are fully inserted into the reactor core, the neutrons continuously emitted

from a start-up source (Sb-Be photo-neutron source) are absorbed by the rods and the reactor remains sub-critical. If the absorber rods are withdrawn from the core (two of them by an electric motor and one pneumatically as in Figure 1.7 than the number of fissions increase the power level of the reactor. The start-up process takes roughly two minutes for the reactor to reach a power level of 250 kW from the sub-critical state. The reactor can be shut-down either manually or automatically by the safety system. It takes about 1/10 of a second for the control rods to fall into the core [3].

Component	Dimension (cm)	Material	Density (g/cm^3)
Shim Rod		B_4C	2.48
Outer diameter	3.2		
Length	40		
Cladding Thickness	0.071	Al	2.7
Regulating Rod		B_4C	2.48
Outer Diameter	2.2		
Length	40		
Cladding Thickness	0.071	Al	2.7
Safety-Transient Rod		B_4C	2.48
Outer Diameter	2.5		
Length	40		
Cladding Thickness	0.071	Al	2.7

Table 1.2: Material and geometrical specifications of control rods.

In steady state type of the TRIGA without pulsing capability, the control rods are the same as mentioned above except that the safety-transient rod is replaced by a powdered boron carbide safety rod that is 3.2 cm in outside diameter.
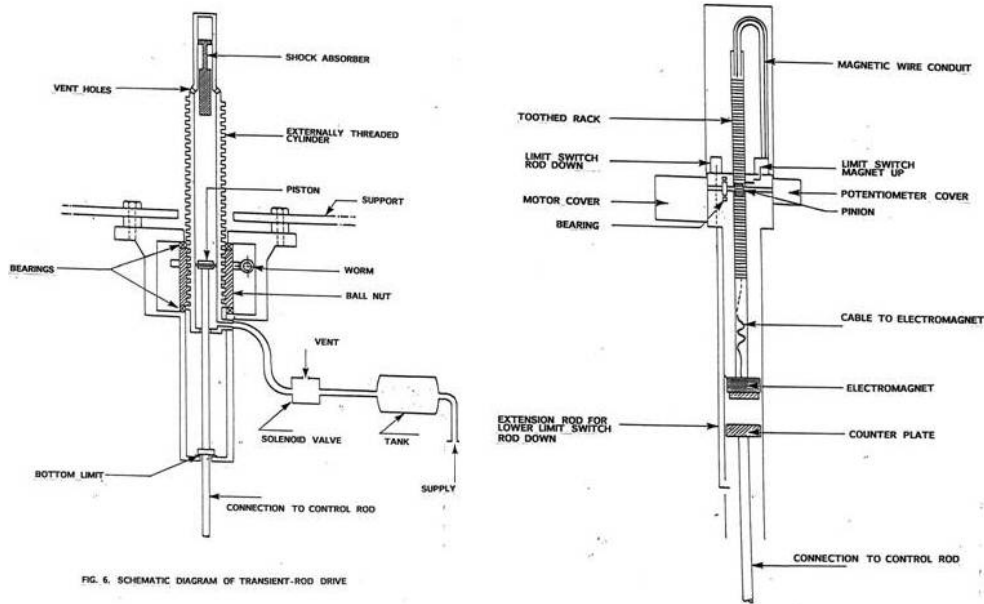
Figure 1.7: Control rod drive mechanism for all three control rods [3].

1.3.3 Neutron Source

The cylindrical photoneutron Sb-Be neutron source element has two cylinders inside (inner Sb cylinder and outer Be cylinder). The innder cylinder has a diameter of 1 cm while outer Be cylinder has thickness of 0.5 cm. This source element has total length of 40.4 cm. The Sb emits gamma radiation which induces (gamma, n) reaction in the outer Be-cylinder. During the normal operation this source emits 6×10^6 neutrons per second [10].

1.3.4 Graphite Dummy Element

These elements are filled with nuclear grade graphite and occupy those grid positions which are not filled by FE(s). Their dimensions are same as FE. The current reactor core has only one graphite element in F-ring as shown in Figure 1.5 [6].

1.4 Reactor Simulation Tools

One of the main motivations for computer simulations of physical system is that one eliminates the approximations. The sytsems which are un tractable with analytical methods can be studied with computer simulation tools. This approach allows one to study complex system and gain insight their behaviour. The computer simulation provides a tool of assessing the validity of the computational model by comparing its simulated results with experiments. Another big advantage of these tools is to fill the gap between theory and experiment. For example computer simulations can simulate such quantities or behaviours which are impossible to measure experimently [11].

Since the application of computers, the reactor simulation remains a convenient tool to analyze the reactor parameters in the fields of neutronics and thermal hydraulics of coolant flow through the reactor core. Because of the complicated neutron physics, it is not possible to approach the problem as a single, well-defined task. Instead, the solution proceeds in steps, starting from the interactions between neutrons and the target nuclei. The intermediate step in the solution is the so-called lattice calculation, in which the geometry is modeled at the fuel assembly level. The results are then used as input parameters for a three-dimensional reactor simulator calculation, which yields the reactor response under different operating conditions. Practical computer simulations of reactors either use deterministic or Monte Carlo methods. Both methods require extensive neutron reaction data which are obtained from various data bases. The quality of calculations is often limited to that of the data. Prior to discuss the calculation methods, it is an appropriate to discuss the data files and their evaluation [12, 13].

1.4.1 Neutron reaction data files [12]

The evaluated cross-sections are usually found in nuclear data evaluated files like ENDF-B6, JEFF 3.1, JENDL or BROND . The additional step is required and consists of decoding the data files, and producing a new file at the chosen temperature, which will be consistent

with the code and the system studied. For deterministic codes, the reaction cross-section must be calculated and averaged on different energy groups, while Monte Carlo codes require, in general, continuous cross-section values obtained by a list of points and an interpolation procedure. For example, the program NJOY reads an ENDF format file, and writes a specific file for a Monte Carlo code such as MCNP, taking the Doppler effects into account.

1.4.2   Monte Carlo Method versus Deterministic Method [12, 13]

Practical computer simulations of the reactor can be performed either by deterministic or probabilistic methods (i.e. Monte Carlo methods). Deterministic methods, the most common of which is the discrete ordinates method, solve the transport equation for the average particle behavior. The existed deterministic lattice codes are developed mainly for the needs of light water reactor modeling. Its applications are not easy to extend to advanced fuel types and next-generation reactor systems. By contrast, Monte Carlo methods follow the history of individual particles and recording some aspects (tallies) of their average behavior . The average behavior of particles in the physical system is then inferred (using the central limit theorem) from the average behaviour of the simulated particles.

Due to these limitations of deterministic tools and the development of advanced and fast computer systems, the transition to Monte Carlo lattice codes seems natural. The Monte Carlo method is a basic tool in particle transport problems, and it is well suited for tasks requiring the detailed modeling of 3D geometry and physics. The method is used in reactor physics calculations for decades and the applications have mainly been restricted by computer capacity. The use of a Monte Carlo based lattice code also brings all the advantages of the calculation method, and most importantly, the same code can be used for modeling any fuel or reactor type without compromising the reliability of the results. There are no approximations due to discretisation. These methods allow very detailed representations of all physical data. By increasing computer speed, very precise results

can be obtained within few hours. The code reliability lies in the validity of cross-sections, taken directly from evaluations.

1.4.3 Monte Carlo N-Particle (MCNP) transport code

The MCNP (Monte Carlo N-particle transport code) is one of the best known and well practiced Monte Carlo code in reactor physics. Its standard features includes a powerful general source, criticality source, and surface source; both geometry and output tally plotters; a rich collection of variance reduction techniques; a flexible tally structure; and an extensive collection of cross-section data. These features make MCNP more versatile and easy to use. The version MCNP5 1.40 was obtained from the NEA and all the simulations during this PhD studies are executed on a special PC of the licence holder (Prof. Helmuth Böck), the supervisor of this PhD research.

The MCNP always calculates the expected or mean value of some physical quantity (i.e. flux density, current, multiplication factor etc). This mean value is calculated per history as [14].

$$\overline{x} = \frac{1}{N} \sum_{N}^{i=1} x_i \tag{1.1}$$

Where x_i is the contribution of its history to that quantity. Thus, MCNP tally x_i after each history to calculate the estimated or sample mean at the end of each calculation. This code can not give the rate (i.e. flux density) but only the mean response per particle. It needs to give the rate information i.e. in terms of per second. The time information (mostly by experiments) converts the MCNP results into real physical quantity. This is called normalizing the model. The model is always normalized to make some sense of physics. For example

$$Flux \quad (/cm^2 - sec) = MCNP \quad results \quad (probability/cm^2 - history) \times constant \quad (histories/s)$$

This normalization factor or constant (histories/s or cps) can be obtained from reliable experimental values.

1.4.4 MCNP Physics [15]

MCNP follow the particle (neutron in our case) throughout its life similar to theoretical experiment. It tracks the particle from its birth (the source) to its death (absorption, escape). Probability distributions are randomly sampled using transport data to determine the outcome at each step of its life as described in Figure 1.8. Specific techniques are implemented for critical problems (KCODE problems), where the neutron chain length can reach infinity. Following cases should be known:
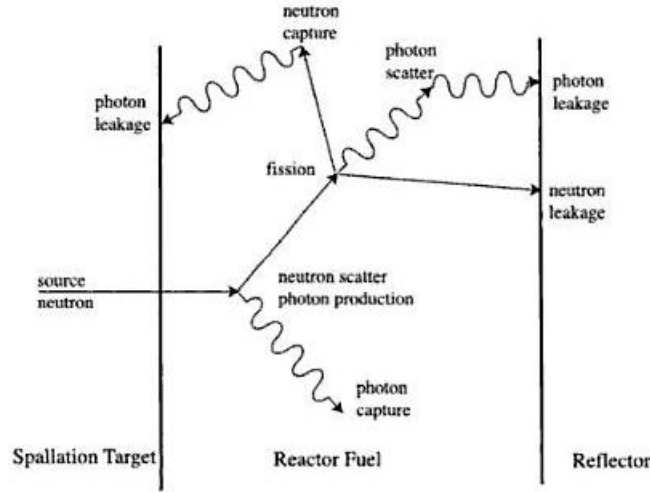
Figure 1.8: Random walk of neutron [9].

Neutron Interaction

Suppose one neutron enters into the a material, this neutron can escape or interact in the material. The probability for a collision to occur between l and $l + dl$ is

$$p(l)dl = exp(-\Sigma_T l)\Sigma_T dl \tag{1.2}$$

Where Σ_T is the macroscopic total cross section. One has to sample l according to this exponential probability law. Let ξ be a random number in $[0,1]$ uniformly distributed. One can write

$$\xi = \int_0^l p(l)dl = 1 - e^{-\Sigma_t l} \tag{1.3}$$

$$l = -(1/\Sigma_t)ln(1-\xi) \tag{1.4}$$

Which can be replaced by $l = -(1/\Sigma_t)ln(\xi)$ because $1-\xi$ and ξ have the same distribution. The probability distribution of l is obtained by estimating the length of the interval $\Delta\xi$ corresponding to interval the dl

$$\frac{\Delta\xi}{\Delta l} = \frac{d\xi}{dl} = exp(-\Sigma_T l)\Sigma_T \tag{1.5}$$

Comparison of equation 1.1 and 1.3 gives that $p(l)$ obeys the distribution given in 1.1. If l is larger than the size of the material than the neutron escapes. Otherwise, an interaction occurs at distance l. About the interaction, MCNP addresses the following aspects of physics where ξ denotes a random number uniformly distributed in $[0,1]$.

Thermal Scattering laws $S(\alpha, \beta)$ treatment

The neutron interaction is affected by the thermal motion of the atom and their binding effects. Depending on the compound (essentially moderators) and on the neutron energy, two treatments are done. For slow neutrons ($En < 4eV$) and for carbon, water, etc., the crystalline structure as well as effects of chemical binding have to be taken into account via an $S(\alpha, \beta)$ treatment. These $S(\alpha, \beta)$ tables are special sets of ENDF files. For higher energies or other compounds, a free gas thermal treatment is applied that assumes the nuclei are present in the form of a mono-atomic gas. This is the MCNP default for thermal neutron interactions.

Neutron interaction with specific nuclides

If the target material is composed of N different nuclei, the interaction occuring with a specific nuclide 'K' if

$$\sum_{i=1}^{i=k-1} \Sigma_T^i < \xi \sum_{N}^{i=1} \Sigma_T^i \leq \sum_{k}^{i=1} \Sigma_T^i \tag{1.6}$$

Where Σ_T^i represents the total macroscopic cross section of the $i - th$ nuclide.

Neutron Capture

MCNP handles neutron capture in two ways i.e. analog and implicit capture. Analog is a true capture where the neutron is absorbed with a probability σ_a/σ_T where σ_a is absorption reaction except (n, n'). While the implicit absorption is useful to obtain better statistics.

Elastic and inelastic reactions

MCNP adjusts the elastic scattering cross-section according to the free gas model while inelastic reactions $(n, n'), (n, f), (n, np)$ are assumed to be independent of the temperature. The elastic scattering probability of the reaction is

$$\frac{\sigma_{el}}{\sigma_{inel} + \sigma_{el}} = \frac{\sigma_{el}}{\sigma_T + \sigma_a} \tag{1.7}$$

The inelastic reaction probability is

$$\frac{\sigma_{inel}}{\sigma_T + \sigma_a} \tag{1.8}$$

If the inelastic reaction happens, the j-th reaction is selected among M atoms as follows

$$\sum_{i=j-1}^{i=1} \sigma^i < \xi \sum_{M}^{i=1} \sigma^i \leq \sum_{j}^{i=1} \sigma^i \tag{1.9}$$

Angular distribution

The direction of outgoing particles is determined by sampling angular distribution tables from the cross-section files for both elastic and inelastic scattering. There are two possibilities for sampling the angular distribution. If the distribution is isotropic for a reaction, the cosine angle is chosen uniformly in an interval -1, 1]. Otherwise, 32 groups of cosine angles are used depending on the nuclear data. This group discretisation could be a limitation of MCNP (mainly sensitive for high energies) [12].

Fission inelastic reactions

In case of a fission reaction, N_p neutrons are emitted according the mean number of neutrons per fission (given in cross-section files) i.e. $\overline{\nu}(E_n)$. MCNP takes these neutrons N_p as

$$N_p = I + 1 \, if \, \xi \leq \overline{\nu}(E_n) - I$$
$$N_p = I \, if \, \xi > \overline{\nu}(E_n) - I$$

Where I is the largest integer smaller than $\overline{\nu}(E_n)$: MCNP select the energies of outgoing neutrons according to applied spectrum (i.e. Maxwell fission spectrum, energy dependent Watt spectrum, evaporation spectrum etc.). However, such treatment is not totally correct, because the N_P follows a Poissonian distribution; for example, if $\overline{\nu}(E_n) = 2.5$, MCNP gives two or three neutrons (in order to have 2.5 on average), but it never gives bigger and smaller neutron number (with the same average).

MCNP Precision

Monte Carlo computes the expected mean value of the required quantity with associated statistical error (or uncertainty) from many histories sampled during the run. This uncertainty (or error) evolves with the number of histories. Indeed, this behavior can reflect

whether the result is statistically well behaved; if this is not the case, the uncertainty will not reflect the true confidence interval of the result which thus could be completely erroneous. MCNP provides a detailed and efficient methods to determine the quality of the confidence interval, as well as methods to improve the precision (i.e. variance reduction techniques).

If the result of a run is ϕ with 'N' histories contributing to this quantity, the uncertainty is $\Delta\phi \propto 1/\sqrt{N}$. To make the error by half, N has to be multiplied by 4. On the other side the computer time is also proportional to N, so the duration of the run is also multiplied by 4. To optimize the case, generally, an MCNP result with an uncertainty less than 10 % is sufficient, but only if the entire volume is visited by particles. MCNP provides the evaluating number (i.e. the Figure Of Merit (FOM) which is defined by

$$FOM = 1/\Delta\phi^2 \times T$$

Where T is the computer time. This number must be approximately constant $T \propto N$ and $\Delta\phi \propto 1/\sqrt{N}$ for the result to be credible.

Variance reduction techniques

The estimated relative error R is proportional to $1/\sqrt{N}$ where N is the number of histories. The computer time T consumed per run of MCNP model is proportional to N. This implies; $R = C/\sqrt{T}$, where C is constant. By this relation, there are two ways to reduce R i.e. increase T or decrease C. The MCNP has a special variance reduction techniques for decreasing C. Here the variance reduction techniques are described briefly while the details of these techniques are available in reference [10]. In truncation technique, the MCNP can operate energy or time cut-offs. By energy cut-off, the particle is killed below an energy threshold. It saves time but it is dangerous specially when low-energy particles produce highly energetic ones (fissions) and thus lead to erroneous results. Similar time cut-offs exist when the particle time exceeds a given cut-off.

Each MCNP cell has an importance I. For example, if a neutron of weight W passes from a cell of importance 2 to one of importance 8, it is split into $8/2 = 4$ identical neutrons each with a weight W=4. Conversely, if the neutron passes from a cell of importance 8 to one of importance 2, a Russian roulette is played and followed with a 25% ((2/8)x100) probability and a weight W/4. These population control methods use particle splitting and Russian roulette to control the number of particles in various regions.This technique can also be applied to the energy range.

1.4.5 ORIGEN2 [16]

In order to calculate the burn-up and relevant material composition of irradiated fuel, burn-up codes are available. Generally, the burn-up codes solve the system of differential equations that describe the evolution of the isotopic vector, taking into account the radioactive decay and the neutron induced reactions during irradiation. Therefore the codes need the decay modes with half-lives, the average cross sections of the neutron induced reactions and the neutron flux density. The most commonly used code is ORIGEN2 v2.2, updated version of ORIGEN2.1, was developed at developed at the Oak Ridge National Laboratory (ORNL), meets the above mentioned requirements.

ORIGEN2 is a one-group depletion and radioactive decay computer code. It makes a relatively unsophisticated one-group neutronics calculation providing various nuclear material characteristics (the buildup, decay and processing of radioactive materials) in easily comprehensive form. It calculates the composition and other related properties of irradiated nuclear materials and forms the basis for the study and design of fuel reprocessing plants, waste treatment and disposal facilities. ORIGEN2 databases contain in total 1700 nuclides divided into three categories: 130 actinides, 850 fission products and 720 activation products. The actinides include all of the heavy isotopes with atomic number Z greater than 90 plus all of their decay daughters, including the final stable nuclides. The fission products include all nuclides which have a significant fission product yield (either binary or ternary) plus some nuclides resulting from neutron captures of fission products. The

activation products include the low-Z impurities and structural materials. For each of these three segments, there are three different libraries: a radioactive decay data library, a cross-section and fission product yield data library, and a photon data library. The cross-section libraries cover the main commercial reactors and fuel types, such as Uranium and U-Pu cycle PWRs and BWRs, Thorium-based fuel PWRs, once-through Uranium cycle CANDUs and U-Pu and Thorium cycle LMFBRs. This work apply PWR cross section library to the TRIGA Mark II as best available option for the TRIGA reactors.

The point-depletion ORIGEN2 is based on one group space independent model for flux density calculations. The rate at which the amount of nuclide (i) changes as function of time is given by following equation

$$\frac{dX_i}{dt} = \sum_{N}^{j=1} l_{ij}\lambda_j X_j + \phi \sum_{N}^{k=1} f_{ik}\sigma_k X_k - (\lambda_i\phi\sigma_i + r_i)X_i + F_i i = 1, 2, 3, ..., N \quad (1.10)$$

Where l_{ij} = fraction of radioactive disintegration by nuclide j which leads to formation of nuclide i;

λ_j = radioactive decay constant;

ϕ = position- and energy- averaged neutron flux density;

f_{ik} = fraction of neutron absorption by nuclide k which leads to formation of nuclide i;

σ_k = spectrum-averaged neutron absorption cross section of nuclide k;

r_i = continuous removal rate of nuclide i from the system;

F_i = continuous feed rate of nuclide i.

This gives N simultaneous equations in N variables (nuclides), which makes the problem relatively simple to solve if the number of equations is reasonably small. The solutions of these simultaneous differential equations by ORIGEN2.1 yields the amounts of each nuclide present at the end of each time step (integration interval). All the time-dependent parameters are set constant at specified time interval, the neutron flux density is calculated

from power or vice versa:

$$\phi \propto \frac{6.242 \times 10^{18} \times P}{\sum_{N}^{k=1} X_f^i \sigma_f^i R_i} \tag{1.11}$$

Where ϕ = instantaneous neutron flux density $(ns.cm^{-2}s^{-1})$;

P = power (MW);

X_f^i = amount of fissile nuclide 'i' in fuel (gram-atom);

σ_f^i = microscopic fission cross section for nuclide 'i' $(10^{-24}cm^2)$;

R_i = recoverable energy per fission for nuclide i (MeV/fission).

Finally the system of simultaneous differential equation is solved to provide the composition of the material at the end of each irradiation step.

ORIGEN2 uses several input and output units to facilitate orderly and flexible code operation. These units and their functions are given in reference. For a basic ORIGEN2 calculation, units 5, 6, 12, and 50 would be necessary, and the rest of the units could be dummied or omitted. The units not used in the basic calculation are required to execute certain ORIGEN2 commands or to provide useful auxiliary information.

The subroutine LISTIT is included in ORIGEN2, which can provide a card input echo. The cards are read on unit 5, printed on unit 6, and written to unit 50, which is a temporary file. Cards that have a dollar sign in the first column of the card are printed on unit 6 but not written on unit 50, thus allowing for the inclusion of comments in the input stream that will not interface with the operation of ORIGEN2. The rest of ORIGEN2 reads the information from unit 50. The units 5, 6, and 50 appear explicitly in the call to LISTIT, which occurs in MAIN.

Chapter 2

DEVELOPMENT OF THE MCNP MODEL

This chapter constitutes three sections. The first section describes the development of the MCNP model of the very first core configuration of the TRIGA Mark II reactor. To start reactor operation, the first core was loaded with only FE type 102 making the initial core as a uniform core. The second part explains the validation of the MCNP model by three different local consistent experiments performed on the first core configuration of the TRIGA Mark II reacor [17, 18, 4]. The first experiment was performed in March 1962 to achieve the initial criticality of the core. The second experiment was carried out in December 1963 to measure the reactivity worths of four FE(s) and one graphite element using the control rods positions. The third experiment was taken from one of the Master thesis performed on the radial and axial measurement of the neutron flux density. The radial thermal flux density was measured in the core while the axial thermal flux density was measured in the CIR using gold foil activation method. The third part of this chapter discusses the results in details.

2.1   The MCNP Model Development

The MCNP5, 1.40 neutronics behaviour simulating computer code has the capability to model the reactor core geometry up to the desired level of achieving the objectives of

the specific research. Having all geometrical and material inventory informations from various sources [3,6,19], the detailed three dimensional MCNP model of the very first core configuration of TRIGA Mark II is developed. The top view of core model and simplified geometry of the FE model is shown in Figure 2.1.

Inside the reactor core, all core components (i.e. FE(s), graphite elements, neutron source element, CIR etc.) are modeled. Each grid position in its exact location of the grid plate has been simulated in this model. Outside the reactor core, this model includes the annular grooved graphite reflector, thermal and thermalizing column, four beam tubes and the water tank up to 100 cm in radial and +60 and -60 cm in axial direction. The reactor started its operation with the achievement of first criticality on 7th March 1962 with a core loading of 57 FE(s) [17]. Therefore the first core configuration consisted of 57 FE(s), dummy graphite elements in F-ring and one source element in F06 position are modeled with the exact dimensions of their constituent materials. The geometrical dimensions of each surface and cell of the model are taken from the chapter no. 1. Once the geometrical part of the model is completed, all relevant material are filled into the corresponding cells. Each cell of the model is flagged with different MCNP color as shown in Figures 2.1 and 2.2.

The input material composition of each cell of the model is taken from shipment documents [7,19]. This model employs the average values of the fuel inventory to all FE(s). Keeping the future plan of calculations (i.e. incorporating the burned material composition to the model) in view, each FE is modeled separately. All components of the FE (that is fuel meat, poison disks, axial graphite reflectors, Al-cladding) have been modeled and shown in Figure 2.2. The geometry of the top and bottom aluminium fixtures is not modeled exactly because it has no significant effect on neutronics of the core. The side view (YZ-view) of the MCNP core model and Al-clad FE is shown in Figure 2.2.

The different colors present the different materials employed in the model as shown in in Figure **??**. The left picture includes the reactor core with FE(s) in the B, C, D and E
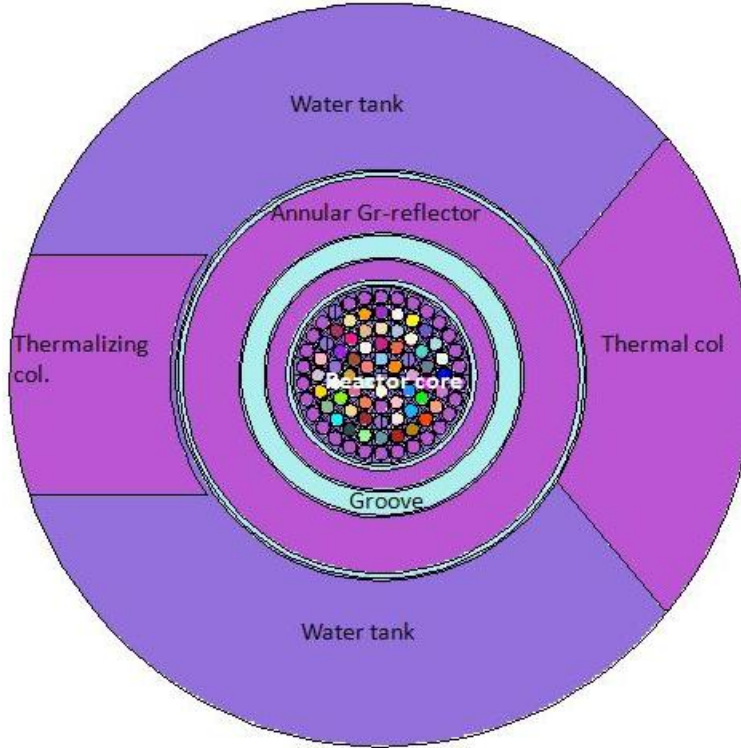
Figure 2.1: Top (or XY) view of the MCNP model of the TRIGA Mark II reactor.

ring while the neutron source (F06) and graphite elements are loaded in the F-ring of the reactor core. Keeping in view that each FE in the core will be treated separately because of its individual different burn up history therefore all FE(s) are assigned different material numbers (different colours) in spite of the fact that all FE(s) are fresh and have the same average material composition. The core is surrounded by an annular graphite reflector. The water inside the reflector groove and outside the reflector is shown in Figure 2.2.

All three control rods are modeled in their exact grid location (i.e. C03, D10 and E21). The geometrical specifications of all control rods are described in the first chapter while material specifications of the control rods are given in Table 1.2. The graphite element, neutron source element and the CIR can be seen the in the model exclusively.

The neutronics code MCNP5 is equipped with a wide variety of source conditions without modifying the actual code. The source is described in the "Data" section of the MCNP in-
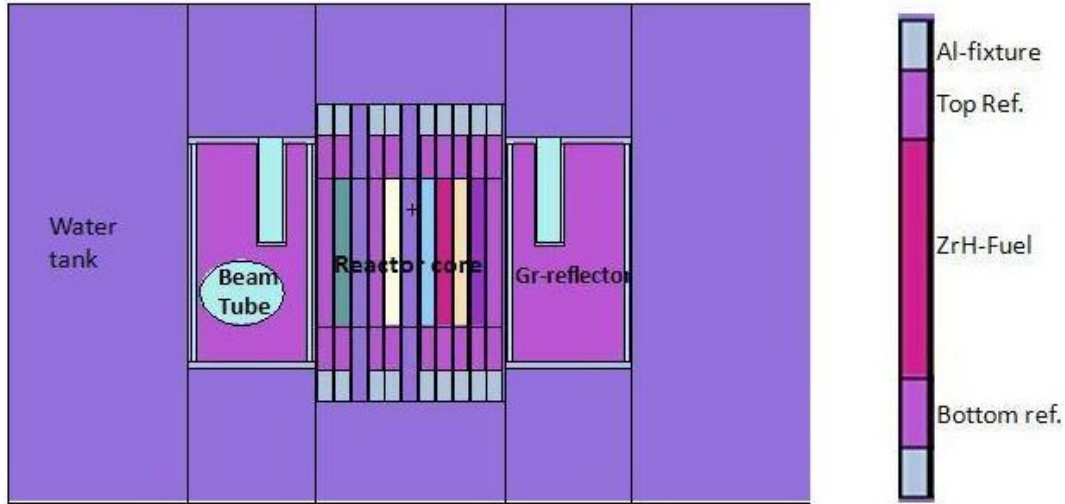
Figure 2.2: Side view (or YZ-view) of the MCNP model of the core and 102-type FE.

put file. Independent probability distributions are available to specify the source variables of energy, time, position, direction, and for other parameters such as starting cell(s) or surface(s) [13]. In addition to the input probability distributions for source variables, certain built-in functions are available for example Watt, Maxwellian, and Gaussian spectra; Gaussian for time; and isotropic, cosine, and mono directional for direction etc. Among all available source cards, the general source (SDEF) source is useful and common in use for reactivity or criticality calculations. Monte Carlo calculation tracks the particle from its birth to its death. The code ends with the end of the last history. In criticality calculation a neutron is followed throughout its life and fission is considered as a cycle termination (like a capture). The reactivity or criticality calculations need to specify the KCODE card in Data block of MCNP model [20]. General cylindrical SDEF source has been employed in this model with following options.

SDEF ERG=d1   SUR=0   AXS=0 0 1   RAD=d3   EXT=d4   POS 0 0 0

Sp1   -3

Si3   0   22.85

Si4   -19.05   19.05

kcode   100000   1   50   200

Its energy is described by the Source Probability card (SP1); its value i.e. "- 3" describes the source energy probability (i.e. Watts spectrum). The axis of the cylinder passes through point POS (0 0 0) in the direction AXS (0 0 1) along z-axis. Neutron positions are sampled uniformly (in volume) within a ring of radius 22.85 (from zero to 22.85) on Source Information card SI3 card). The ring lies in a plane perpendicular to AXS at a distance from POS sampled by EXT card. The distribution of EXT card has been described on SI4 card from Zmin = -19.05 to Zmax =19.05.

This model is run by 10^6 particles, with initial guess of $K_{eff} = 1$. Total 250 cycles are employed skipping the first 50 neutrons generation cycles. This model is based on the first criticality experiment which is explained in the next sections of this chapter.

The MCNP computer program requires extensive neutron reaction data. To perform the precise calculations, the model needs the quality of neutronics data libraries. The evaluated cross-sections are usually available from NEA are ENDF-B6, JEFF3.1 etc. These files contain the parameters of each resonance and sometimes the correlation matrix of these parameters, which allow sensitivity calculations. Because of some missing cross sections (i.e. Samarium, Erbium etc. in ENFD-B6), this model uses JEF3.1 data libraries.

2.2   Model Validation

The reactor simulations using a particle transport code always need its validation for its reliability. The validation is performed either on some standard experiments (benchmarks if available) or on local consistent experiment. There are two main objectives of such verification. The first is to check the consistency of the physical model and data used in a model while second is to determine systematic errors made by approximate simulation of the experiment. MCNP provides good statistics of the calculations and has been proven to simulate the physical interactions correctly. This does not mean that the MCNP model of ATI TRIGA Mark II reactor provides accurate solutions. Therefore, to put full confidence mark in the model, this chapter compares the MCNP calculations to available historical

experimental results of the first criticality experiment, reactivity measurements and flux density mapping experiment in the first reactor core configuration. These experimental results are obtained from the first log books [17,18] and a dissertation performed on neutron flux density measurement in the first core [4]. This section includes the results of past the experiments and compares them with MCNP calculations. These experiments are:

- First Criticality Experiment;

- Reactivity Worth Distribution Experiment;

- Flux Mapping Experiment.

2.2.1   First Criticality Experiment

This historical experiment was performed on 7th March 1962. It started with core loading of different components. Initially, the core was loaded with two FE(s) with identity number 2145 in position B06 and 2147 in C09, one source element in position F06 and 31 dummy graphite elements in other position of F-ring. Two pneumatic systems were installed in F-ring positions i.e. F11 and F21. All these components are shown in Figure 2.3. After then, the FE(s) were added to the core one by one, recording the count rates both in control rods up and down positions. By the addition of 56th FE i.e. 2118 in E23 position, the core was observed as in just sub critical state. The historical first criticality signal appeared when the 57th element (i.e. 2075) was added to core into E24 position. The excess reactivity of 15.7 cents was measured by the calibrated control rod positions [17]. The core configuration of the first criticality experiment is shown in Figure 2.3.

The described experimental procedures are applied to the developed MCNP model with 200 cycles of iteration on a nominal source size of 100000 particles per cycle. Keeping all three control rods in the up positions, the model with core loading of 56 FE(s) is executed. The simulated results the model confirm the experimental observation of sub-criticality with core loading of 56 FE(s). This gives the value of the effective multiplication factor (K_{eff}) as
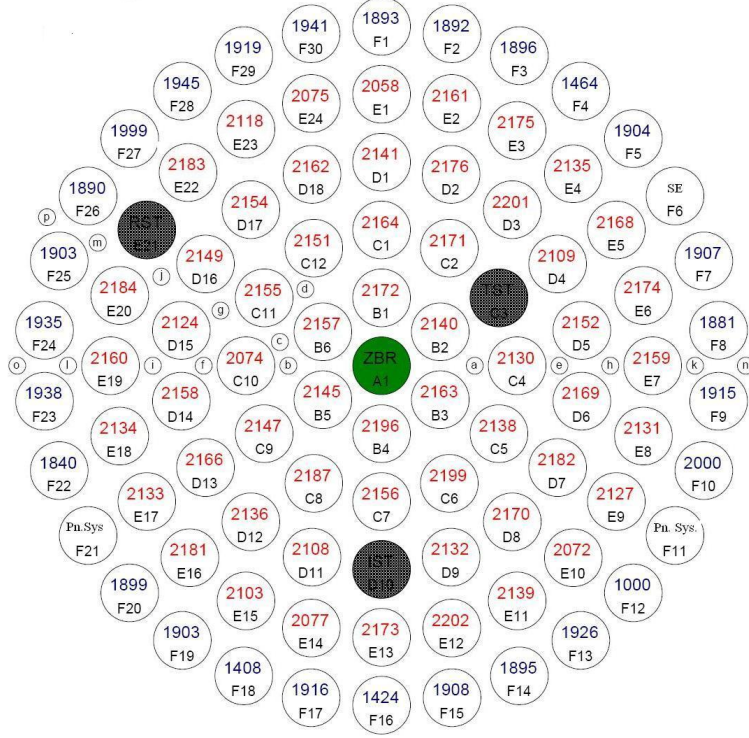
Figure 2.3: The initial critical core configuration.

0.99788 with a standard deviation of 0.00021 which corresponds to a negative reactivity of 29.11 cents. When the 57th FE is added to the core in E24 position, the execution verifies the initial criticality achievement by calculating the K_{eff} as 1.00114. This value of K_{eff} corresponds to 25.0 cents of positive reactivity. The summary of MCNP calculations and experimental observations is shown in Table 2.1. The reasons of the deviations between the experimental and theoretical values are explained in the next section.

Number of FE(s)	MCNP K_{eff}	Experimental K_{eff}
56	0.99529	subcrtical state
57	1.00183	1.00114
Core excess reactivity (cents)	25.0	15.7

Table 2.1: The MCNP results comparison with measurements for the first critical core.

44

2.2.2   Reactivity Worth Distribution Experiment

This experiment was performed on 12th December 1963, about 1.75 years after the first criticality experiment. The actual reactor core during the experiment was as burned core with the burn up history of about 1.75 years. This section only demonstrates the experimental results of the past experiment for the analysis of the simulated results. The developed model does not incorporate any composition changes with time. The reactivity worth calculations are performed applying the MCNP model. To keep the discrepancies at a aminimum possible level, the core was almost kept clean from Xenon. The reactivity worth distributions are calculated using MCNP code and compared with the available experimental values taken from reference [18]. In this experiment, one graphite element (F01) and four FE(s) from four FE(s) from different rings (B01, C01, D01, E01) were selected for reactivity worth measurement using core excess reactivity method. The control rod positions were kept to working positions at 100 watts (i.e. the transient control rod was kept fully out, the regulating rod at 15 cm out and the shim-safety rod at 25.5 cm out of the core). The core experimental core configuration is shown in Figure 2.4.

The same experimental conditions are applied to calculate the reactivity of above mentioned elements except of three control rods positions . The control rods are readjusted at different positions because of the presence of fission products in the core. This model calculates the reactivity worths of five elements on the control rod positions (i.e. transient rod full out, regulating rod 18 cm out and shim-safety rod 29 cm out of the core). To calculate the reactivity worth of a graphite element, the model replaces a graphite element by a simple water filled element of the same dimensions. The reactivity difference between these two configurations (with and without graphite element) determines the required worth of agraphite element. The same methodology is applied to compute the other four FE(s). Table 2.2 provides the comparison between the MCNP and the experimental results.
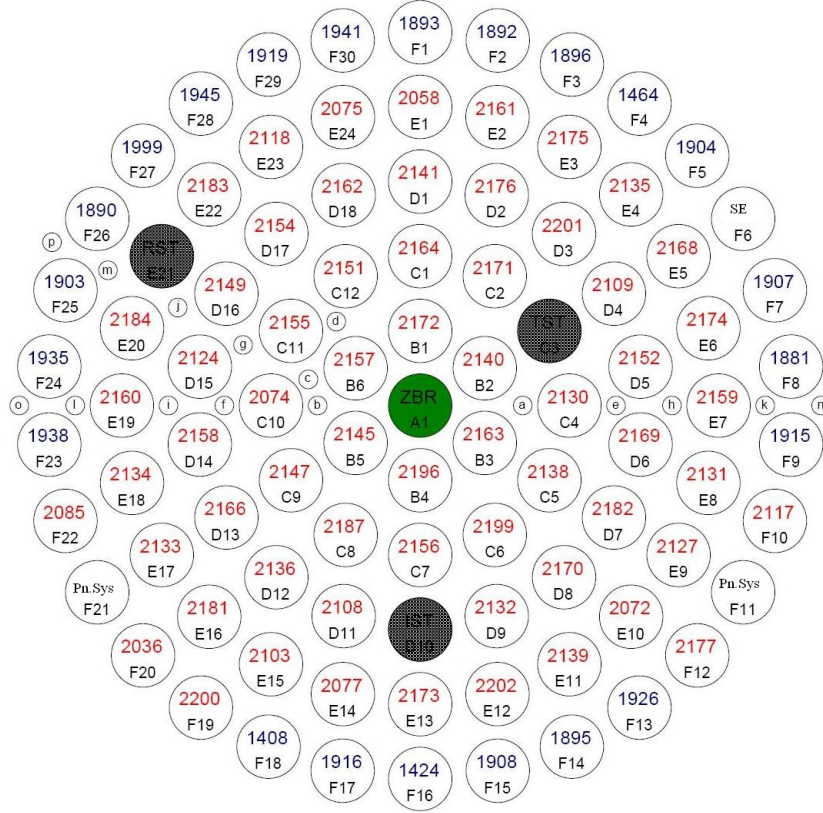
Figure 2.4: First core configuration of TRIGA Mark II at 100 watts.

Configurations	K_{eff}	MCNP reactivity (cents)	Exp. reactivity (cents)	Percent difference
GE 1893 (F01)	1.00027	11.9	10.5	8.4
FE 2058 (E01)	0.99723	53.6	56	4.3
FE 2141 (D01)	0.9958	73.4	65	12.9
FE 2164 (C01)	0.99367	102	80	22.5
FE 2172 (B01)	0.98918	153	143	6.9

Table 2.2: Comparison of MCNP results with experimental observations.

2.2.3   Flux Mapping Experiment

In the previous two experiments, the model is validated by calculating the K_{eff} parameter which describes the global (avergae) behaviour of the reactor core. While the complete validation of the model needs its confirmation at both, global and the local levels. In spite of above two verifications, its further assessment requires the analysis of some local

parameter. Therefore, to raise the further level of validity, another experiment is taken from one of the Master Thesis performed to measure the radial and axial flux densities at selected positions in the core [4]. This experiment was performed in 1963-64. The core configuration of this experiment has been shown in Figure 2.4 where the green "ZBR" represents the CIR while 16 positions are marked with small alphabets (a, e, h, k, n, b, c, d, g, j, m, p, f, i, l, and o) and indicate the small irradiation channels (each with diameter of 8 mm) along the radius of the core.

The radial and axial information of the neutron flux density in the reactor core is essential for the effective utilization of the research reactor. The neutron flux density distributions at various irradiation positions (a, e, h, k, n, b, c, g, j, m, p, f, i, l, and o) and the water filled CIR of the TRIGA core are investigated using the gold foil activation measurement technique. These measurements are performed at mid plane of the core in radial direction while at each 5 cm along the CIR in axial direction [4].

The MCNP computer program also provides seven standard tallies types for the out put [13]. These tallies provide the results per "starting" particle except in KCODE criticality problems, which are normalized to one fission neutron. To convert these tally results into real physical parameter (neutron flux density, reaction rate, fission density etc.), one needs to normalize the MCNP results to some experimental value. This model calculates the multiplication factor by using KCODE card. It is important to note that all the standard MCNP tallies need criticality calculations (KCODE card) when they are applied.

Radial Flux density in the Core

In addition to seven standard tallies, the FMESH tally is the latest edition which covers three dimentional regions of space independent of the problem geometry. In this neutronics study, the MCNP model applies the superimposed mesh tally card, FMESHn, to calculate the radial flux density distribution in the core. With this capability, MCNP estimates the particle flux density (particle/cm^2), averaged over a mesh cell. The tally multiplier card

together with mesh tally can be applied to scale the results to appropriate units of flux density i.e. particle/cm^2.s. In these calculations, the MCNP results are normalized to the measured flux density at the axial centre point of the CIR. The MCNP, mesh tally plots for radial flux density distribution is shown in Figure 2.5.
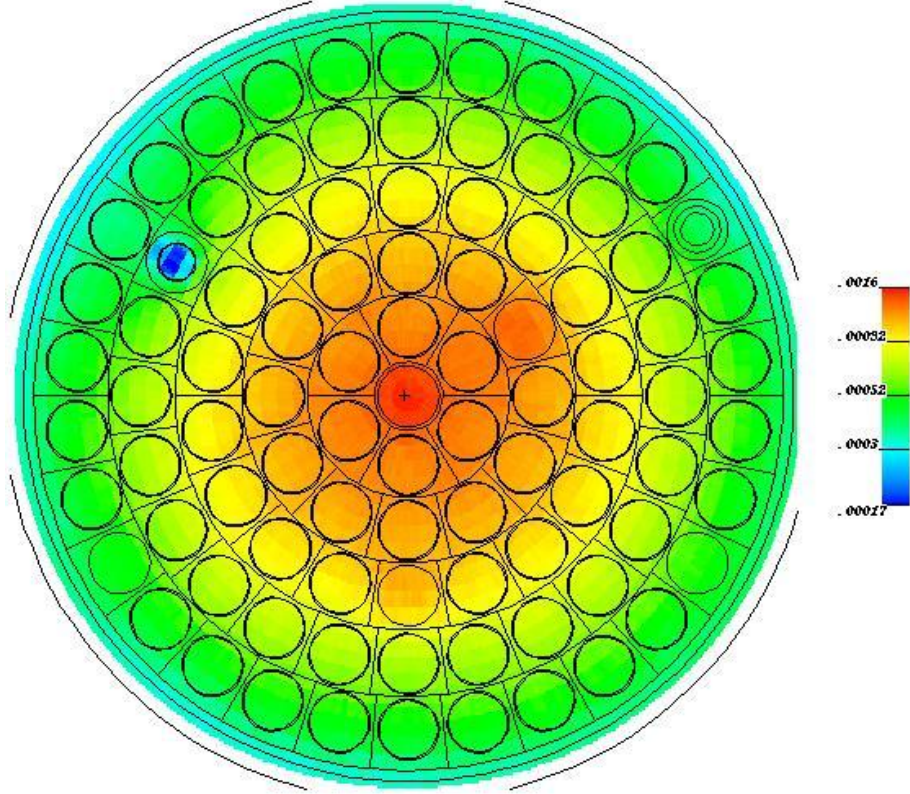
Figure 2.5: The mesh tally plot for radial thermal flux density in the reactor core.

Figure 2.6 presents the comparison of experimental and MCNP calculated radial thermal flux density distribution in the core. In Figure 2.6, the radial flux denisty is highest at the center and decreases radially. The MCNP predicted values are symmetrical to experimental results except the at ends of the core. The calculated results underestimates the experimental results inside the core while overestimates the measured values close to the reflector. These deviations are discussed in next section.
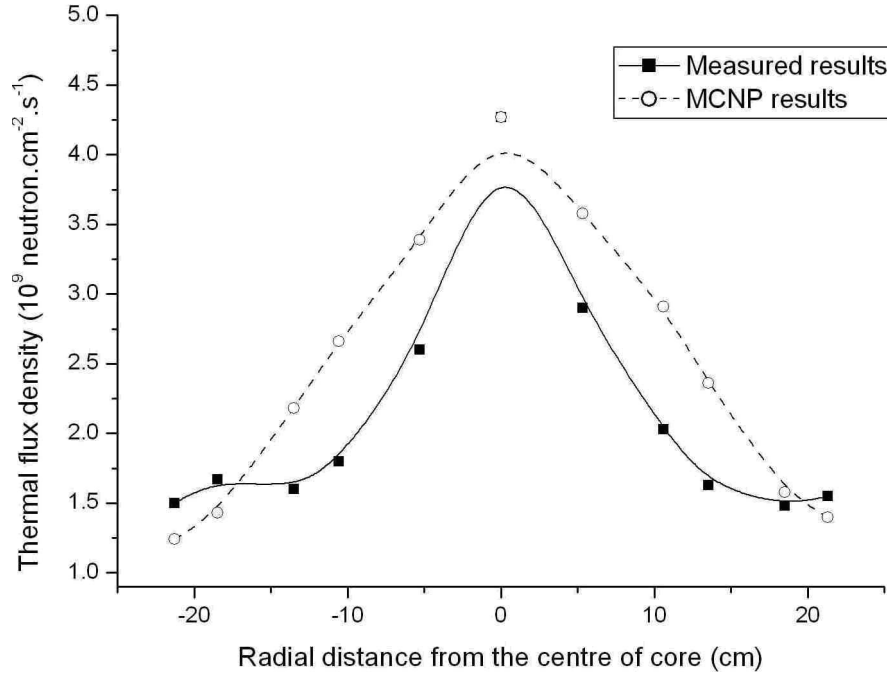
Figure 2.6: The theoretical and experimental the radial flux density distribution in the core.

Axial Flux density in the CIR

The axial flux density in the CIR of the reactor core was measured in the flux density mapping experiment using same gold foil activation method. About ten gold foils are installed at each 5 cm along the CIR. These foils are irradiated at a thermal power of 100 Watts for 1.05 hours [4]. For further validation of the model, the axial flux density in the CIR is calculated for each centimeter of axial length using the FMESH tally capability of MCNP package. The MCNP tally plot and its comparison of the axial flux density with measurements are shown in Figure 2.7. The comparison looks symmetrical about its peak. The calculations and measurements agree that the flux density is maximum at the center and decreases axially following the cosine shape.
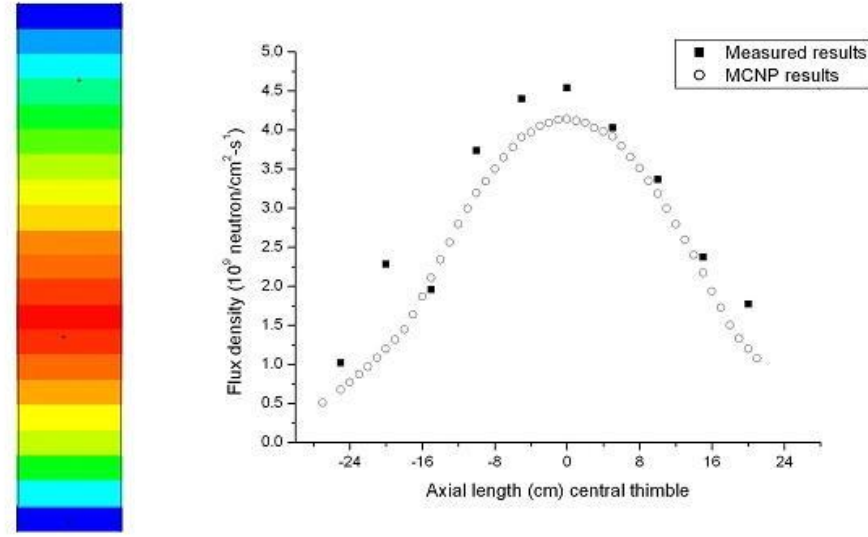
Figure 2.7: MCNP mesh tally plot (left) and its axial thermal flux density comparison (right).

2.3 Discussion of Results

The differenes between the simulated and experimental results for all three experiments are discussed in this section. The developed MCNP model makes some geometrical and material assumptions for example employing average material composition for each FE. These assumptions may become the common reason of deviations between the calculations and measurements. In the following, the results are analyzed separately for each experiment.

2.3.1   The MCNP Model Assumptions

Before analyzing the theoratical results based on historical experiments, this section briefly describes the geometrical and material uncertainities assumed in the model. To develop this model, the geometrical and material informations have been collected from various reliable documents, for example different TRIGA users, TRIGA manual [6], shipping documents [7] and emails from General Atomics [19]. From the shipment documents, there are slight variations in the fuel meat for each FE. Therefore, to keep the model consistent, the average

value (mass and length) of the fuel meat is used for all FE(s). Moreover, the top and bottom aluminium fittings of the FE are simplified to one geometry in the model instead of the actual complicated geometry. That is the geometry of the fittings are considered exactly as cylindrical and are shown in Figure 2.2.

The inventory of the fuel material is slightly different for each FE. The model uses the average value of each component of the fuel material (U-238, U-235, U-236 etc). The Hydrogen to Zirconium (H/Zr) ratio used in the fuel meat is very sensitive to reactivity changes. In fact, this ratio is slightly different in each FE while the model employs the average value of H/Zr ratio to all FE(s).

2.3.2   The First Criticality Experiment

The Table 2.1 compares the calculations and measurements of the first critical experiment. The theoretical and experimental results agree that the core is in just subcritical state with core loading of 56 FE(s). Also both results confirm the state of initial criticality on loading of 57th FE into the core. On addition of 57th element, the core reactivity was measured 15.7 cents while model calculates it as 25.0 cents. As the reactivity of the whole core is a global parameter therefore the difference of 9.3 cents for whole core is acceptable variation keeping in view the possible source of errors in cross sections and reaction rates.

It has been mentioned that the model employs the average value of fuel inventory. The deviations between actual fuel mass and its average value in different positions of the core may contribute in the uncertainty of these results. Despite the efforts were focussed on collecting the accurate geometrical and material data of the fuel, the very small uncertainty either in the dimensions or material composition of the fuel may play role in these deviations.

2.3.3   The Reactivity Worth Distribution Experiment

The Table 2.2 demonstrates the experimental and calculated values of reactivity worth distribution experiment. As mentioned, this experiment was performed to measure the reactivity of four FE(s) in different ring positions and one graphite element in F01 position. The deviations between calculations and experimental observation may be due to the model assumptions.

The theoratical and experimental results in the Table 2.2 agree that the closer an insertion of reactivity to the center of a core, the larger is the effect. The proportion is also influenced by the surrounding environment near the inserted position. However, the discrepancy between the calculated values and the experimental data gradually increased as the insertion position is closer to the centre of core. It may be due to the geometry of the reactor core lattice. In such a lattice, generally, a FE worth for a well-thermalized, small, compact and uniform core is approximately proportional to the square of the thermal neutron flux density, integrated over the entire fissile volume of the FE [21]. Therefore the fuel in the inner ring is always more reactive than in the outer rings. This behavior can also be observed in the flux density profile of the reactor core.

2.3.4   The Radial and Axial Flux Mapping Experiment

Figure 2.5 and 2.8 show the simulated thermal flux density distribution in the mid plane of the core. This flux density profile looks symmetrical in the core i.e. it has a maximum in the center and decreases in the radial direction. Figure 2.8 clearly presents the flux density depression due to the regulating and safety-transient control rod positions and also reflects the shadow effects of the shim control rod. The simulated radial themal flux density distribution exhibits the fact that the thermal flux density is maxium in the CIR and decreases radially.

A comparison of the simulated results with the experimental observations of the flux density
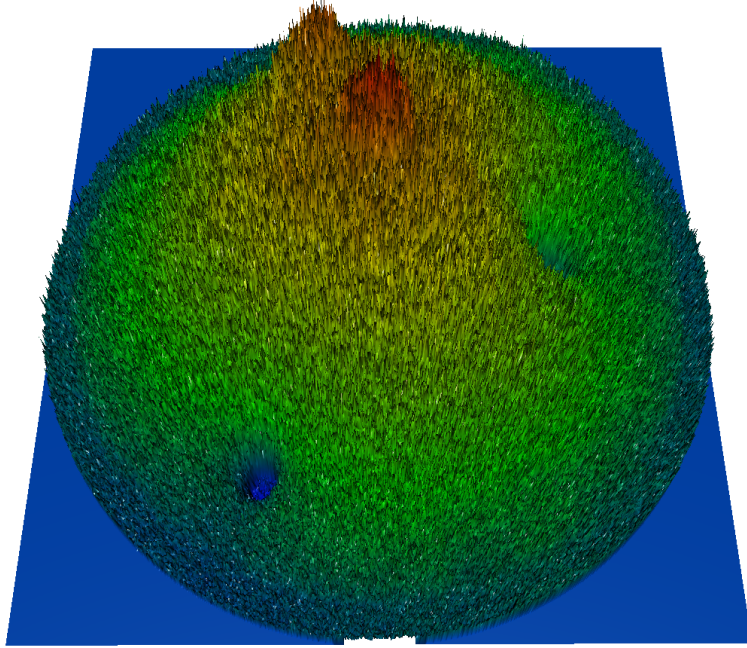
Figure 2.8: The thermal fux density distribution in the mid-plane of the reactor core.

at selected radial and axial positions of the reactor core is shown in Figure 2.6 and 2.7 respectively. It is observed that the MCNP model captures the experimental behavior in the core as shown in Figure 2.6. MCNP thermal flux density, on both sides of the core, represents the experimental behavior i.e. the flux density is maximum in the CIR and decreases radially. Though the trends are similar but MCNP overestimates the flux density in the core and underestimates the flux density values at points very close to graphite reflector. It is obvious that the MCNP model estimates the thermal flux density inside the core employing fresh fuel while actual fuel in the experiment is burned fuel. Fresh fuel is more reactive than the burned fuel, therefore, probably, the MCNP code results overestimate the experimental values.

The slight peaks at the edges of the core (as seen Figure 2.6), are due to the annular graphite reflector. The difference between calculations and measurements at the edges may be because of the density difference of the graphite reflector. The actual density of the reflector is still not confirmed. The model uses 1.6 g/cm^3 as graphite density while the actual density may be slightly higher than 1.6 g/cm^3.

Chapter 3

BURN UP CALCULATION AND EXPERI-
MENTAL VALIDATION

The TRIGA Mark II reactor core has been operating for the last 48 years. The previous chapter described the development of the MCNP model and its validation. So for this model is employed with the fresh fuel. With elapsed time to keep the reactor operating, the additional three different types of FE(s) were added to the reactor core since its initial criticality. Starting with 57 FE(s), the current core has 83 FE(s) of three different types. To analyze the current core, the already developed model needs some important modifications. One of these modifications is to calculate and incorporate the material composition of burned fuel in the current core. Burn up is one of the key factors to determine the isotopic composition of spent or burned fuel. This chapter describes the fuel depletion equation, its solution, the development of the ORIGEN2 model to determine the burn up and its relevant material composition. To confirm these reactor physics calculations, the gamma spectroscopy of the Cesium (Cs-137) isotope of six SFE(s) is performed and explained in this chapter. Applying the confirmed ORIGEN2 model, the burn up and its relevant material composition of all 83 FE(s) are calculated to apply the already developed MCNP model of the TRIGA core.

3.1 Fuel Depletion Equation

During the reactor operation, the nuclear fuel undergoes long-term changes in its properties over its lifetime. These changes are determined by the changes in the composition due to fuel burn up and the manner in which these are compensated. The nuclear power economics is strongly affected by the efficiency of fuel utilization to produce power, which in turn is affected by these long-term reactivity changes associated with fuel burn up [15].

During the irradiation, the fuel nuclei are transmuted by neutron capture, fission and subsequent decay. The fission of the fissile nucleus produces two intermediate fission products. The fission products tend to be neutron-rich and subsequently decay by beta or neutron emission (usually accompanied by gamma emission) and undergo neutron capture to be transmuted into a heavier isotope, which itself undergoes radioactive decay and neutron transmutation. The fissile nuclei also undergo neutron transmutation via radiative capture followed by decay or further transmutation. The general fuel depletion equation satisfied by a fission product species j is

$$\frac{dn_j}{dt} = \gamma_j \Sigma_f \Phi + \sum (\lambda^{i \to j} + \sigma^{i \to j} \Phi) n_i - (\lambda^j + \sigma_a^j \Phi) n_j \tag{3.1}$$

Where Φ is neutron flux density, γ_j is the fraction of fission events that produces a fission product species j, Σ_f is macroscopic fission cross section, $\lambda^{i \to j}$ is the decay rate of ith-isotope to produce jth-isotope (α, β, neutron, etc, decay). And $\sigma^{i \to j}$ is the transmutation cross section for the production of isotope j by neutron capture in isotope i. The increase in total fission product plus their decay products is give as

$$\frac{dn_{fp}}{dt} = \sum_j \frac{dn_j}{dt} = \sum \gamma_j \sigma_f \Phi \tag{3.2}$$

The solution of this depletion equation needs an integration over the depletion time from t_i to t_{i+1}) and the given flux density. Assuming the flux density is constant in interval

$t_i < t < t_{i+1}$, the depletion equation can be written in the matrix notation as

$$\frac{dN(t)}{dt} = A(\Phi(t_i))N(t) + F(\Phi(t_i)) \qquad t_i < t < t_{i+1} \tag{3.3}$$

The general solution of this set of equations is of the form

$$N(t_{i+1}) = exp\left[A(t_i)\Delta t\right] N(t_i) + A^{-1}(t_i)\left\{exp\left[A(t_i)\Delta t\right] - 1\right\} F(t_i) \tag{3.4}$$

The accuracy of the solution depend on depletion time (Δt_{burn}) being chosen so that $(\lambda^i + \sigma_i^a)\Delta t_{burn} << 1$ for all isotopes. Therefore it is economical to reformulate the depletion equations to eliminate short lived isotopes that do not change the overall results. There exist number of computer codes that solve the production-destruction equations for input neutron flux density [15]. The ORIGEN2 is such a neutronics computer code that provides the solution of these equations. This solution incorporates the build-up of radio nuclides and their decay during irradiation.

3.2 Burn up

The burn up indicates the useful lifetime of the fuel in the reactor core. It is defined as the amount of energy (MWd or kWh) extracted per unit mass of fuel. In other words, reactor power P (assumed constant) times the irradiation time T equals the energy generated in the reactor in that period. That is

$$burnup = \frac{P \times T}{M} \tag{3.5}$$

Where M is mass of fuel only, excluding the oxide and other structural material in the fuel. Note that the burn up can really describe the state of a single FE or even a fuel rod, if the actual T of that element is taken exactly $[http://www.ricin.com/nuke/bg/burnup.html]$. The actual burn up of the fuel in a reactor is determined by the physical and mechanical changes resulting from irradiation and high temperature in the fuel and the cladding, and

also by the decrease in reactivity due to the decrease in fissile material and the accumulation of fission product poisons [22].

By definition, consequently, the burn up is directly related to the fission reaction rate in a given FE. Ideally, burn up can be assessed by measuring the amount of fissile material left in the fuel. However, due to limitations of existing passive non-destructive methods, it is difficult to measure directly the remaining fissile material in irradiated fuel. This is mainly because of the existence of very strong gamma lines in the irradiated fuel that will overwhelm the direct signatures from the fissile material. Therefore, passive burn up measurements are conducted indirectly using the spontaneous emission of gamma by the fission products that result upon irradiation of the fuel.

In this work, six 102 type SFE(s) are selected for theoretical and experimental studies. The ORIGEN2 reactor code is selected for theoretical studies while gamma spectroscopy of the fission product gamma line is employed for experimental studies. This experimental approach utilizes gamma ray lines, which are emitted by radio-nuclides that are either directly produced by the fission reaction (primary fission products) as in the case of Cs-137 $T_{1/2}$ = 30.23 years) or by radio-nuclides that are produced upon the capture of a neutron by a primary fission product. Examples of that are Cs-134 ($T_{1/2}$ =2.06 years and Eu-154 ($T_{1/2}$ =8.6 years), which are produced in negligible amounts by U-235 fission.

The SFE(s) used in this work have different irradiation histories and removed from the core with different irradiation times. Most of them were removed before the year of 2000 as in table 3.1. Therefore, because of long cooling/decay time, most of the produced Cs-134 had been decayed. And by the measurements, there is no significant existence Cs-134 in the FE(s) due to its shorter half life of 2.06 years. Therefore, the Cesium isotope Cs-137 is considered as burn up indicator for typical TRIGA Mark II fuel.

3.2.1   Burn up Calculations of TRIGA Mark II Fuel

During the past reactor operation, some 102-type FE(s) were removed from the core and stored into the fuel storage rack for radioactive cooling. The six of these SFE(S) were chosen for their burn up study. The identification number (ID no.) of these SPE(S) are 2156, 2196, 2077, 2124, 2184 and 2176. Because of the versatile nature and safe experimental capabilities of the reactor, all of these selected FE(s) were reshuffled during their irradiation history except FE no. 2196 which was placed in one fixed position for whole irradiation period [8]. During the operation history, these SFE(S) were even taken out from the core for different durations and reloaded again to the core as described in Table 3.1. A schematic and simplified diagram of 102-type FE is shown in Figure 3.1.
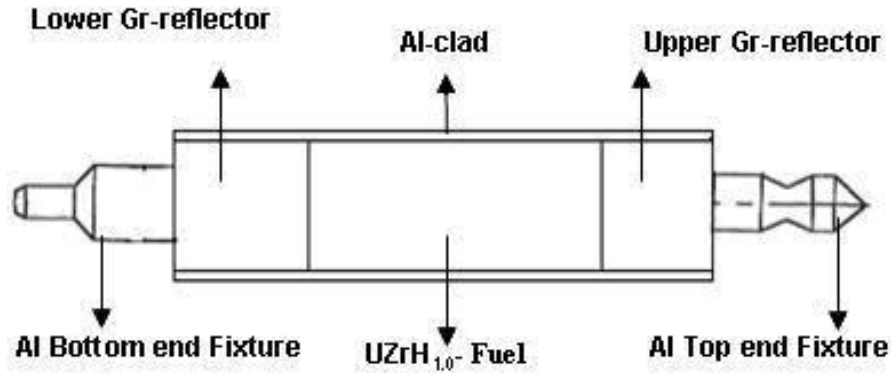
Figure 3.1: Schematic diagram of Aluminium clad (102-type) FE.

Because of the long cooling (decay) time in the storage, most of the SPE(s) have almost decayed their Cs-134 concentration. Therefore, this work concentrates only to determine the burnup by measuring the Cs-137 concentration. The TRIGA Mark II of Vienna operates at 250 kW, at this very low burn up, the Cs-137 concentration is proportional to the burn up at this low fuel consumption [22]. Therefore the burn up calculations are verified through the spectroscopy of Cs-137. Being a proved and widely used technique, the gamma scanning of six selected SFE(S) is performed. The schemes of their loading, reshuffling and removal from the core are described in the Table 3.1 [8].

Fuel ID no.	Action	Date	Core position
2124	loaded to the core	09-03-1962	D15
	Removed from the core	06-08-1985	Out from core
	Reloaded to the core	17-10-1985	D15
	Removed from the core	29-11-1985	Out from core
	Reloaded to the core	21-11-1991	F06
	removed from the core	04-03-1995	Out from the core
2176	Loaded to the core	09-03-1962	D02
	Removed from the core	07-08-1985	Out of the core
	Reloaded to the core	11-10-1985	D02
	Removed from the core	09-02-1999	Out of the core
	Reloaded to the core	04-12-2000	F25
	Discharged from core	08-02-2001	Out of the core
2184	Loaded to the core	09-03-1962	E20
	Shuffled in the core	25-04-1974	C11
	Removed from the core	06-08-1985	Out of the core
	Reloaded to the core	12-10-1985	D16
	Removed from core	08-02-1997	Out of the core
2156	Loaded to the core	09-03-1962	C07
	Shuffled in the core	25-05-1974	E11
	Removed from the core	09-01-1982	Out of the core
	Reloaded to the core	11-06-1987	F01
	Removed from core	12-06-1987	Out of the core
2077	Loaded to the core	09-03-1962	E14
	Removed from the core	06-09-1968	Out of the core
	Reloaded to the core	08-05-1973	B03
	Shuffled in the core	24-05-1974	E09
	Discharged from core	04-08-1979	Out of the core
2196	loaded to the core	09-03-1962	B04
	Removed from the core	08-08-1970	Out of the core

Table 3.1: Loading and reshuffling schemes of the selected SFE(S) in the core.

The main efforts of this chapter are

- calculation of the average burn up and its relative Cs-137 isotopic composition employing ORIGEN2

- its validation by the method of high-resolution gamma spectroscopy

- calculation of the axial burn up re-redistribution implying axial gamma spectrometric measurements.

The log books describe every reactor event during the operational history. These events include the experiments carried out, reactor start up, shutdown records and some unusual events etc. These log books are well maintained and managed at Atominstitute on yearly basis. For each year, the reactor power (MW) and its relative burn up in MWd is documented on a daily basis. The operation length (days) and its corresponding burn up (MWd) are calculated for the whole operation history of the reactor. Using the total operation length and its MWd, the Full Operating Length (FOL) in days and average power at FOL in MW are calculated for the input of the ORIGEN2 reactor code.

For example, the FE no. 2196 was loaded to the core on 07-03-1962 in the position B04 at a reactor power of 100 kW. This FE remained at the same position and same power until 27-07-1964. On 28th of July 1964, the reactor power was raised to 250 kW keeping the same position of the element. This element was removed from the core on 07-08-1970 and placed into the storage tank. The log books provide the burn up of 4.1322 MWd and 69.504 MWd from reactor operation 07-03-1962 to 27-07-1964, and from 28-07-1964 to 07-08-1970 respectively. The Table 3.2 presents the details of the irradiation history calculation from the log book for the ORIGEN2 input.

From	To	FOL days	MWd	FPD	Power (MW)	FLP(MW)
07-03-1962	27-07-1964	872	4.13	41.3	0.0014516	6.879x 10^{-5}
28-07-1964	07-08-1970	2202	69.504	278.0	0.003629	0.0004582
08-08-1970	06-11-2008	13971				

Table 3.2: Irradiation history of fuel ID no. 2196 from log books.

The Table 3.2 introduces the terms such as Full Power Days (FPD), Full Operation Length (FOL) and Full Length Power (FLP). From the Table 3.2, the total number of days from 07-03-1962 to 27-07-1964 become 872 and are called FOL. During this FOL , the reactor produced the energy of 4.13 MWd. If the reactor was operated at 100 kW continuously, it would produce energy 4.12 MWd in 41.2 days. These 41.2 are called FPD. The reactor power for FOL is called FLP. The Table 3.2 presents the irradiation power of FE no. 2196.

The Full Power Days (FPD) were calculated from MWd [8]. The power (MW) from the log book is distributed in the core by using power factors described in Table 3.4. The FLP is calculated by using simple proportional relation. The total weighted average power of both operations becomes 0.00029533 MW for the whole duration of 3074 days. This whole operation of 3074 days was divided into steps with each step length of 300 days. These irradiation steps with weight average power were applied as input to the ORIGEN2 Model. Similarly the irradiation history in terms of FOL in days and average power (MW) at FOL, of each SFE, is shown in Figure 3.2.

This series of calculation are carried out for the same type of FE(s) i.e. 102 type fuel. The only difference is their individual irradiation histories and resulting burn up. The accuracy of the ORIGEN2 burn up model for each FE depends on its location in the core, number of reshuffling and on the precision of operational records from log books. Keeping all these factors in view, the FE 2196 is identified with the simplest irradiation history because it was placed and kept only in one position and finally removed from the core without any reshuffling. The same element was also used as reference element during burn up calculations by the reactivity method [23].

The Cs-137 activity of each burned FE is calculated using ORIGEN2 under their given irradiation conditions. These FE(s) were measured through gamma spectroscopy at the scale of one centimeter. The experimental results were found close to the calculated values, confirming the ORIGEN2 model for burn up and isotopic computation of TRIGA burned fuel.
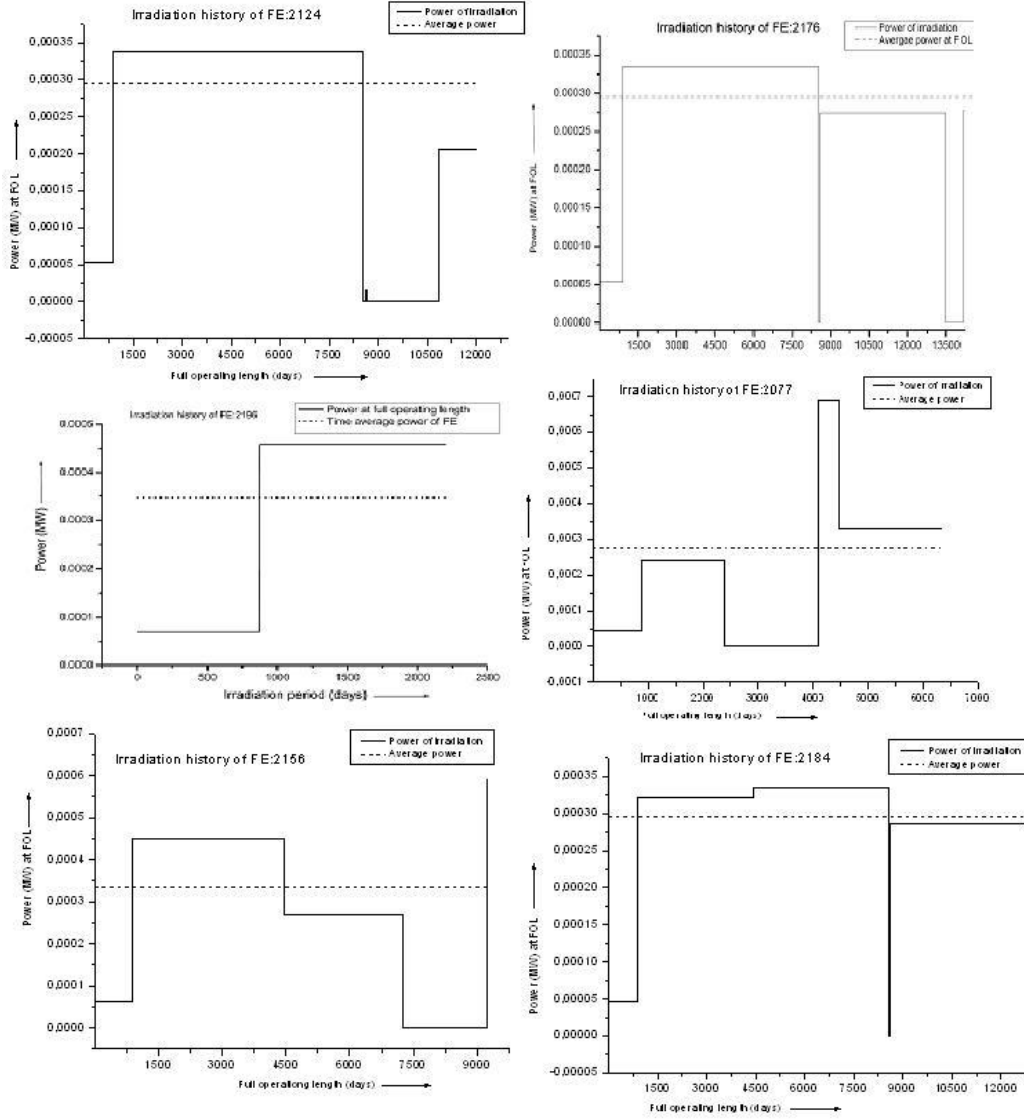
Figure 3.2: Irradiation history of each SPE at full operating length (FOL).

3.3 Development of the ORIGEN2 Model

The reactor physics code ORIGEN2 is chosen for activity and burn up calculations, which can simulate the build up and decay of nuclides during irradiation. ORIGEN2 uses a matrix exponential method to solve a large system of coupled, linear, first-order ordinary differential equations with constant coefficients [16]. The above mentioned SFE(S) were calculated for their material composition and burn up using ORIGEN2. As all selected

FE(s) have different irradiation histories therefore each FE is calculated independently. Based on Full Operation Length (FOL), the irradiation history of each FE is divided into appropriate number of equal steps. The step length of each irradiation interval is set to 300 days. A weighted average power (MW) is applied to all irradiation steps. The irradiation power history of each element is shown in Figure 3.2.

The ORIGEN2 model for TRIGA FE is developed to calculate the average burn up and its relevant material isotopic composition. This model needs the following three main inputs for these calculations. The accuracy of these calculations depends on the following inputs of the model.

1. Library selection

2. Fuel irradiation history

3. Material inventory

The ORIGEN2 neutronics code is not equipped with cross section libraries for TRIGA reactors. The fission cross section and fission product yield libraries for TRIGA fuel either has not been developed or it is not known if any one existed. Therefore on the basis of previous published work on this subject [24], the PWR library is found appropriate for TRIGA reactors and applied to this ORIGEN2 model. The 102-type TRIGA FE(s) were modeled using available PWR cross-section and fission product yield libraries.

The fuel irradiation part of ORIGEN2 model has a key importance in the calculation. The quality of results depends on the accuracy of the irradiation history provided to the model. The irradiation history of each FE in terms of FOL and power (MW) is taken from reactor operation log books.

The shipment documents [7] of the reactor fuel provide the material inventory of each FE. Using the shipment documents and email correspondence with General Atomics [19], the

material composition of each component of fuel is applied to the model. The material inventories for selected six SFE(S) , used in the model, are given in Table 3.3.

Material	FE: 2124	FE: 2176	FE: 2176	FE: 2176	FE: 2176	FE: 2176
U-235	35.99	36.34	35.65	36.61	35.72	36.93
U-238	145.7	147.09	144.3	148.2	144.61	149.51
U-234	0.37	0.37	0.37	0.37	0.37	0.37
U-236	0.37	0.37	0.37	0.37	0.37	0.37
Hydrogen	22.46	22.46	22.46	22.46	22.46	22.46
Zirconium	2038.52	2038.52	2038.52	2038.52	2038.52	2038.52

Table 3.3: TRIGA Al-clad fuel composition (in grams) for ORIGEN2 calculations.

3.3.1   Irradiation Model

All described SFE(S) are calculated separately because of their different individual irradiation histories. These elements were loaded to the core on the same date, March 9, 1962 but in different ring positions. The history of their loading, reshuffling and discharge from the core is described in the Table 3.1. Using the total irradiation length and Megawatt hour (MWh) from the log books, the full operation length FOL (in days) is calculated for each SPE. Using the irradiation power of each FE at specific location and FOL, the weighted average power of each SPE at FOL is calculated and applied to ORIGEN2 model. The irradiation power is taken from log books and distributed using power factors described in Table 3.4 [25]. By incorporating the decay time of each SFE till the date of measurement, the burn up and the radioactivity of each SPE is calculated.

$$P_{Irr} = \frac{Total \quad Thermal \quad Power}{Number \quad of \quad FE(s)} \times P_f \tag{3.6}$$

Where the total thermal power of the reactor is 250 kW and P_f is the power factor with different values for each ring. The ring power factors for all six rings (A to F) of the core are given in Table 3.4

Core ring	A	B	C	D	E	F
P_f	1	0.9	0.8	0.7	0.6	0.5

Table 3.4: Power factors of TRIGA Mark II reactor core.

3.4 Gamma Spectroscopy

Generally, the burn up of nuclear reactor fuel is estimated computationally using reactor physics computer programs. However, to validate and benchmark the computational methods and their results, fuel assay measurements are performed off-line (i.e. after the reactor is shut down), and, in most cases, the fuel is removed from the core and allowed to cool for a period of time that may extend to years. The Post Irradiation Examination (PIE) which needs expensive fuel transportation, conventional hot-cells to study and final disposal of destroyed rods etc. are usually avoided. Therefore Non-Destructive Testing (NDT) methods are preferred.

The burn up and its relevant nuclide composition of an irradiated fuel are usually needed for reactor fuel management, criticality safety, when dealing with SPE and validation of reactor physics calculations. Among several NDT techniques, the gamma spectroscopy of irradiated fuel is considered as more advantageous one because of giving an extensive information and the simplicity of measurement. This greatly helps the tasks of acquiring the gamma-ray spectra, isolating the full energy peaks that represent the radio-nuclides of interest, and determining the peak areas that are converted to activities and related to burn up. The past studies prove that methods based on activities of certain long-lived fission products are the most popular ones [26]. Obviously, in case of the TRIGA fuel spectroscopy, the on-line measurements may present several challenges due to the high activity of the fuel. The distinctive fuel inspection unit, with sufficient lead shielding combat these challenge of high activity. This system is unique, not because of sufficient lead shielding, but due the capability of scanning each millimeter of fuel with high precision and accuracy. This system minimizes the high activity effects at the working station.

65

The gamma spectroscopic measurements are performed in the reactor hall of Atominstitute but outside the reactor tank. More than adequate shielding is provided to the system by the high density fuel transfer cask and fixtures of the fuel inspection unit. About 2 to 3 μSv per hour dose rate is recorded at the contact surface of the cask and working station. The experimental setup which consists of the fuel transfer cask, an inspection unit, the beam collimator and coaxial High Purity Germanium p-type detector (HPGe), is shown in the Figure 3.3 and 3.4.
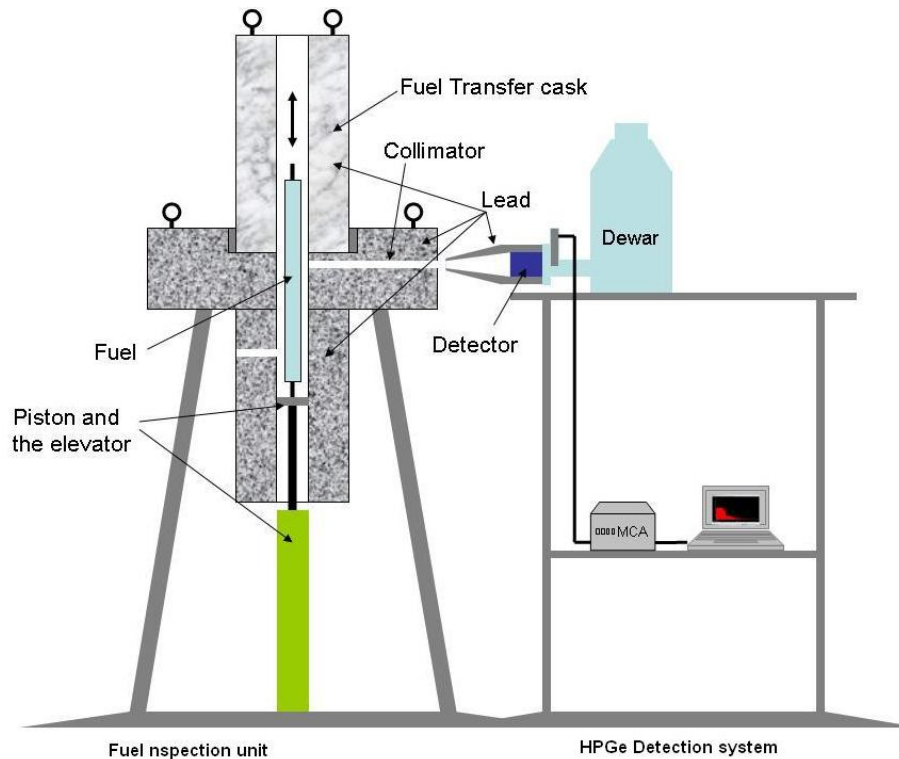
Figure 3.3: The experimental setup developed at ATI.

The FE to be measured is mounted to the fuel inspection unit through the fuel transfer cask where it can be moved vertically with an adjustable speed. The transfer of the fuel cask to the fuel inspection unit is shown in Figure 3.5. Although this fuel elevator system has ability to scan each millimetre of the SPE accurately in the axial direction however a one centimetre scale us selected for each measurement conveniently. To avoid any overloading of gamma spectrometer, the collimator with 5 mm diameter is used and the distance between
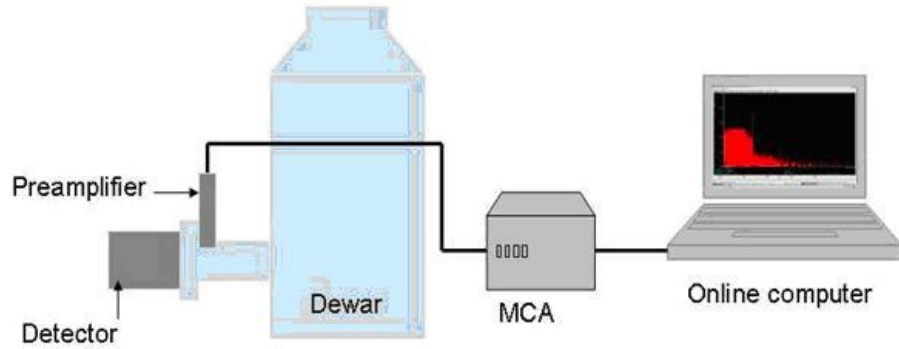
Figure 3.4: The schematic diagram of the experimental setup for gamma spectroscopy.

detector and fuel rod is kept about 10 cm. To minimize the statistical and counting errors, the time for each measurement is selected as 300 seconds. The dead time of the detector is recorded up to 16 %. The axial position of the rod to be scanned is indicated by a digital monitor fixed on the fuel inspection unit.

Figure 3.5: Fuel transfer to the fuel inspection unit at Atominstitute.

The signal from the instrument (detector) is transferred to the on-line computer with a

calibrated gamma spectroscopic software. Using suitable fast electronics, the 300 seconds were set to record the gamma ray spectrum for each centimetre and saved this spectrum on removable hard disk for further detailed analysis i.e. identification of Cs-137 peak and corresponding peak area etc. Figure 3.6 illustrates one example of the typical plenum gamma ray spectrum with Cs-137 peaks. The counting errors were controlled up to 1.0%
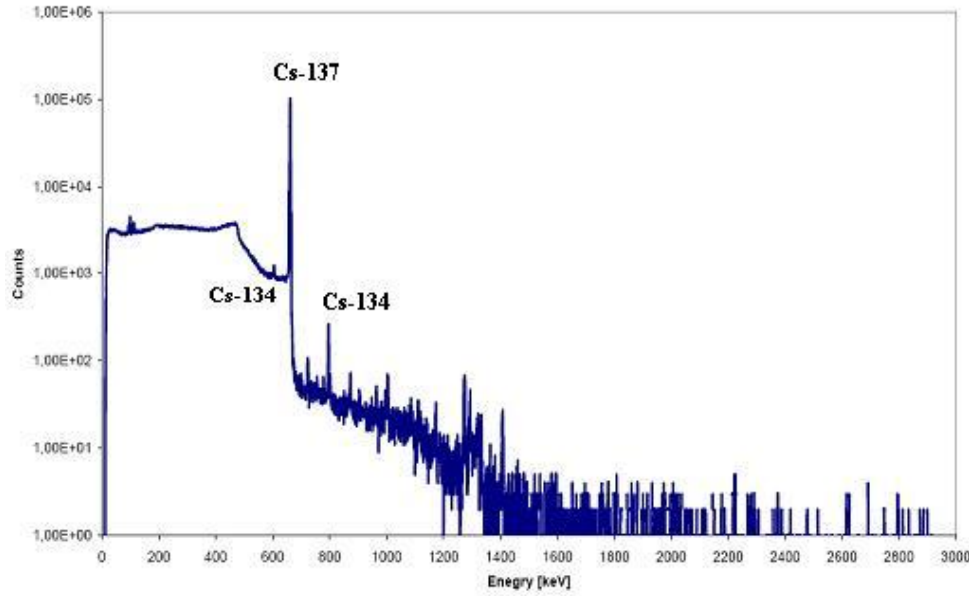
Figure 3.6: The typical gamma spectrum of TRIGA FE.

(in one standard deviation). The counting dead times were in generally controlled to be $\leq 16\%$ and were corrected during the counting period. The spectrum analysis provides the counts per second of Cs-137 (net peak area) which gives experimental activity using following relation [26]

$$A_{exp} = \frac{C}{\epsilon \times \gamma \times f} \tag{3.7}$$

Where

C = Photo peak area (cps)

ϵ = Absolute efficieny

γ = Gamma ray branching ratio

f = Self shielding factor

3.4.1 Self Shielding Factor

The self-shielding factor "f" in equation 3.7 is incorporated to make the correction for that fraction of gamma-rays, which are emitted from fission products (FPs), but not detected due to fuel self absorption. Under the given geometrical conditions, this factor is calculated according to the fission product distribution and the gamma- ray attenuation coefficient of the fuel rod. The Monte Carlo shielding code MCNP5 [13] is applied to calculate this factor. For this purpose, a fuel scanning machine and a fresh Al-clad FE is simulated by MCNP5 as shown in Figure 6. In the simulation, homogeneous distribution of Cs-137 is applied. The two calculations were performed, one using flux-tally (F2) with Cs-137 distribution and second applying the same F2 tally but without Cs-137 inside the FE. The MCNP model for these both cases is shown in Figure 3.7. The ratio of F2-tally results for both cases provides the value of self shielding factor "f". In our case, this factor is determined as 15 % of total Cs-137 emission.
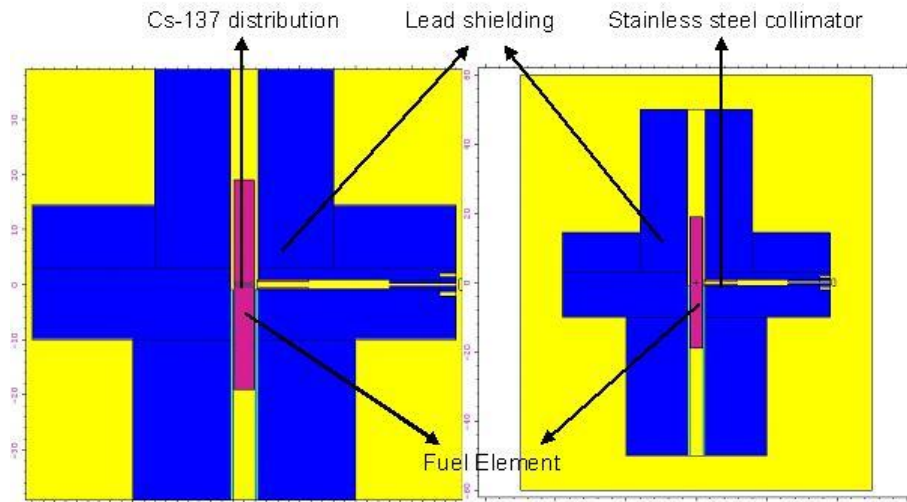
Figure 3.7: The MCNP model for self shielding factor "f" calculation.

3.5   Results and Discussions

The gamma spectroscopic results of Cs-137 along the length of FE no. 2196 are shown in Figure 3.8. The Cs-137 distribution along the FE looks symmetrical about the center i.e. Cs-137 reaches a maximum at the center while it decreases along both sides symmetrically. At both ends of the fuel meat, there are two slight peaks of Cs-137. As it is described that each FE has two axial graphite reflectors at both ends of the fuel meat (Figure 3.1) therefore the obvious reason of these peaks is due to the presence of upper and lower graphite reflector of the FE.
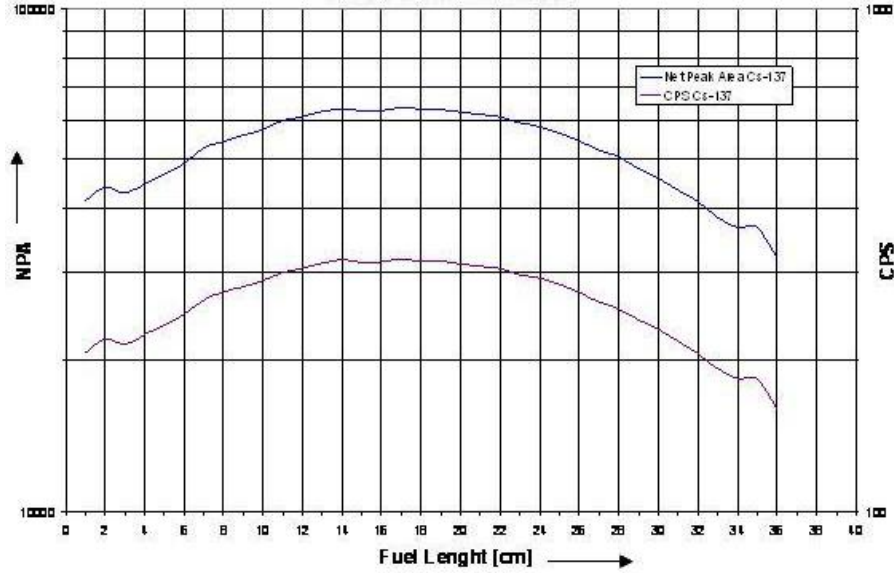
Figure 3.8: The axial distribution of Cs-137 in FE no. 2196.

Table 3.5 compares the calculated and measured results of the average Cs-137 activity (Bq) per centimeter for each SFE. The percent difference between the theoretical and experimental values varies from 0.82 % to 12.64 % and depends on the irradiation history of the FE.

The graphical comparison of calculations and measurements is given in Figure 3.9. The main possible factors causing the deviations between calculations and measurements are

FE no	burn up (MWh)	Calculated Cs-137/cm (Bq)	Measured Cs-137/cm (Bq)	Percent (%) Difference
2196	25.68	1.35E+09	1.36E+09	0.82
2077	30.92	1.72E+09	1.60E+09	6.87
2156	58.08	3.52E+09	3.60E+09	2.29
2124	25.68	4.59E+09	4.44E+09	3.21
2184	25.68	6.60E+09	7.09E+09	7.49
2176	25.68	7.22E+09	6.31E+09	12.64

Table 3.5: Comparison of ORIGEN2 calculations and spectroscopic measurements.

highlighted below.

- the TRIGA reactor is operating since 1974 with mixed core of three different types of fuels. Most of these FE(s) were reshuffled during their long history therefore the percent deviation between calculations and measurements vary from element to element depending on their individual irradiation histories and different positions in the core [23].

- the basis of the calculation in MWh, were taken from log books since 1962, therefore due to long history, any significant documentation mistake in the log books may contribute to these variations.

- as the PWR libraries of ORIGEN2 are employed, hence the ORIGEN2 model has its own contribution due to cross section uncertainties.

These percent differences between the calculations and measurements of the Cs-137 activity are reasonable and confirm that the corresponding burn up calculations of the selected SFE(S) are reliable.

The spectrometric analysis provides the Cs-137 axial distribution for given FE(s). As is is mentioned that the Cs-137 production and burn up are proportional [22] therefore applying this axial distribution of Cs-137, the relative axial burn up distribution of each measured SPE can be calculated with reasonable accuracy. For example the relative axial burn up
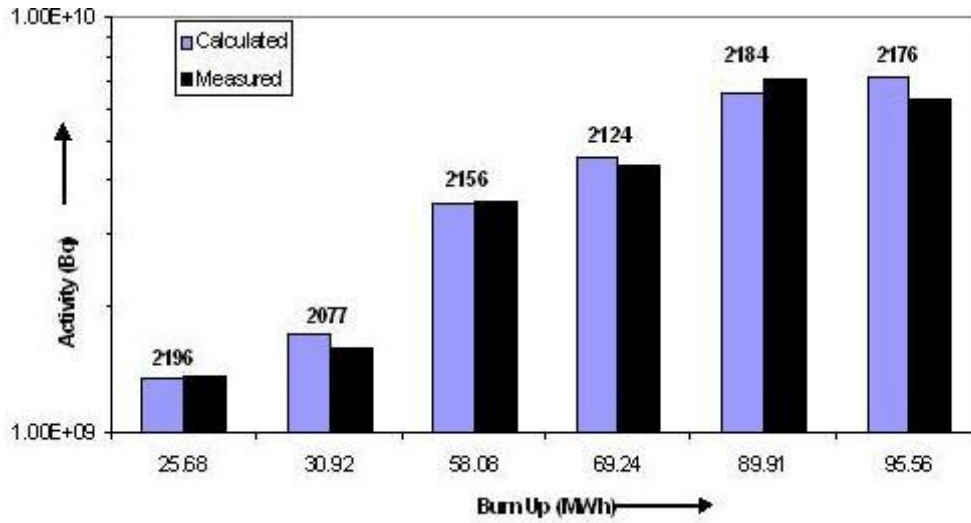
Figure 3.9: Graphical comparison between gamma spectroscopic values and ORIGEN2 results.

profile of SFE no. 2196 is shown in Figure 3.10. Two slight peaks at both ends of the fuel meat are due to the presence of two axial graphite reflectors incorporated in the FE.
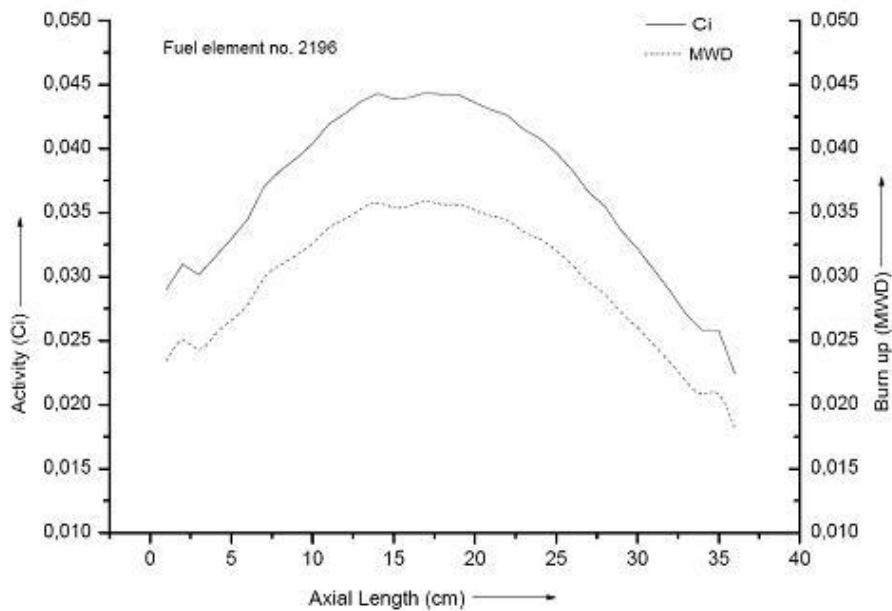
Figure 3.10: The measured Cs-137 and relative axial burn up profile of SFE no. 2196.

Chapter 4

CURRENT CORE MODEL

The confirmed ORIGEN2 model for type 102 fuel is modified for type 104 and FLIP fuel. This chapter presents the ORIGEN2 results of all 83 FE(s) of the present core and incorporates the burned fuel composition into the MCNP model, resulting into the current core model. In this thesis, the current core model refers to the model incorporated with the burned fuel composition at 29th June 2009. For this reason, with the ORIGEN2 burn up results, the 83 FE(s) of the current core are divided into 16 groups with their group burn up values. An average burn up of the group is applied to all FE(s) in that particular group. That is, the FE burn-up value closest to an average value of the group represents that group. The FE representing a particular group is called 'group indicator' of that group. The material composition of all sixteen group indicators approximates the material composition of the core. This approximation is called burn-up group approximation. This approximated material composition is applied to the MCNP model of the current core. The chapter also demonstrates the confirmation of the current core model through some local consistent experiments performed at the ATI. The current core model employs JEFF3.1 cross section library.

4.1   ORIGEN2 Calculations of the Current Core

The burn-up calculations and its confirmation for six selected 102-type SPE(s) have been described in the previous chapter. The current core has three different types of FE(s), therefore its analysis needs the burn-up information of all three types of FE(s). This section presents the burn-up calculations of the remaining two types of FE(s), 104-type and FLIP FE(s). Relying on the developed 102-type SPE ORIGEN2 model, the required modifications are applied to the model for the other two types of fuels. In the first modification, the material inventory of FLIP and 104-types FE are taken from the shipment documents [7] and incorporated into the ORIGEN2 model of the respective fuel types. The average values of the fuel components (in grams) for all three fuel types are described in Table 4.1 and are applied to the ORIGEN2 model for burn up calculations.

Fuel type	U-235	U-238	U-234	U-236	hydrogen	Zirconium	Erbium
102-type	36.13	146.03	0.36	0.36	22.46	2043.6	0
104-type	39.12	192.2	0.38	0.38	35.7	2053.5	0
110 or FLIP	135	59	1.35	1.35	17.57	2015.2	36.52

Table 4.1: Average values (in grams) of the material inventories of all three types of FE(s).

The irradiation part of the model plays an important role in its accuracy. Many FE(s) in the current core are located in the core since its first criticality. Therefore, because of the very long and different irradiation histories of the FE(s), the required information (MWh) are carefully extracted from the log books. The fresh fuel material composition from the Table 4.1 and irradiation history from the log books for each FE are applied to the ORIGEN2 model to calculate the accumulated burn-up and its relevant material composition during the whole fuel history. The burn-up results (MWh) for all FE(s) are calculated and given in Table 4.2. In this Table, the identity numbers (ID no.) of the 102-type FE start with digit '2' and '3', ID nos. of 110 (FLIP) start with '7' and the remaining ID numbers starting with 4, 5, 8, 9, 10 are used for 104-type FE(s).

To reduce the manual extraction of an effective material composition for each FE from

Grp. no.	ID no.	MWd	Grp. no.	ID no.	MWd	Grp. no.	ID no.	MWd
1	9200	0.322539	8	2157	4.33695	9	2074	4.80953
1	10198	0.322539	8	2133	4.33695	9	2130	4.80953
2	10197	0.322539	8	2103	4.33695	9	2151	4.80953
2	10916	0.322539	8	2154	4.33695	9	2155	4.80953
2	10145	0.322539	8	2133	4.33695	9	2160	4.80953
3	10144	0.322539	8	2145	4.33695	9	2171	4.80953
3	10143	0.322539	8	2170	4.33695	9	2175	4.80953
4	8257	0.322539	8	2132	4.33695	9	2181	4.80953
4	10077	0.322539	8	2161	4.33695	9	2075	4.80953
4	10076	0.322539	8	2168	4.33695	9	2109	4.80953
-	-	-	9	2159	4.33695	9	2141	4.80953
5	9591	0.322539	9	2108	4.33695	9	2182	4.80953
5	10075	0.322539	9	2152	4.33695	10	4304	4.80953
5	9589	0.322539	9	2158	4.33695	10	4305	4.80953
5	9590	0.322539	9	2162	4.33695	11	4303	4.80953
6	2172	0.322539	9	2166	4.33695	11	5127	4.80953
6	2200	0.322539	9	2169	4.33695	12	5284	4.80953
7	2184	0.322539	9	2187	4.33695	12	5128	4.80953
7	2136	0.322539	9	2201	4.33695	13	7302	4.80953
7	2138	0.322539	9	2202	4.33695	13	7306	4.80953
7	2127	0.322539	9	2199	4.33695	13	7309	4.80953
8	2173	0.322539	9	2134	4.33695	13	7308	4.80953
8	2139	0.322539	9	2174	4.33695	13	7307	4.80953
8	3456	0.322539	9	2118	4.33695	14	7304	4.80953
8	2163	0.322539	9	2164	4.33695	14	7305	4.80953
8	2135	0.322539	9	2149	4.33695	15	7301	4.80953
8	2140	0.322539	9	2183	4.33695	15	7303	4.80953
8	2058	0.322539	9	2131	4.33695	16	3457	4.80953

Table 4.2: Group structure of all 83 FE(s) on the basis of their burn-up results.

the out put of the ORIGEN2 and formatting into MCNP material card, the total 83 FE (s) of the current core are divided into 15 groups on the basis of their burn-up (MWh). The group structure of all 83 FE(s) is described in Table 4.2. Each group is represented by its average burn up value and the FE with the burn-up value close to average value of the group, is called group indicator. The current core has 15 group indicators. This means that the material composition of the current core is approximated by the material composition of the 15 group indicators. The FE no. 3457 of group no. 5 is a 102-type FE and its fuel properties can not be grouped with 104-type fuel. Therefore, this FE is placed

into separate group with number 16. Thus, the total number of groups become 16. The table 4.3 gives the list of group indicators of 16 burn-up groups.

Grp. no.	Avg. MWd	Grp. indicator	Grp. no.	Avg. MWd	Grp. indicator
1	0.353813	10198	9	4.745256	2164
2	0.770131	10196	10	5.1019	2164
3	1.346325	10143	11	4.74897	2164
4	2.251723	10077	12	3.879295	2164
5	2.732158	10075	13	2.873812	2164
6	3.48944	2172	14	3.51812	2164
7	3.855723	2136	15	4.19128	2164
8	4.31424	2157	16	2.61299	3457

Table 4.3: Sixteen burn up group indicators of the current core.

4.2 Material Composition of the Burned Fuel

The analysis of the current core parameters of the TRIGA Mark II research reactor requires complete information of its burn up and relevant material composition. The experimental methods, due to their limitations, are not sufficient to provide the detailed information of the burned fuel material composition. Therefore methods of calculation are more common and more practical than experimental methods. In the calculations of the current fuel composition, the ORIGEN2 model is developed for all three types of FE(s) present in the current core to predict the burn up and the burned fuel isotopic composition. These calculations are confirmed by gamma spectroscopic experiments of 6 selected 102-type SPE(s), as described in Chapter 3.

The ORIGEN2 computer program is equipped with data libraries of total 1700 nuclides. These nuclides are divided into three segments i.e. 130 actinides, 850 fission-products and 720 activation products. This code can generate 28 out put tables. Out of these 28 tables, it prints different tables of material composition with different units (i.e. gram-atoms, atom-fraction, grams, weight-fraction etc) [16]. In these calculations of burned fuel, the out put of the ORIGEN2 code contains a large number of isotopes of all three segments

(actinides, fission products and activation products). To incorporate all these isotopes into the MCNP model is not a practical approach. Therefore only those isotopes are considered that are important for reactivity calculations.

The influence of each particular fission product on K_{eff} is investigated for different burn ups to estimate the relative importance of different isotopes. By excluding a particular isotope from the K_{eff} calculations, the relative influence of the isotope on K_{eff} is taken from reference [27] which explains the effective isotopes and their influence on criticality calculations for three different burn-ups (3%, 10% and 20%). On the basis of this sensitivity study, the actinides, fission products and their influence in reactivity, described in Table 4.4 are selected for MCNP application of the current core of the TRIGA Mark II, Vienna. These isotopes are extracted from the ORIGEN2 output in grams, converted it into weight fraction and then applied to the MCNP model for the current core analysis. In addition to these sensitive isotopes, the isotopes in the original fuel (U-234, U-235, U-238, H, Zirconium etc.) are also extracted from the ORIGEN2 out put for MCNP applications.

Nuclides	MCNP ZAID	20% burn-up (pcm)	Nuclides	MCNP ZAID	20% burn up (pcm)
54-Xe-135	54135	973	Pseudo FP		47
62-Sm-149	62149	645	62-Sm-152	62152	64
62-Sm-151	62151	284	94-Pu-240	94240	216
94-Pu-239	94239	-840	42-Mo-95	42095	36
60-Nd-143	60143	384	36-Kr-83	36083	24
92-U-236	92236	168	62-Sm-150	62150	30
61-Pm-147	61147	102	44-Ru-101	44101	19
45-Rh-103	45103	179	55-Cs-135	55135	17
54-Xe-131	54131	118	63-Eu-153	63153	20
55-Cs-133	55133	105	62-Sm-147	62147	31
43-Tc-99	43099	79	93-Np-237	93237	12
60-Nd-145	60145	55	94-Pu-241	94241	-17
63-Eu-155	63155	20			

Table 4.4: Effective istopes for 20% burn up of TRIGA Mark II reactor [27].

4.3 Current Core MCNP Model

The burn-up calculations of all FE(s) of the current core are performed from March 7, 1962 to 29th June 2009 for MCNP application. The relevant material composition is applied to the MCNP model to develop the current core model. The current core describes the state of 29th June 2009. With reference to the first core configuration (Figure 2.3), following modifications are applied to develop the current core model.

- Addition of new FE(s) to keep the reactor into operation over its history.

- The source element position is shifted from F06 to F28.

- One pneumatic transfer system is changed from F21 to F08.

- There is only one graphite element left (F09) in the current core.

All these modification can be seen in the current core configurationas shown in Figure 4.1.


Figure 4.1: Current core configuration of the TRIGA Mark II research reactor (June 2009).

4.3.1   Development of Current Core MCNP Model

The original MCNP model, developed for the initial core, is modified to the current core model keeping the same geometrical and material inventory assumptions. Two main modifications are performed in the original model. First, to keep the reactor into operation, different types of FE(s) have been added to the core over its history. This resulted the current core into a complete mixed core of three different types of FE(s) i.e. 102, 104 and 110 or FLIP type fuel. Therefore, these additional FE(s) are modelled and included to the origional MCNP model. The second modification, the burn-up accumulated from the initial start up to 29the June 2009 is incorporated by applying the new material composition. This new material composition is calculated by the ORIGEN2 and corresponds to the current status of the burn-up as described in Table 4.2. This current core model employs the JEFF3.1 cross-section data libraries.

The top view of the complete current core model is shown in Figure 4.2, which includes the current reactor core, the annular graphite reflector, four beam tubes and the thermal column and the radiographic collimator. The radiographic collimator, due to its negligible effect on the reactor core, still needs to be modeled correctly.

The close view of the current core MCNP model can be seen in Figure 4.3. It is already described that all 83 FE(s) of the current core are divided into 16 groups on the basis of their burn up values. Therefore MCNP assigns 16 different colors to the 16 groups of FE(s). In the top view of the MCNP model, the different types of FE(s), the CIR, control rod positions, neutron source element in F-ring and inner cladding (yellow) of the annular graphite reflector are shown in the Figure 4.3.

The YZ (side) view of the current core model is shown in Figure 4.4. This picture of the model shows the water tank, beam tube, annular reflector, reflector groove and the current reactor core.
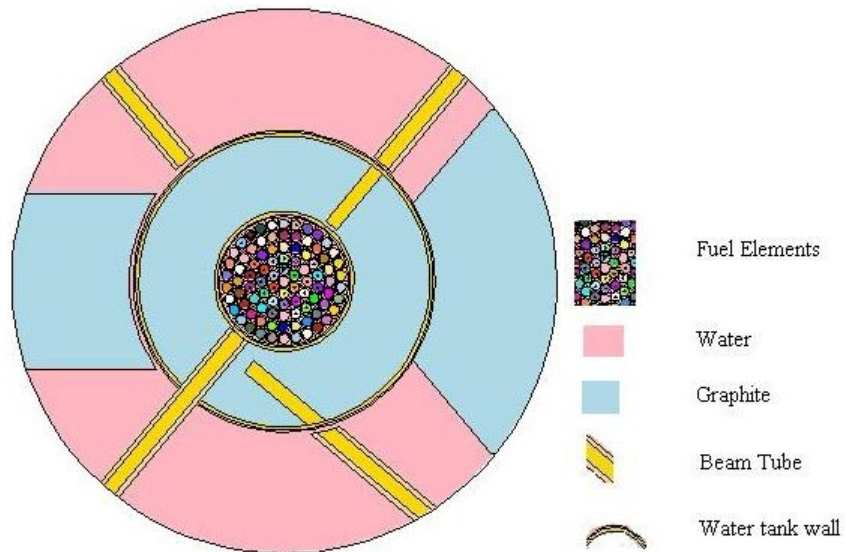
Figure 4.2: Top (or XY) view of the MCNP model of TRIGA Mark II research reactor
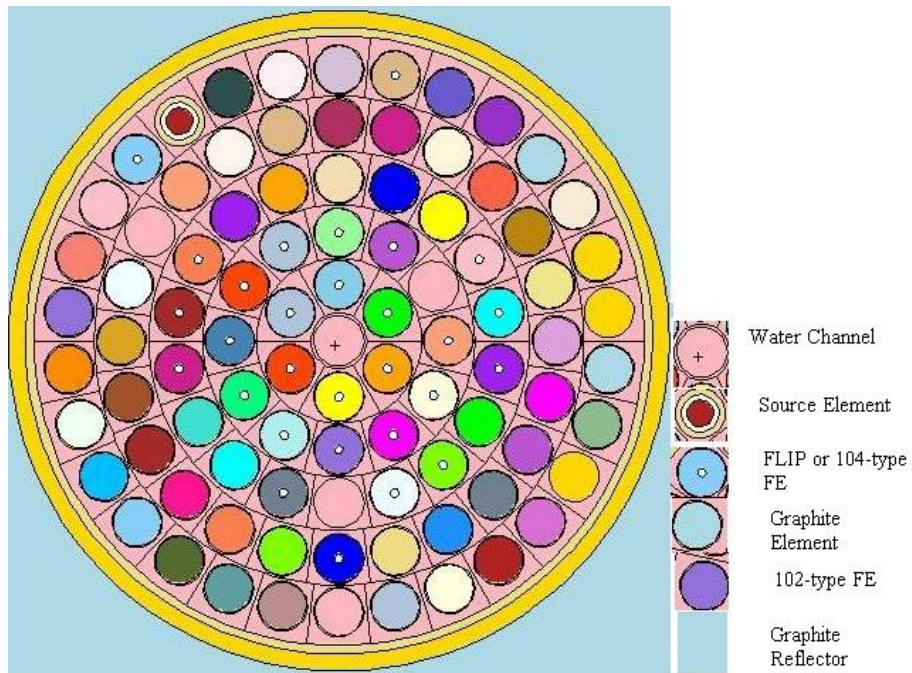
Figure 4.3: MCNP Top (XY) view of the current core of TRIGA Mark II reactor.
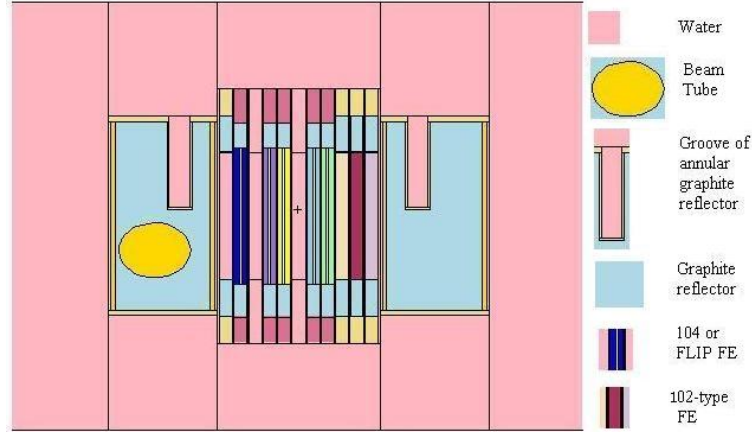
Figure 4.4: Side (YZ) view of the current core MCNP model.

4.4 Model Validation

The reliability of the model needs its confirmation using a standard (if benchmarks are available) or local consistent experiments. Such validation provides the information about the consistency of the model and the systematic errors made by the simulation. To verify the current core MCNP model at both local and global levels, several local experiments are performed at the TRIGA Mark II research reactor of the ATI. These experiments include criticality experiment, reactivity distribution experiment; radial and axial flux density measuring experiments. The first two experiments measure the global parameter i.e. K_{eff}, while the third experiment measures the neutron radial and axial flux density as local parameter.

4.4.1 Critical Experiment

To perform this experiment, 10 FE(s) are chosen in the current reactor core. These selected FE(s) are marked with "+" sign in Figure 4.5 and have least effect of the control rods. These FE(s) are removed from the core and placed in the in-tank storage positions. The selected positions of FE(s) are B05, B06, C09, C10, D13, D14, E17, E18, F21 and F22.

The start-up source is kept in the core throughout the experiment duration. The FE(s)
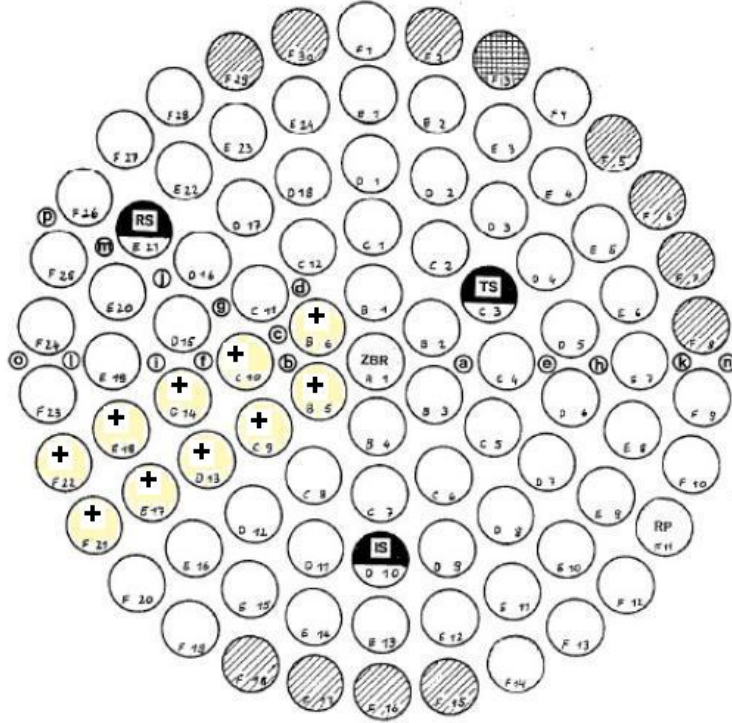
Figure 4.5: Core map with selected positions in the critical experiment.

are added to the core one by one in an order as B05, B06, C09, C10, D13, D14, E17, E18, F21 and F22. After the addition of each fuel rod, the signal (counts per second) from the fission chamber indicates the increase in the reactivity. According to this experiment, the criticality signal is reached when 78th FE (2109 in D13 position) is added to the core keeping all three control rods in fully out position.

The S73d (or S73u) represents the neutron count rate when 73 FE(s) are in the core with all three CR(s) in fully down (or fully up) positions. Similarly the symbol Sxxd (or Sxxu) is used for the neutron count rate after loading of each FE in CR(s) fully down (or fully up) positions. The ratios (Sxxd/S73d and Sxxu/S73u), after each addition , are calculated. The experimental observations are shown in the Figure 4.6. The brown line in this figure shows that reactor core approaches criticality on insertion of 78th FE (2109) with all CR(s) in completely up positions. With CR(s) completely down positions, the linear extrapolation shows that the core would be critical on addition of approximately 88

FE depending on the loading scheme and fuel reactivity.
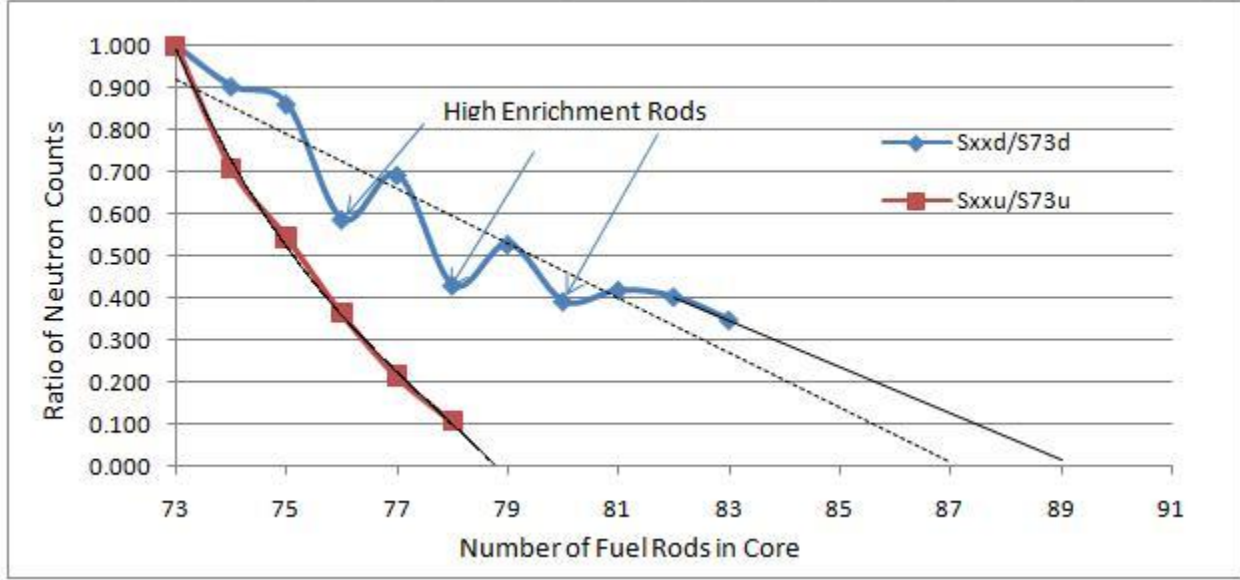
Figure 4.6: Experimental results of the critical experiment at the TRIGA Mark II reactor.

The current core MCNP model, incorporating the burned fuel composition, is modified for the critical experiment. The model is applied for each addition of a FE, in both positions of CR(s) i.e. fully withdrawn and fully down positions. For each MCNP model run, 50000 particle histories with 100 cycles of neuron life are applied for reactivity calculations. The simulated results are shown in Figure 4.7, confirming the experimental fact that the core attains the criticality on addition of 78th FE keeping all control rods in fully up position. Keeping all three CR(s) fully down positions, the core would achieve its criticality on addition of approximately 88th FE depending upon the extrapolation size. If the linear fit from 73rd to 83rd is extrapolated, the curve approaches to criticality ($K_{eff}=1$) on addition of 89th FE (i.e. 88.1211 FE) to the core, as shown in Figure 4.7.
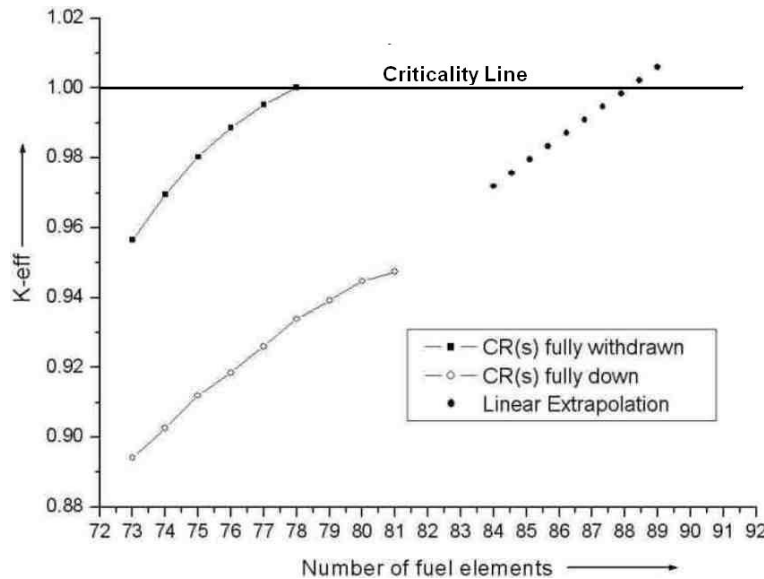
Figure 4.7: MCNP results of the critical experiment at the TRIGA Mark II research reactor.

4.4.2   Reactivity Distribution Experiment

The effective multiplication factor of the core gives the average behavior of the core. To validate the model at some selected positions, the reactivity distribution experiment is performed to measure the reactivtiy worth of five FE(s) in different ring positions. Keeping the burn-up group approximation and control rod effects into consideration, five FE(s) are selected for this experiment. The fuel identification numbers (positions) of the selected FE(s) are 10077(B05), 10198(D05), 7301(C01), 2133(E16) and 2184(F20). Using the shim rod calibration performed on 29 June 2009, the reactivity worths of these FE(s) are measured and are given in Table 4.5. This reactivity distribution experiment is performed at the core configuration of Figure 4.1, where each mentioned FE is replaced by water during its measurement. The reactivity difference between two shim rod positions gives the reactivity worth of the measured FE. The reactivity distribution experiment is applied to the MCNP model of the current core to calculate the reactivity worths of the selected FE(s). This model keeps the same geometrical and material approximations. These calculations are performed with total 150 cycles of iteration on a source size of 50000 particles per

84

Sr. No.	FE No.	Shim rod position 1	Shim rod position 2	Reactivity diff. (dollar)
1	10077	220	398	1.29
2	7301	221	326	0.80
3	10198	220	294	0.58
4	2133	220	280	0.48
5	2184	220	254	0.27

Table 4.5: Measurements of reactivity worths of five selected FE(s) of the core.

cycles. To decrease the statistical error estimates, the first 25 cycles are skipped. For each execution of the model, the calculating FE is replaced by water. From the output, K_{eff} for each FE is taken to calculate the corresponding reactivity worth in dollars using the effective delayed neutron fraction 0.0073 (or 0.73%). The calculated results are given in Table 4.6. The comparison between theoretical and experimental results is shown in Figure

Sr. No.	FE No.	K_{eff} (core)	K_{eff} (FE)	Reactivity
1	10077	1.00972	0.99878	1.48
2	7301	1.00972	1.00482	0.67
3	10198	1.00972	1.00620	0.56
4	2133	1.00972	1.00597	0.50
5	2184	1.00972	1.00775	0.27

Table 4.6: MCNP calculations of reactivity worths of five FE(s) of the core.

4.8. The difference between calculations and measurement will be discussed in the section 4.6.2.
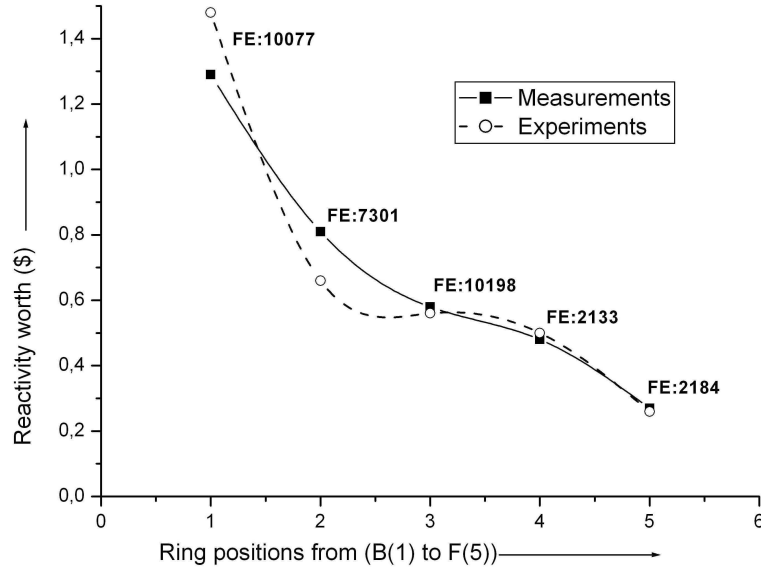
Figure 4.8: The comparison between MCNP and experimental results.

4.4.3   Neutron Flux Density Distribution Experiment

To raise the validity level of the model, the radial and axial neutron flux density distribution experiments are performed on the current core configuration (Figure 4.1). In these experiments, the radial flux density is measured in selected irradiation holes of the reactor core. For the axial flux density measurement, the core rings A, C, E and F are selected.

Radial Neutron Flux Density Distribution

For the radial neutron flux density distribution experiment, the gold foil activation method is used. In this experiment, six irradiation channels (CIR, b, f, I, l and o) are selected for the flux density measurement as they have the smallest effect on control rods. Six aluminium sample holders, each containing two gold foils (with and without cadmium cover), are inserted into the described irradiation vertical holes of the core, along the profile shown in red marked horizontal line in Figure 4.9. These samples are irradiated at a power level of 10 W for 10 minutes. The samples are then stored in storage tank for one hour to allow the aluminium sample holders to decay to background levels. The activity of each gold foil

is measured using 4π detector.
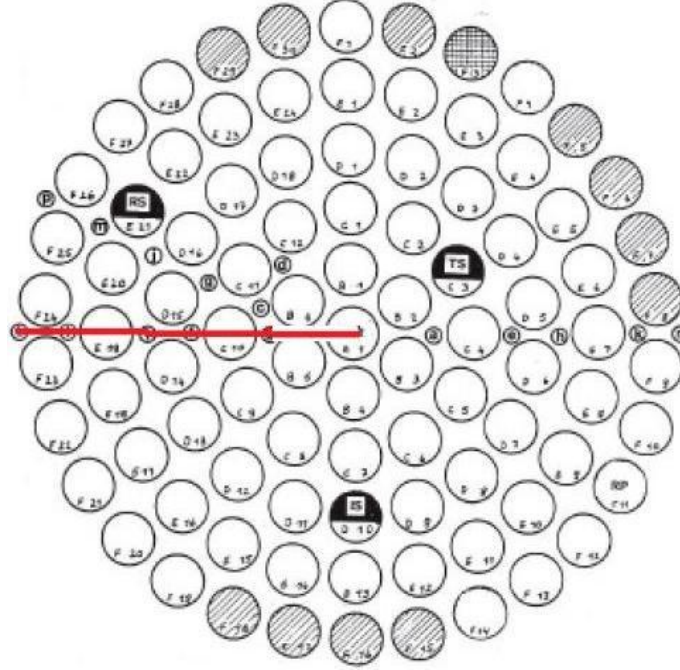
Figure 4.9: The selected profile of the radial flux density measurements.

To calculate the radial thermal flux density, the MCNP model is modified. The superimposed MESH tally capability of MCNP is utilized for these calculations. The MCNP model employs the SDEF source with total 250 cycles of iteration on a source size of 500000 particles per cycles. To decrease the statistical error estimates, the first 50 cycles are skipped. The MESH tally provides results in particles/cm^2. To compare with real experimental observations, the theoretical results are normalized to a real thermal flux density at the center of the CIR in the same environment. The MESH tally is applied to a circular disk of 25 cm at the mid plane of the reactor core. By the MESH tally, the radial length of 25 cm is divided into 100 small intervals while the circumference is divided into 720 intervals (each of 0.5 degree). The MCNP MESH tally plot of radial thermal flux density distribution in the core is given in Figure 4.10. To compare the calculated neutron flux density with measurements, the theoretical flux density values are normalized to the measured flux density in mid point of CIR channel. The comparison of MCNP normalized results with
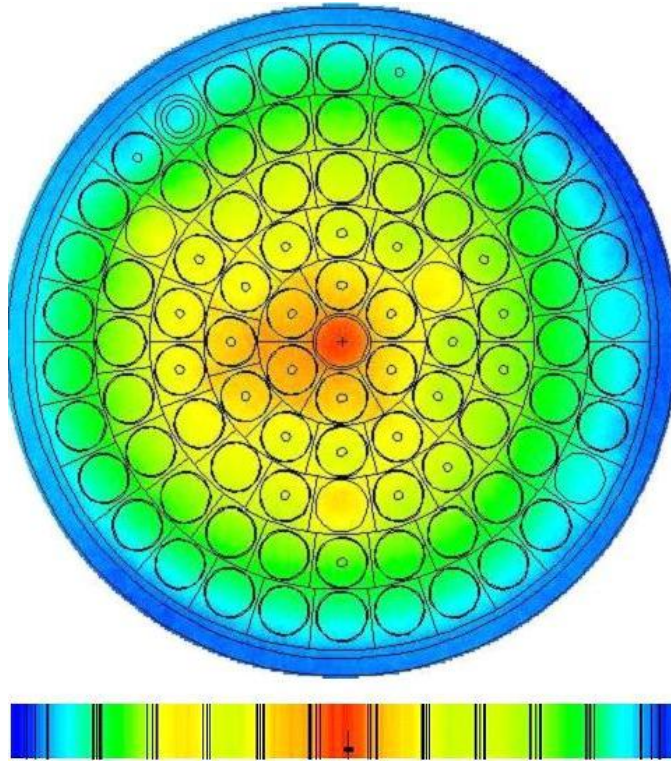
Figure 4.10: Top (XY) (upper) and side (YZ) (lower) views of the MCNP MESH tally plot of radial thermal neutron flux density distribution.

experimental observations is shown in Figure 4.11.
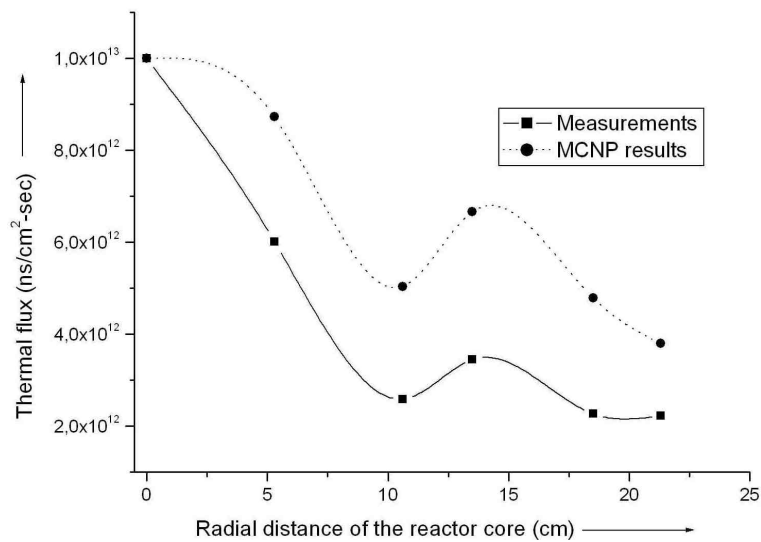
Figure 4.11: Comparison of theoretical and experimental results.

Axial Neutron Flux density Distribution

The core positions A (CIR), C08 (7303), E17 (2108) and F21 (2103) are selected for the axial neutron flux density distribution of the reactor core. For this purpose, the FE(s) are replaced by water filled tube. A aluminium sample holder, shown in Figure 4.12, is inserted into the water filled tube to measure the axial neutron flux density distribution in the selected ring positions. Nine axial positions are marked on each sample holder with 5 cm separation, for these measurement. The central point is marked as zero-point. The gold foils (with and without cadmium covers) are irradiated in selected ring positions for 10 minutes at a thermal power of 10 Watt. The neutron flux density of each marked position is calculated from the measured activity of gold foil.
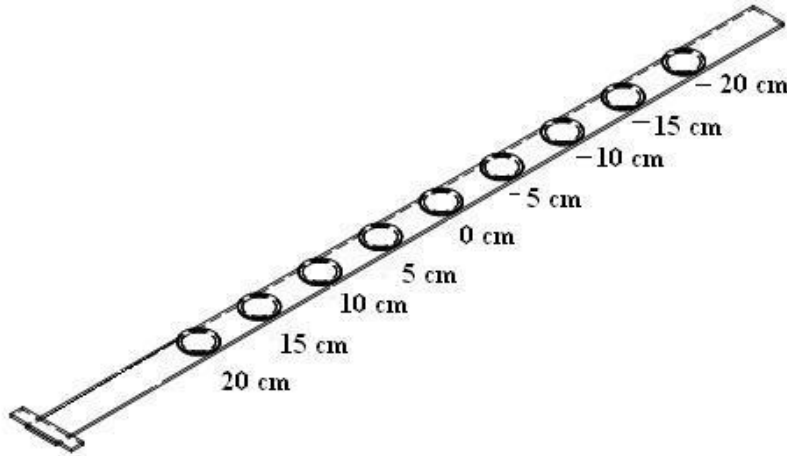
Figure 4.12: Sample holder used for axial neutron flux density distribution experiment.

The experimental results of the axial neutron flux density distribution in selected ring positions are given in Table 4.7. These measured results are given in unit of 10^{12} neutrons/cm^2.s. The middle point or zero point refers to the mid plane of the reactor core. The neutron flux density at the center of the mid plane is 1.081×10^{13} neutrons/cm^2.s and is used to normalize the axial neutron flux density distribution.

The MCNP model of the current core is modified for axial neutron flux density calculation. According to the experimental procedures, FE(s) no. 7303, 2108 and 2103 in positions

Position	20 cm	15 cm	10 cm	5 cm	0 cm	-5 cm	-10 cm	-15 cm	-20 cm
A1	3.44	6.10	8.28	9.84	10.81	10.95	9.49	7.36	5.03
C08	3.44	6.10	8.28	9.84	10.81	10.95	9.49	7.36	5.03
E17	3.44	6.10	8.28	9.84	10.81	10.95	9.49	7.36	5.03
F21	3.44	6.10	8.28	9.84	10.81	10.95	9.49	7.36	5.03

Table 4.7: The experimental axial neutron flux density in unit of (10^{12} neutrons/cm^2.s) in selected ring positions.

C08, E17 and F21 respectively, are replaced by the water channel. The MESH tallies are applied to the axial length of each selected channels (CIR, C08, E17, F21). The separate simulation for each position (CIR, C08, E17 and F21) is executed to calculate the thermal flux density for each centimeter of their axial length. The MCNP MESH tally results of the axial thermal neutron flux density for each described ring position is shown in Figure 4.13. The comparison between theoretical and experimental results are shown in Figure 4.14.
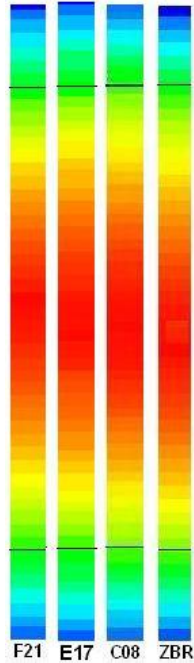
Figure 4.13: MESH tally plots of the axial neutron flux density distribution in selected channels.
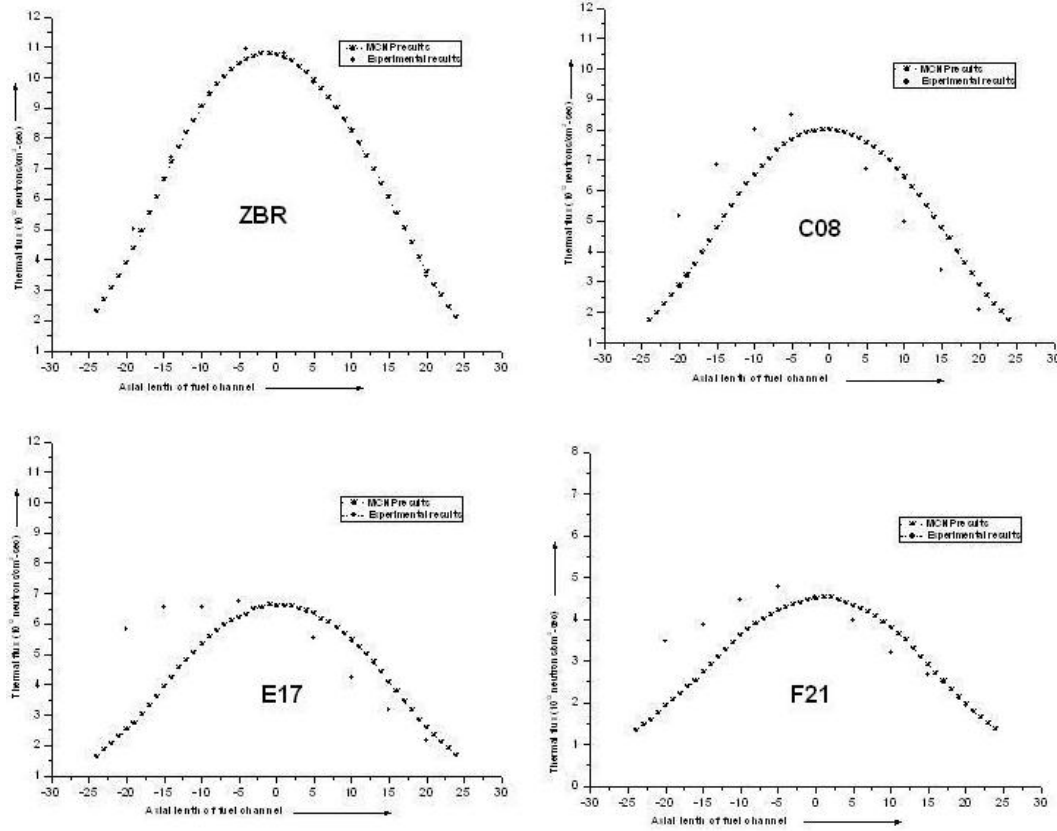
Figure 4.14: Experimental and MCNP results of the axial thermal neutron flux density distribution.

4.5   Discussions of Results

The current core model is verified by three different local consistent experiments as described in previous section. This section discusses the possible reasons of deviations between between the calculations and the measurements.

4.5.1   Criticality experiment

Both the MCNP results in Figure 4.7 and the experimental results in Figure 4.6 agree on the fact that the core reaches the criticality when 78th FE (2109 in position D13) is added to the core. The simulation calculates the K_{eff} and gives about 1.31 cents positive reactivity insertion when FE 2109 is inserted into the core while the experimental

curve in Figure 4.6 confirms the positive reactivity insertion but gives no value due to its experimental limitations. In case of CR(s) fully down position, both experimental and theoretical results agree and show that the reactivity of each FE is different. This may be because of each FE has different fissile material composition and hence has different effect on the core reactivity.

Both Figures 4.6 and 4.7 agree that the core does not reach its criticality on addition of all 83 FE(s) keeping all three CR(s) in fully down position. This is due to the shut down margin of all three CR(s). If the linear fit of the experimental data points (Figure 4.6) is extrapolated, the core may become critical on addition of the 88th FE approximately. In case of MCNP results, when a linear fit of the theoretical data is extrapolated, the core would attain its critical state on addition of 88th FE in the core assuming that each additional FE insertion follow the average reactivity trend.

4.5.2   Reactivity distribution experiment

Figure 4.8 compares the theoretical (MCNP) and experimental results of reactivity distribution experiment. This experiment is performed with the core configuration as shown in Figure 4.1. Generally, the MCNP results are consistent with the experimental results. The calculations are closer to the experimental results in the outer ring positions (i.e. D, E and F) than the inner ring positions (i.e. B and C-ring) of the core. It may be because of, when FE is inserted into the core, more severe local neutron flux density distribution is deformed in inner ring position than the outer rings (D, E and F). The other possible reason of the deviations between MCNP and experimental observations is the burn-up group approximation. All FE(s) in the same groups are considered with same material composition while in reality each FE of the group has a slight different material composition. Further, the calculations are performed with a fixed control rod positions while, in the experiment, the control rod positions are re-adjusted during each measurement of FE.

4.5.3   Radial and axial neutron flux density distribution

Radial neutron flux density distribution

The Figure 4.15 presents the thermal neutron flux density in the mid plane of the current core of TRIGA Mark II Vienna research reactor. The flux density depression due to the shim rod and shadowing effects of two control rods can be seen clearly. The Figure 4.15 also indicates that burn up rates of the FE(s) on the opposit side of the shim rod are not symmetrical.
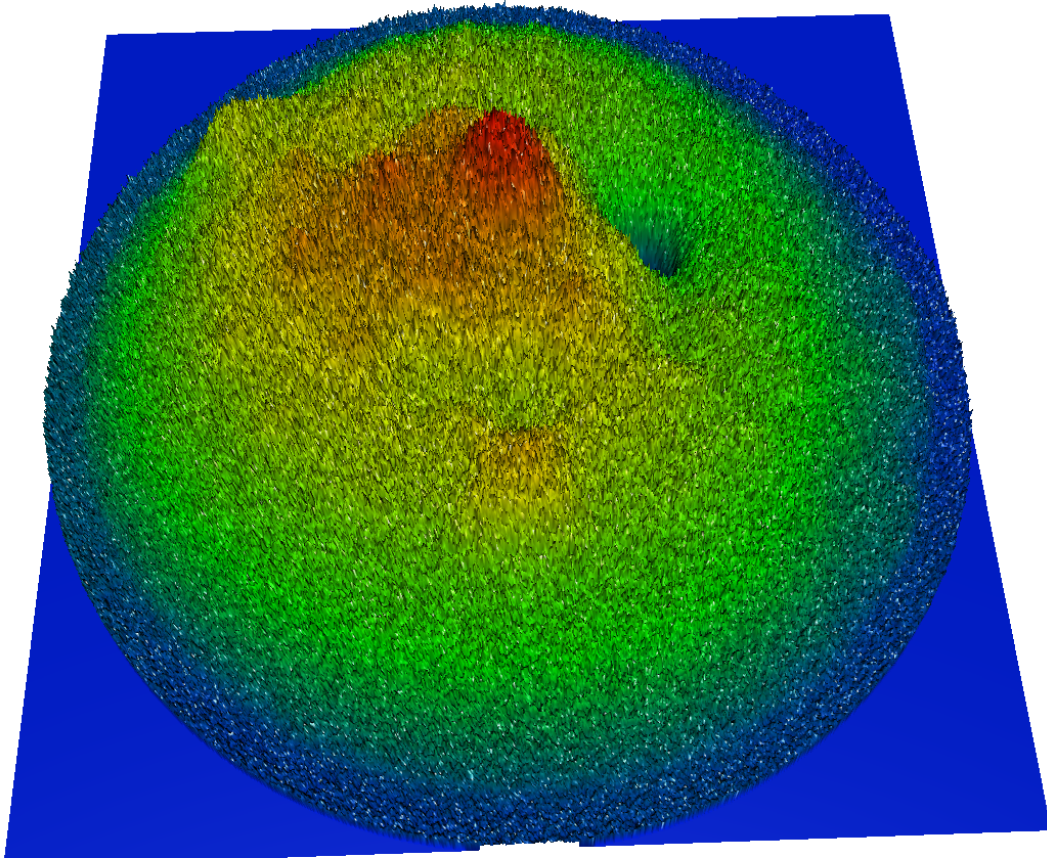
Figure 4.15: Thermal neutron density flux density distribution in the mid plane of the current core.

The Figure 4.11 presents the comparison between the MCNP and the experimental radial neutron flux density distribution results. The peaks in the flux density are due to burn

up differences between the FE(s) in different ring positions. For example, the FE(s) in in B, C and D ring (SS clad FE) are more reactive than FE (s) in E and F rings (2074 and 2163) respectively. The burn up group approximation may play its role in the deviations of the MCNP predictions. It may also be due to the fact that the whole range of fission products is not included in the model therefore it may give the difference between MCNP predictions and and the measurements.

Axial neutron flux density distribution

The Figure 4.14 compares the MCNP results with experimental observations of the axial neutron flux density in four different positions of the reactor core. In all four locations, the axial neutron flux density follows the cosine curve, i.e. maximum at the center and decreases along both sides of the axial length. It is commonly observed in all cases that the neutron flux density is higher in the lower part than the upper part of the core. This is due to the control rods effects which are mostly kept in the upper part of the core. It is also observed in case of C08, E17 and F21, that the calculated neutron flux density in upper part of core is deviating more than the neutron flux density in lower part. The possible explanation may be the distribution of burned fuel material composition in the FE. The ORIGEN2 computer code is a geometry independent program and gives an average material composition per FE. In the current core MCNP model, this new simulated material composition is distributed uniformly which is different than the actual case.

Chapter 5

PERTURBATION ANALYSIS

It is frequently of interest to calculate the change in the core multiplication due to small disturbances in the field of reactor physics. These disturbances can be created either by geometry or composition changes of the core. Fortunately if these changes (or perturbations) are very small, one does not have to repeat the reactivity calculations. In this chapter, the small perturbations are created in the Central Irradiation channel (CIR) of the TRIGA mark II reactor core to investigate their effects on the core reactivity. Three different kinds of perturbations are considered for this study. A cylindrical void (air), heavy water (D_2O) and Cadmium (Cd) samples are inserted into the CIR separately and their neutronics behavior along the axial length of the core is analyzed. The neutronics code MCNP is employed to calculate these perturbations. The theoretical predictions are confirmed experimentally on the reactor core. The behavior of void in the whole core and its dependence on position and void fraction is also studied in this chapter.

5.1 Perturbations in the CIR of the Core

The operational safety of the reactor needs the information of reactivity effects on the core caused by small perturbations. These perturbations can be created by the insertion of small samples into the region of maximum flux density in the core. For this purpose, the

CIR is used due to its highest flux density. The TRIGA Mark II research reactor has about 16 irradiation channels for sample irradiation. The CIR is the largest irradiation hole in the centre of the cylindrical reactor core and can be seen from the top of the reactor core as shown in Figure 5.1. For the perturbation study of the TRIGA Mark II reactor core, three
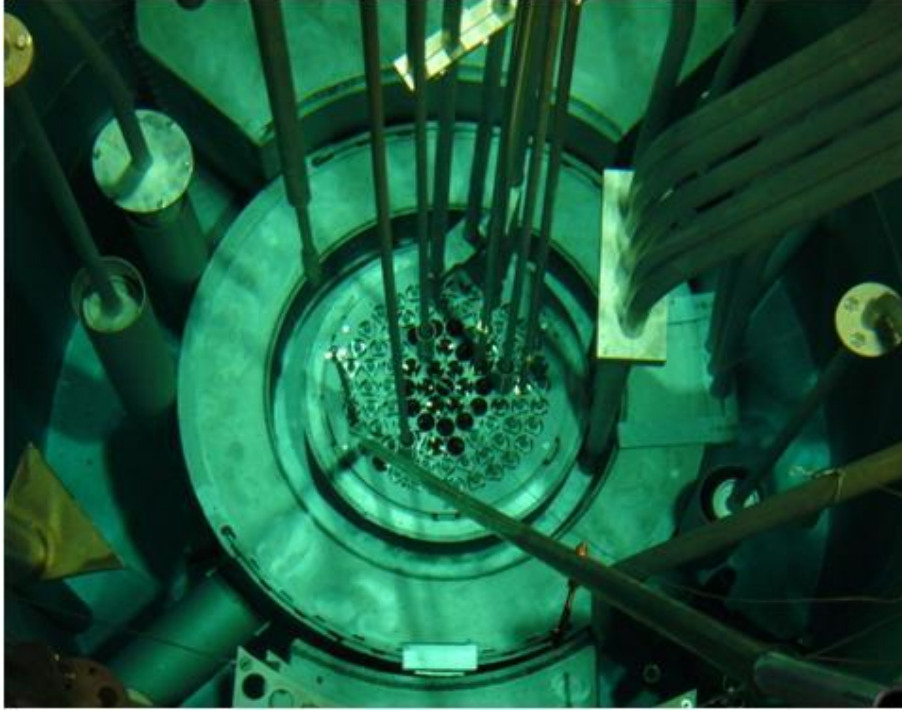
Figure 5.1: Top view of the TRIGA Mark II core.

different experiments are performed on the reactor. In the first experiment, a cylindrical void of 66.47 cm^3 is inserted into the core. This sample is moved along the length of the core in 5 cm steps to study its neutronics effect. The same experiment is repeated with a cylindrical heavy water (66.47 cm^3) and a cylindrical Cadmium (1.25 cm^3) sample.

To calculate the effect of each sample on the core reactivity, the value of effective delayed neutron fraction (β_{eff}) is needed. Therefore the MCNP model is applied to calculate the β_{eff} of the current mixed core.

5.2   Effective Dealyed Neutron Fraction (β_{eff})

The fission event emits fast neutrons and more than 90% of them are emitted within 10^{-14} s and are called prompt neutrons. However, less than 1% of total fission neutrons are emitted within a few minutes from the subsequent decay of radioactive fission products. These are called delayed neutrons and play a fundamental role in the reactor safety. The control and accident analysis of a nuclear reactor and the conversion of the reactor period into reactivity require the knowledge of the effective delayed neutron parameters as well as their decay constants.

The β_{eff} is used as a scale to obtain the reactivity in the $\Delta k/k$ unit from the measured reactivity in dollar unit. As the reactivity is always calculated in $\Delta k/k$ unit, the unit of the reactivity needs to be converted to the other one in order to compare the measured and the calculated values.

MCNP Calculation of β_{eff}

The effective delayed neutron fraction β_{eff} in the TRIGA Mark II is calculated by the MCNP5 transport code using prompt method [28], which requires two calculations. Therefore

$$\beta_{eff} \cong 1 - \frac{k_p}{k} \tag{5.1}$$

Where k is the multiplication factor for total neutrons (i.e. prompt and delayed) while k_p represents the eigen value for prompt neutron only. The required value of k taking both prompt and delayed neutrons into account is usually acquired in the straight calculation mode of the MCNP5 criticality calculation.

Using the KCODE mode, the mean values of both prompt and delayed neutrons (if these are included in the cross-section libraries) are used in criticality calculations. To prevent the influence of the delayed neutrons, $TOTNU$ card with entry NO is used to obtain the value of effective multiplication factor for prompt neutrons k_p. A $TOTNU$ card with

NO calculates k_p, for all fissionable nuclides for which prompt values are available. If the $TOTNU$ card is used and has no entry after it, the total average number of neutrons from fission (ν) using both prompt and delayed neutrons is used and the total effective multiplication factor k is calculated [28].

The MCNP model of the current core is modified for both cases i.e. $TOTNU$ without any entry and with NO entry. Keeping all three control rods in completely out positions, the two separate executions are performed to calculate k and k_p. Both simulations are executed with KCODE employing 500000 histories, 100 neutron cycles skipping first 25 cycles. The calculated results are given in Table 5.1. The calculated value of β_{eff} is 0.007256 which is very close to reference value 0.0073. The reference value is taken from GA, the designer of the TRIGA Mark II reactor.

	Multiplication factor	number of neutrons/fission
All neutron	1.01438± 0.00018	2.443
Prompt neutron	1.00684± 0.00017	2.427
Effective delayed neutron fraction	0.007256±0.00024	

Table 5.1: β_{eff} calculation using MCNP model of the TRIGA reactor.

5.3 Perturbation Experiment [29]

This experiment is performed in the CIR of the reactor core. Three cylindrical samples were prepared for this perturbation study. The void and heavy water sample have volume of 66.42 cm^3 while Cadmium sample has volume 1.25 cm^3. All three samples are used in a polyethylene bottle with negligible neutron absorption cross section. This experiment is performed at low power of 10W. First of all, the void sample is inserted into the CIR and moved vertically in each 5 cm step from bottom to top of the core. For each 5 cm step, the reactivity effect is recorded using the regulating control rod position. This experiment is carried out in auto-mode of the reactor control system to maintain the power at 10W. The same procedure is repeated for heavy water and Cadmium samples.

During the experiment, a withdrawal of the control rod while Cadmium sample is moved,

indicates that due to the high neutron absorption, the Cadmium reduces the reactivity of the core. The experimental results are given in Table 5.2 for each measured sample.

Sample pos.	MCNP reactivity effect(dollar)			Exp. reactivity effect (dollar)		
	Cadmium	D_2O	void	Cadmium	D_2O	void
5	-0.03894	-0.01074	0.03491	-0.0048	0.0	0.0312
10	-0.02282	-0.03089	0.0282	-0.0192	0,0024	0.0264
15	-0.05641	-0.00671	0.0	-0.0696	-0,0192	0.0264
20	-0.07388	-0.01208	-0.01355	-0.0696	0,048	0.0024
25	-0.07388	0.06575	-0.04966	-0.2736	0,0816	-0.0288
30	-0.33511	0.11072	-0.07916	-0.31268	0,0936	-0.048
35	-0.35940	0.12421	-0.07916	-0.324	0,0936	-0.036
40	-0.36210	0.09500	-0.06514	-0.2904	0,0696	-0.0144
45	-0.26095	0.10020	-0.01477	-0.2208	0,0384	0.0144
50	-0.13977	0.08721	0.01746	-0.1056	0,0096	0.0072
55	-0.05910	0.03624	0.023	-0.036	0.0	-0.0024
60	-0.03223	-0.04163	0.00537	-0.0048	0,0024	-0.0072
65	-0.00806	-0.0188	0.01746	-0.0072	0,0024	-0.0168

Table 5.2: Experimental observations of perturbation study in the CIR of TRIGA reactor.

5.4   MCNP model of the Perturbations

The MCNP model of the current core is modified for the perturbation experiment in the CIR of the TRIGA Mark II research reactor as shown in Figure 5.2 and 5.3. For each sample position, the model was executed separately. This modified model employs SDEF general source card along with KCODE. Each simulation is run for 500000 histories, 200 neutron cycles skipping first 50 cycles. The standard deviations for such reactivity calculations range from 0.00021 to 0.00023.

The model employs the density of void, heavy water and Cadmium as 1.15e-3, 1.1044 and 8.65 g/cm^3 respectively. The comparison between the MCNP theoretical predictions and experimental observations is show in Table 5.2.
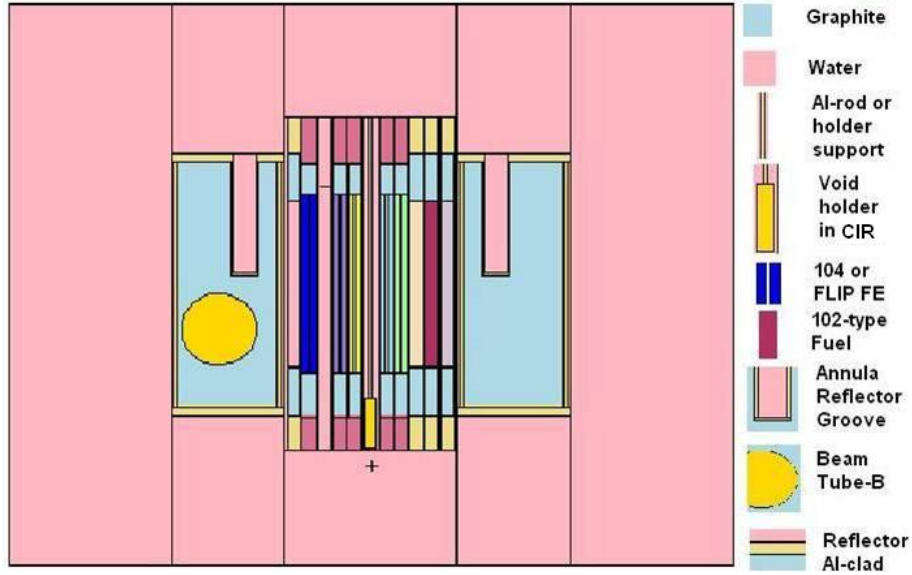
Figure 5.2: MCNP model for the perturbation study of the TRIGA Mark II.
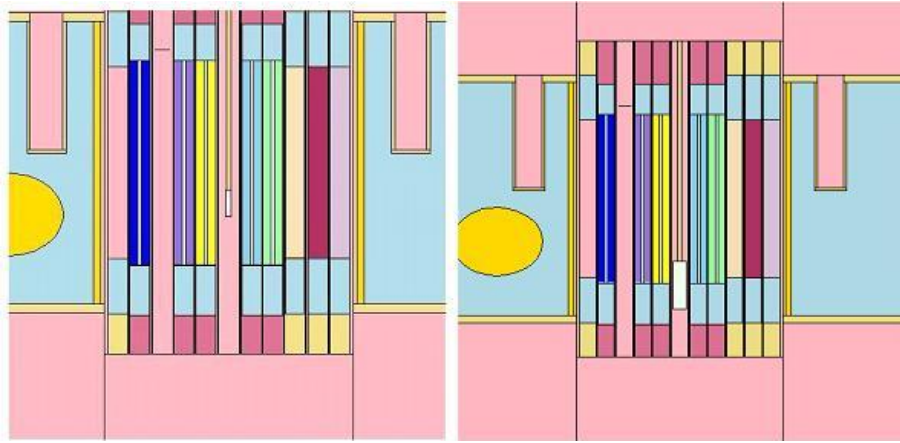
Figure 5.3: MCNP model of the Cadmium sample (left) and of the heavy water sample (right).

5.5 Void Coefficient of Reactivity

The void coefficient describes how the moderator density effects the reactor. In an extreme case, a reactor can loose all of its water coolant. In this case the moderation is reduced which in turn reduces the nuclear reactions, causing fewer neutrons to sustain the fission process. For example BWRs are moderated by water. When the temperature increases, the

water density either decreases or boils, reducing the number of interactions per unit volume of moderator and hence reduces the moderations. This reduces the reactor power. There is also increase in fast neutrons absorptions in U-238 nuclei, thus reducing the number of neutrons available for fission. Both these effects tend to turn the reactor down.

Generally, the dominant reactivity effect in water moderated reactors arises from the changes in the moderator density, due to either thermal expansion or void formation. The principal effect is usually the loss of moderation that accompanies a decrease in moderator density and causes corresponding increase in resonances. In most of the cases, the void coefficient is negative. However, if some significant amount of chemical shim (boric acid) is added to moderator, this reactivity coefficient becomes positive because the reduction in moderation decreases the amount of poison concentration and hence the microscopic absorption cross section. In this case, to achieve a negative moderator coefficient, one has to limit the concentration of poison in the moderator [30].

The core reactivity, for given value of k_{eff} is determined by the relation [31]

$$\rho = \frac{k_{eff} - 1}{k_{eff}} \tag{5.2}$$

Generally the reactivity coefficient is defined as the change in reactivity for a given change in parameter [31]. Mathematically written as

$$\gamma_\xi = \frac{\Delta\rho}{\Delta\xi} \tag{5.3}$$

Where ξ is reactor parameter that affects reactivity and $\Delta\rho$ is the corresponding change in reactivity. If the ξ represent void fraction then γ_ξ defines the void coefficient of reactivity. The actual value varies from reactor to reactor. In this work, the effect of a void on the TRIGA core reactivity is studied.

5.5.1 Void Coefficient of TRIGA Mark II reactor

The void coefficient of reactivity is not an independent parameter but it is coupled with other reactor safety parameters like fuel temperature, water temperature [31]. Table 5.3 shows that the void coefficient is a function of its position and void fraction (percent void). The Table 5.2 shows the reactivity effect due to void is different for each 5 cm along the CIR of the TRIGA research reactor.

Void location	Void coeff.	Void fraction (%)	Void coeff.
A-ring	0.02	0	0.60
A,B-ring	-0.04	5	-0.11
A,B,C-ring	-0.02	10	-0.06
A,B,C,D,E-ring	-0.08	15	-0.65
Whole core	-0.11	20	-0.04

Table 5.3: void coefficient dependence on position and void fraction.

The void coefficient of TRIGA reactors varies from 10-15 cents/%-void [19]. Its value for the TRIGA Vienna is -11 cents/%-void, confirming the fact that TRIGA reactor is under moderated reactor.

5.6 Results and Discussions

5.6.1 Void effect in the centre of the core

Figure 5.4 compares the MCNP results with experimental verifications of the void effects from bottom to top of the CIR of the TRIGA Mark II research reactor. It is seen that the void coefficient increases from bottom to centre and then decreases from centre to top. At bottom and top of the reactor core, the void coefficient is slightly negative while in the centre of the CIR it is positive. The reason of this trend may be due to the fact that both ends of the core provide leakage routes to the neutrons while there is no leakage route in the centre of the reactor core.

The void coefficient is positive at the centre. Actually there are two phenomenal effects of the void on the core reactivity. First, the moderation is reduced when water is replaced by void. Second, the neutron absorption in water is reduced due to less water. Both experimental and MCNP results prove that neutron absorption is dominant over the moderation.
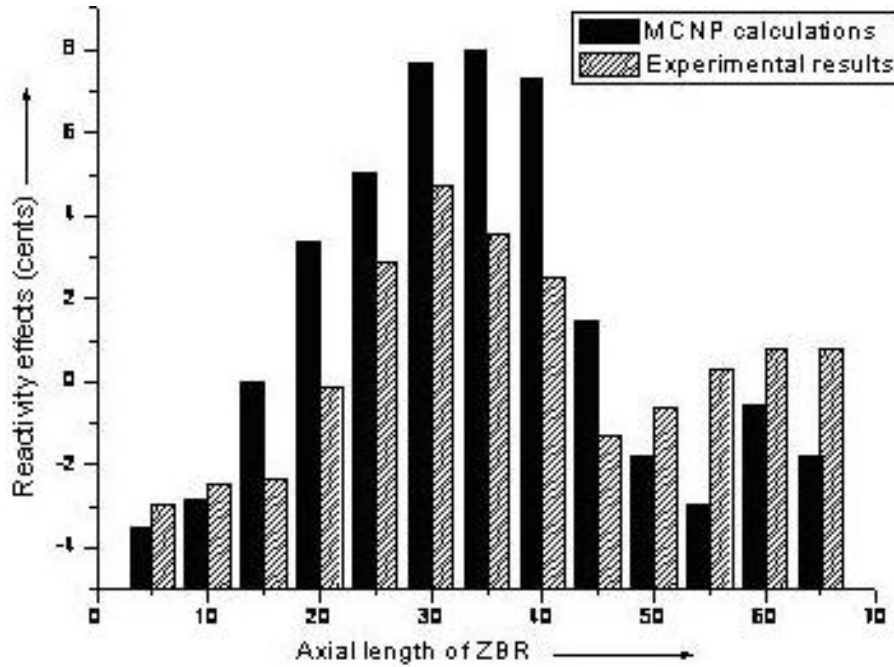
Figure 5.4: Void effect along the axial length (bottom to top) of the CIR.

5.6.2 Heavy water effect in the centre of the core

Figure 5.5 provides the graphical comparison between theoretical and experimental results of heavy water effects along the axial length of the CIR of the TRIGA Mark II reactor core. The heavy water, due to smaller absorption cross section than ordinary water, introduces positive reactivity in the centre and negative reactivity in the bottom and top regions of the core. The main possible reason of the deviations between experimental and theoretical results may be due to composition difference of heavy water used in the experiment and MCNP model of the reactor.
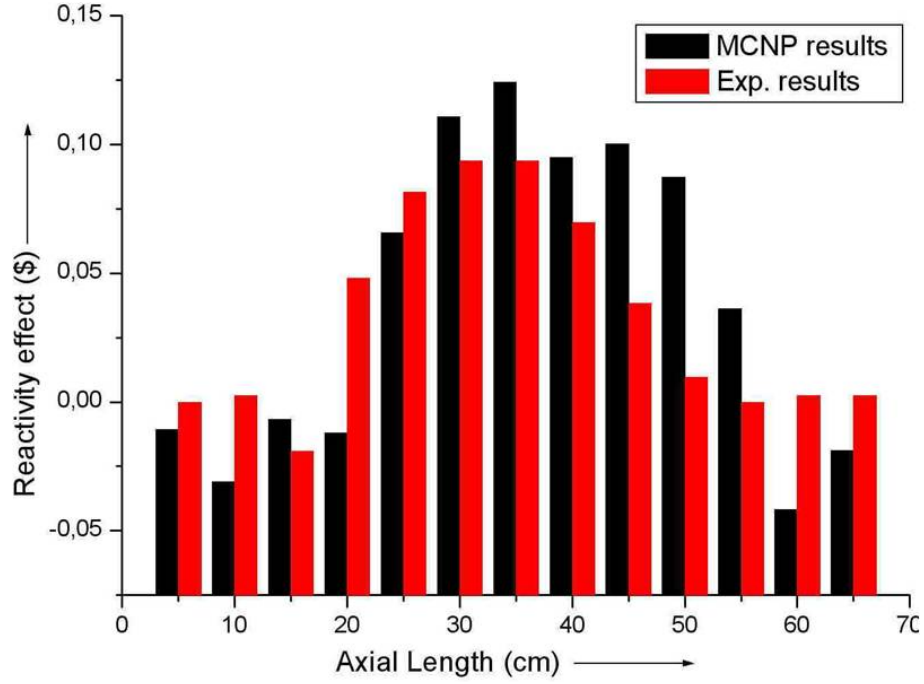
Figure 5.5: Heavy water effect along the axial length (bottom to top) of the CIR.

5.6.3 Cadmium effect in the CIR

When Cadmium capsule is moved from bottom to top of the reactor core along CIR, it exhibits clear and prominent effect due to its high absorption cross section for thermal neutron as shown in Figure 5.6.

The comparison between theoretical estimations and experimental observations of the Cadmium effect in the CIR of the core has been shown in Figure 5.7. It is seen that Cadmium introduces a negative reactivity throughout the axial length of the CIR. It is interesting to note that Cadmium introduces a stronger negative reactivity in the center than at the bottom and top ends of the core. This behavior is due to the dominant effect of neutron absorption over the leakage.
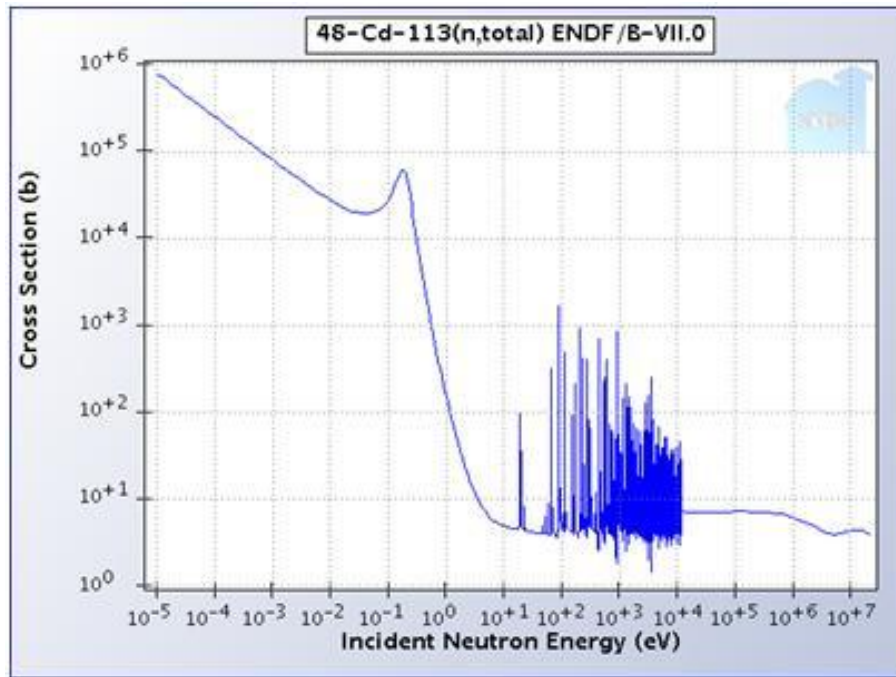
Figure 5.6: Cadmium total cross section as function of neutron energy.
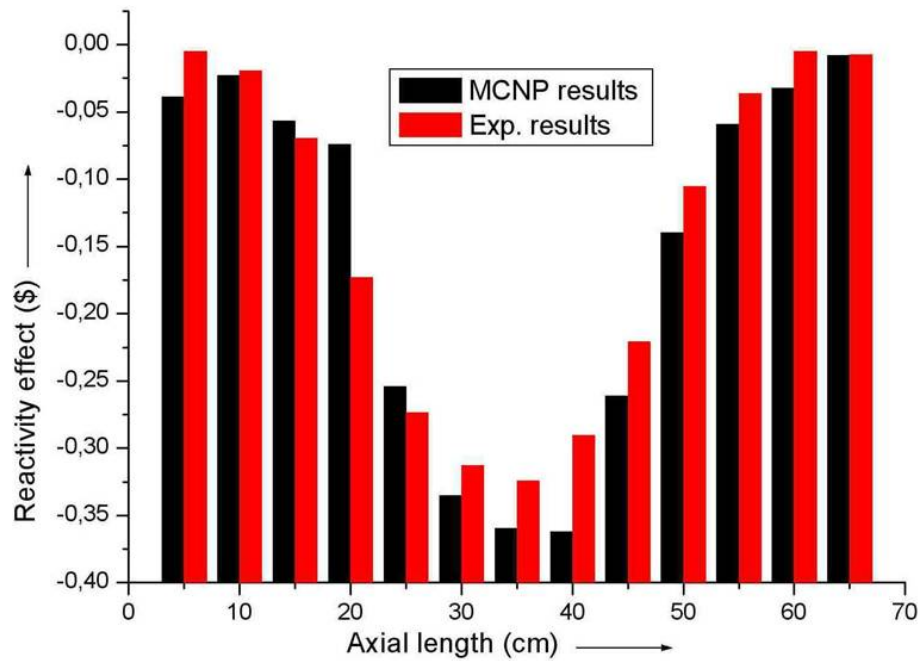
Figure 5.7: Cadmium total cross section as function of neutron energy.

5.6.4   Void coefficient of reactivity

Table 5.3 shows that the void effect depends on the void fraction and its position in the core. The reactivity effect per percent void is not same when 5%, 10%, 15% and 20% void is introduced into the moderator. This may be because of the neutronics effects which are coupled with neutron moderation. The void in the moderator reduces the moderation which causes the spectrum hardening. The spectrum hardening directly affects the fission process in the fuel due to the Doppler effect and hence the fuel temperature [31]. When the void fraction is increased, coupling effects comes into play. These effects increases if the void fraction is inceased. To keep the coupling effects at a minimum possible level, the void coefficient is calculated at the lowest void fraction introduced into the moderator. This thesis calculates the void coefficient at 1% void fraction.

It is also seen from the Table 5.3 that the effect of void is different in different ring positions. As the neutron flux density is higher in the inner rings than in the outer rings therefore void effects are dominant in the inner rings than in the outer ring positions. For example, the void coefficient is positive in the CIR of the core and is negative in the whole core.

Chapter 6

EXTENDED MCNP MODEL

The experimental facilities outside the reactor core are focussed in this chapter. Like in-core irradiation facilities, the TRIGA Mark II research reactor of Vienna is equipped with several irradiation facilities outside the core as described in chapter 1. To calculate the radiation shielding or other nuclear engineering related parameters outside the reactor core, the current core model is extended to the complete biological concrete shield including the four irradiation beam tubes, thermal column and radiographic collimator. The term "extended model" in this chapter refers to a complete MCNP model including the complete biological shielding and the experimental facilities outside the reactor core. To save computational costs and to incorporate the accurate and complete information for the individual Monte Carlo (MC) particle tracks, the Surface Source Writing (SSW) capability of MCNP is utilized. The variance reduction techniques are also invoked to improve the statistics of the problem and to save computational efforts. This chapter describes the calculations of the neutron flux density in the thermal column and in one of the selected beam tubes (i.e. BT-A), using the MCNP5 neutron transport code. To validate these calculations with experiments, neutron flux density measurements using the gold foil activation method are performed on selected positions in the thermal column and in one of the selected beam tube (i.e. BT-A).

6.1 TRIGA Experimental Facilities

The in-core experimental facilities of TRIGA Mark II reactor are described in chapter 4. Outside the core, this reactor has four beam tubes, one thermal column and one radiographic collimator (dry irradiation room) to supply thermal neutrons for following experiments;

1. neutron scattering experiments to study neutron and solid state physics;

2. neutron radiography/tomography;

3. ultra cold neutron physics experiment;

4. neutron activation analysis.

The top and side views of these experimental facilities are shown in Figures 1.1 and 1.2. Though these facilities are briefly discussed in chapter 1 and this chapter describes the geometrical and material details of the thermal column and the four beam tubes. The calculations using MCNP5 computer code and measurements using gold foil activation techniques are performed and analysed at the thermal column and the beam tube 'A'.

6.1.1 Thermal Column

The thermal column of the ATI reactor is a large, boral-lined, graphite-filled aluminium container with outside dimensions 1.2 x 1.2 meters in cross section and 1.6 meters in depth. It is divided into two parts; the inner part of the graphite which is right at the peripheral of the graphite reflector, and the second part which is the outer part right behind the door of the thermal column. The thermal column liner is seal-welded container fabricated from 12.7 mm aluminium plate; the outer portion is embedded in the concrete shield and the inner portion is welded to the aluminium tank. The exterior surfaces of the column, which are in contact with the shield, are coated with plastic for corrosion protection. The

inner part of the column extends to the graphite reflector and matches the contour of the reflector over a 100 degree angle. The outer part is a pile of AGOT nuclear-grade graphite stringers stacked in layers crossway and along the thermal column as shown in Figure 6.1. The stringers measure 10.16 x 10.16 cm^2 with a length of 127 cm except for the lower most and the upper most layers which measure 10.16 x 3.18 cm^2 with the same length. The aluminium container is open toward the reactor room. In a vertical plane, the column extends approximately 33 cm above and below the annular graphite reflector, with the centrelines of the column and the reflector coinciding.

The five graphite blocks serve as removable foil stringers. These blocks have the same dimension but are machined 1.6 mm undersize for easy removal and insertion. The central block is aligned with the stringer access plug in the thermal column door. Thus, this central stringer can be removed and inserted without having to move the entire door. To gain access to the other four stringers, the thermal-column door must be rolled back on its tracks. Each of the five stringers is tapped at the face end for a -13 threaded hole for insertion of a removal tool.

Surrounding the graphite on the inside of the aluminium casing on all four sides, there are 3.2 mm sheets of Boral. These extend inward from the column opening, a distance equivalent to the thickness of the biological shielding. The Boral sheets, which are incorporated in the design to reduce the number of capture gammas in the surrounding concrete shield, are held in place by countersunk aluminium screws. To provide continuous support of the graphite, a piece of aluminium sheet of the same thickness as the bottom Boral sheet extends to the inner end of the column. This aluminium sheet is also held in place by countersunk screws.

The outer face of the thermal column is shielded by a track-mounted door approximately 1.21 meter thick. The door is filled with heavy aggregate concrete with density 3.5 cm^3. The door is supported on a four welded carriage which rolls on two steel rails.

Figure 6.1: Graphite pile of stringers from the thermal column door side.

Thermal Column Experiment [32]

The thermal neutron flux density measurements are performed on the outer surface of the thermal column of the TRIGA research reactor by using the gold foil activation method. Without Cadmium covers and Cadmium covered gold foils, of diameter of 5 mm and an average weight of 0.0084 g, are used in this experiment.

For the experimental purpose, the concrete door of the thermal column is opened and the gold foils are fixed on 13 different positions in the thermal column as shown in Figure 5.1. The air gap between the thermal column and the concrete door is about 2 cm. These gold foils are irradiated at a reactor power of 250 kW for the duration of 10 minutes. After reactor-shutdown, the gold foils are collected and the activities are measured using a 4Π beta counter system at ATI. The results of these measurements are given in Figure 6.2 [29].
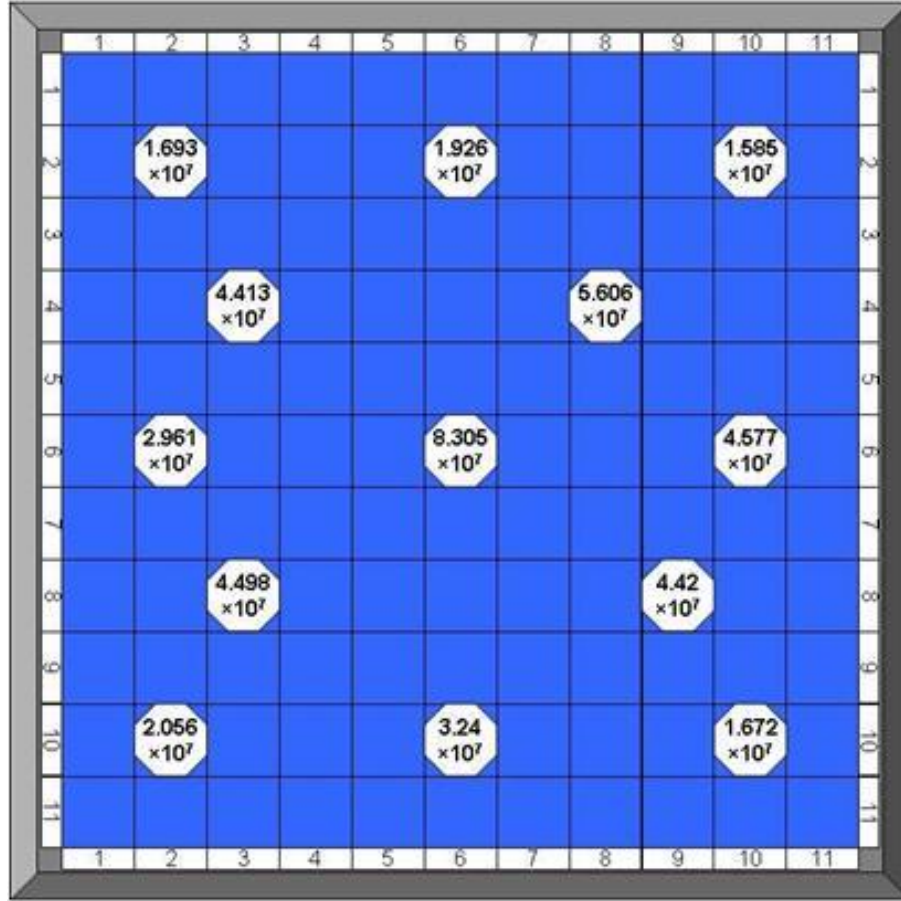
Figure 6.2: Experimental thermal flux density at thermal column surface of the TRIGA Mark II research reactor of Vienna (250 kW) [5].

6.1.2 Beam Tubes

To satisfy the experimental irradiation requirements outside the reactor core, there are four Beam Tubes BT(s) i.e. BT-A, BT-B, BT-C and BT-D. Three of these BT(s) i.e. BT-A, BT-B, and BT-C are radial while the fourth one (BT-D) is tangential to the reactor core. All four BT(s) have the same radial dimensions i.e. 15.2 cm as inner diameter. The top view of these BT(s) can be seen in Figure 1.1. The four BT(s) penetrate the concrete shield and the aluminium tank and pass through the reactor tank water to the reflector. These tubes provide neutron beams and gamma radiation for a variety of experiments. These tubes also provide the irradiation facilities for large specimens (up to 15 cm) in a

region close to the core. Two of the radial tubes terminate at the outer edge of the reflector assembly but are aligned with the cylindrical void in the reflector graphite. The third (i.e. BT-A) tube, specifically developed for neutron activation, penetrates into the graphite reflector and terminates at the inner surface of the reflector, just at the outer edge of the core. In order to have BT voids in the reflector graphite pass beneath the rotary specimen rack, their horizontal centrelines are located 7 cm below the centreline of the core.

The tangential BT (BT-D) terminates at outer surface of the reflector, but is also aligned with the cylindrical void, which intersects the piercing tube in the graphite reflector. This tube provides a radiation source giving a minimum amount of core gamma radiation. The graphite voids maximize the total radiation streaming down the tube. The piercing tube that penetrates the reflector consists of following four major components;

1. the portion of the tube that's is embedded in the concrete shielding;

2. the tube section and flange welded to the aluminium tank;

3. tube section welded into the reflector assembly;

4. a bellow assembly that connects the two tubes sections and compensates for construction tolerance.

The other BT(s) are divided into two sections, one embedded in the concrete shield and the other welded to the aluminium tank. A gap between the sections (of all 4 tubes) embedded in concrete and the sections welded to the tank prevent stresses resulting from thermal expansion in the aluminium tank [6].

Beam Tube Experiment

The neutron measuring experiment using the gold foil activation method has been performed in BT-A on 28th March 2007 [33]. In this experiment, six gold foils (with and without Cadmium cover) have been irradiated and measured using the barite concrete

barrel of 60 cm length. The separation between these gold foils was kept constant as 12 cm. The foils were irradiated at a reactor power of 100kW. The first point (position zero in these results) of measurement is coincident with inner cladding of the annular graphite reflector. The experimental results are given in Table 6.1.

Position	Total flux density	Flux density($\leq 0.4eV$)	Flux density($\geq 0.4eV$)
0	$1.08x10^{11}$	$6.94x10^{10}$	$3.11x10^{10}$
12	$3.12x10^{10}$	$2.03x10^{10}$	$9.51x10^{9}$
24	$1.03x10^{10}$	$6.59x10^{9}$	$2.86x10^{9}$
36	$3.47x10^{9}$	$2.20x10^{9}$	$9.30x10^{8}$
48	$1.17x10^{9}$	$7.25x10^{8}$	$2.76x10^{8}$
60	$4.12x10^{8}$	$2.65x10^{8}$	$1.18x10^{8}$

Table 6.1: Experimetal flux density (neutrons $cm^{-2} - sec^{-1}$) in BT-A [33].

6.2   Extended MCNP Model

A detailed MCNP model of the ATI reactor core, incorporating the addition of new FE(s) over its history and burned fuel composition, is developed by using a 3-D continuous-energy Monte Carlo code [34] and verified by standard experiments performed at the Atominstitute. This model includes all components of the core, i.e. all three types of fresh fuel elements, three control rod elements, graphite reflector elements, surrounding annular reflector with the rotary specimen rack well and reactor tank.

MCNP5 computer code uses point-wise cross-section data. For neutrons, all reactions given in a particular cross-section evaluation (such as ENDF/B-VI) are accounted for. Thermal neutrons are described by both the free gas and $S(\alpha, \beta)$ models [5]. This model uses continuous energy cross-section data and $S(\alpha, \beta)$ scattering functions from JEFF3.1 as ENDF lacks some important cross sections for TRIGA reactors. To perform the calculations outside the TRIGA core (e.g. at the thermal column and in any of the BT(s)) the already developed model is extended to the biological shielding of the reactor with all four BT(s), radiographic collimator and thermal column as shown in Figure 6.3 and 6.4.
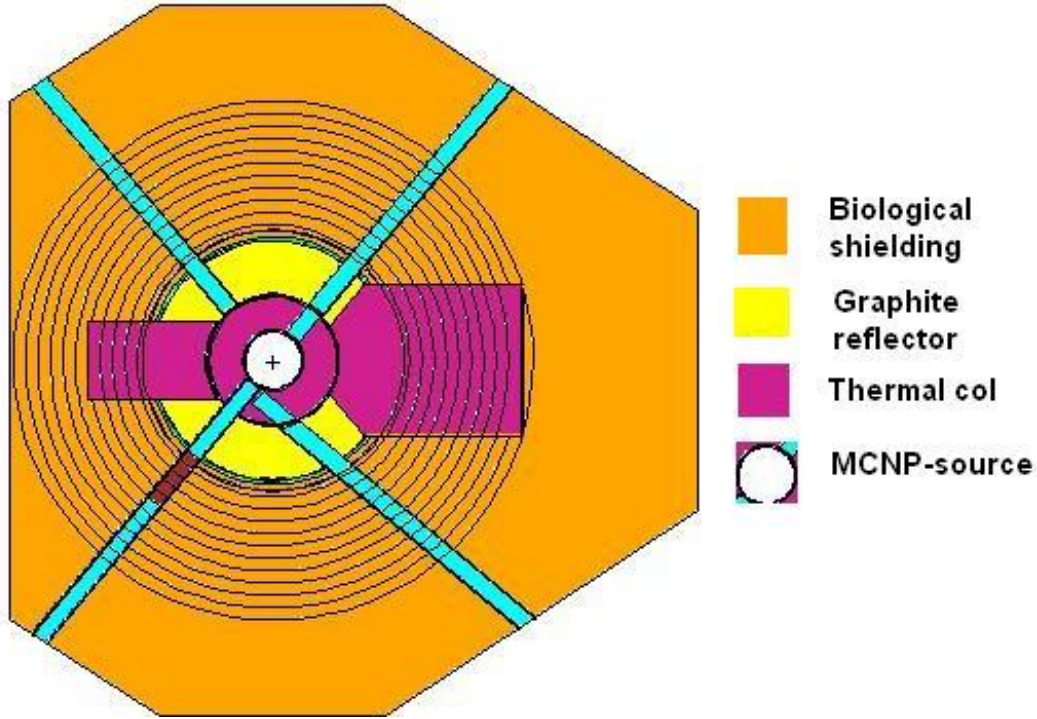
Figure 6.3: Top view (XY) of MCNP extended model of complete TRIGA reactor.
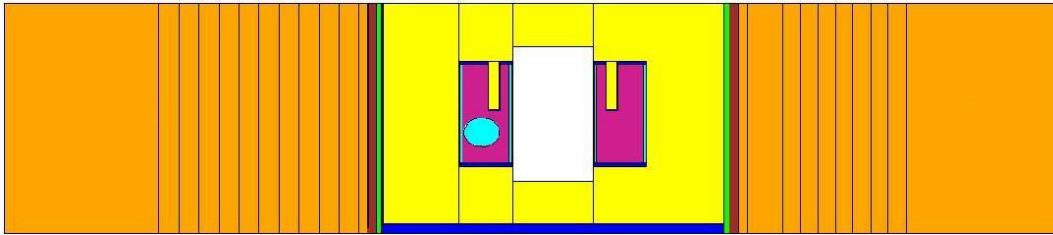
Figure 6.4: Side view (YZ) of MCNP extended model of complete TRIGA reactor.

The prominent advantage of the MC method is the capability of treating complex geometries. However, it is recognized that the convergence of MC calculation for large-scale systems is very time-consuming or even not achievable. The accurate and complete information for the individual MC particle tracks are required in order to perform quality of calculations. The MCNP-code provides a SSW capability to generate a WSSA-format file which contains all required messages of individual particle tracks crossing a given surface. This capability is employed to reduce the computational cost and to keep the quality of calculations. In the application of MCNP, a common surface is first specified in the

MC model. In the MC simulation, the particle tracks of interest crossing this surface are recorded in the WSSA-format file [35]. The execution of the model first needs to be run with SSW card to generate WSSA file. Then, the second execution is performed with SSR card and by changing the WSSA by RSSA file.

In an extended MCNP model, to avoid the computational costs and to incorporate the accurate and complete information for the individual MC particle tracks, SSW capability to generate a WSSA-format file is applied to generate MCNP surface source on the outer cylindrical surface, top and bottom surface of the core (surface no. 34, 6 and 10 in this model). This source-file contains all required messages of individual particle tracks crossing a given surface. The MCNP model with and without core (surface source), all four beam tubes, the thermal and the neutron radiography collimator is shown in figure 6.3 and 6.4.

When this model is executed to calculate the thermal flux density in the thermal column and one of the beam tubes, it is seen at the output, the track entering into the cells are decreased and vanished in bulk biological shielding cell. This situation also gives very bad statistics. Therefore, to solve this problem, MCNP provides several techniques that can be tried to solve this problem, one obvious solution is to run more particles, but it may become very expansive with respect to computational cost. Avoiding the computational cost by the brute force approach of running more particles, this model applies another variance reduction technique. For this purpose, the bulk shielding outside the reactor tank is divided into symmetrical cylindrical cells as shown in Figure 6.4. The neutron importance in these cells is increased from the inner cells to the outward cells in symmetrical orders.

6.2.1 MCNP Model of Thermal Column

To calculate the thermal column flux density, superimposed mesh tally is invoked into the extended model by FMESH card using appropriate settings of available geometrical and other required MCNP cards. The FMESH card allows the user to define a mesh tally superimposed over the problem geometry. Results are written to a separate output file,

with the default name MESHTAL. By default, the mesh tally estimate the track length of the particle flux density, averaged over a mesh cell, in units of particles/cm^2, and is normalized to "per starting particle", except in KCODE criticality calculations.

For thermal flux density analysis, FMESH is applied to one face of the thermal column where measurements are performed at 13 different locations. The coarse mesh for each location is selected so that one graphite block is represented by one tally mesh. The MCNP5 model of thermal column is given in Figure 6.5 which shows mesh tally plot of the model. Each point of measurement (as shown in Figure 6.1) is marked with plus sign i.e. "+". The mesh tally is applied to (11x11) matrix of the thermal column excluding
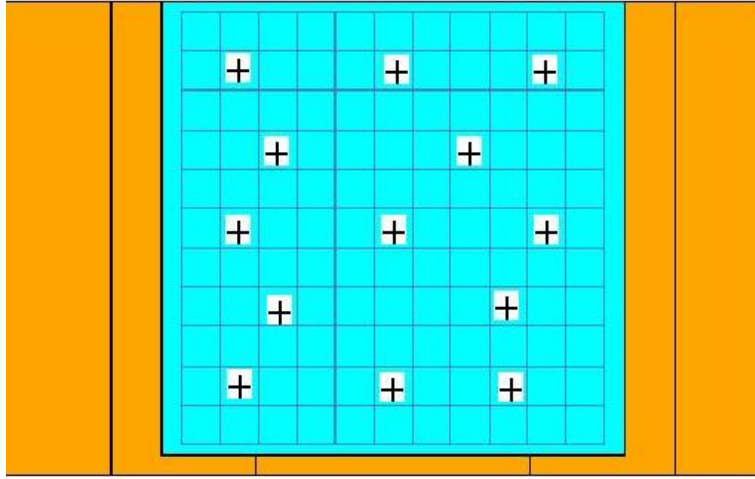
Figure 6.5: MCNP model of thermal column of TRIGA reactor.

the upper most and lower most graphite layers. The thermal flux density is measured on (2x2), (2x6), (2x10), (4x3), (4x8), (6x2), (6x6), (6x10), (8x3), (8x9), (10x2), (10x6) and (10x10) positions and compared with corresponding MCNP calculations. The model is run on source size (NPS) 1.0E+7 with Surface Source Reading (RSSA) file. The MCNP MESH tally plot of thermal column is given in Figure 6.6.

Figure 6.6: MESH tally plot of the thermal column of the reactor.

6.2.2   MCNP Model of Beam Tube A
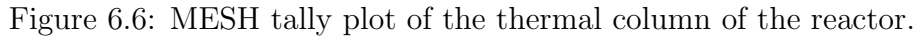
The thermal flux density measuring experiment is performed in BT-A. In the experiment, a 60 cm concrete barrel is prepared at Atominstitue. The six gold foils are installed at its central line at each 12 cm. This barrel with gold foils is inserted into the BT-A. The extended model is modified for BT-A experiment. The barite concrete compositions (of measuring barrel and TRIGA bulk shielding) applied to the extended MCNP model is described in Table 6.2 [33,36]. To calculate the thermal flux density in the BT-A, a MESH tally capability of the MCNP code is utilized on the axis of the barrel. The MCNP model of BT-A is shown in Figure 6.7. The calculated results are given in units of particles per cm^2 at the output file MESHTAL. These results are normalized to the first (initial) point to convert the results into real flux density units.
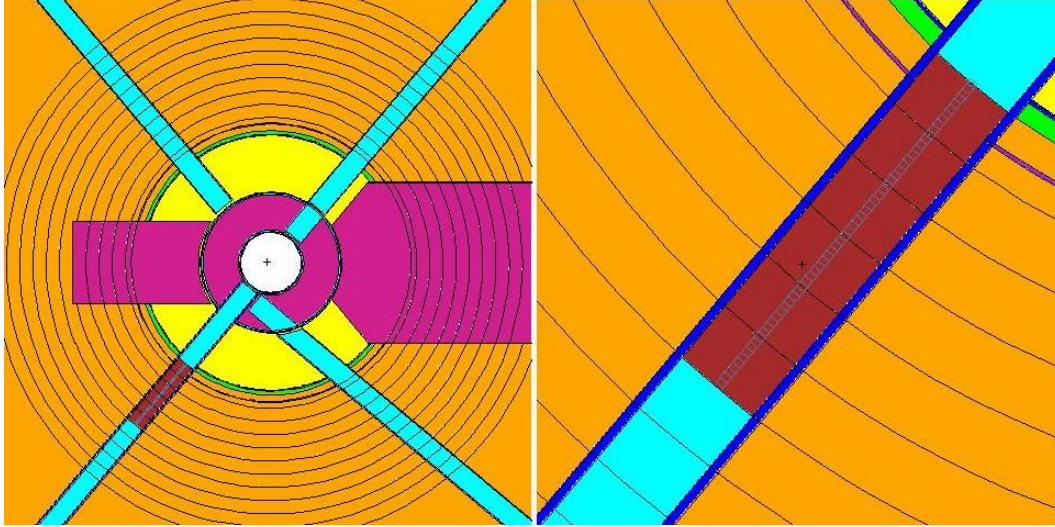
Figure 6.7: MCNP extended model (left) and MESH applied BT-A model (right).

Material	MCNP ID	Barrite concrete barrel	Barrite concrete bio-shield
Elelement	ZAID	Wet. fraction	Wet. fraction
H	1001	0.0037	0.003585
C	12000	0.0023	0.001195
O	8016	0.3163	0.003116
Mg	25055	0.0032	——
Al	13027	0.0069	0.0042
Si	14000	0.0360	0.010157
S	16000	0.1160	0.107858
Ca	20000	0.0570	0.050194
Fe	26054	0.0047	0.047505
Sr	38088	0.0153	——
Ba	56138	0.4407	0.46340
P	1000	——	0.003000
Mn	25055	0.0004	——

Table 6.2: Barite concrete material composition employed in MCNP model [33, 36].

6.3   Results and Discussions

6.3.1   Thermal column

The thermal flux density measuring experiment in the thermal column is described. In this experiment, the thermal flux density is measured on (2x2), (2x6), (2x10), (4x3), (4x8), (6x2), (6x6), (6x10), (8x3), (8x9), (10x2), (10x6) and (10x10) positions at reactor power of 100 kW and 250 kW as shown in Figure 6.2. The MESH tally is applied to (11x11) matrix of the thermal column excluding the upper most and lower most graphite layers. The modified extended MCNP model is executed for thermal column experimental results. The calculated results are shown in Figure 6.8, showing the maximum thermal flux density at the centre of the thermal column and minimum flux density at the corners. These experimental observations are compared with those of theoretical predictions in Table 6.3.
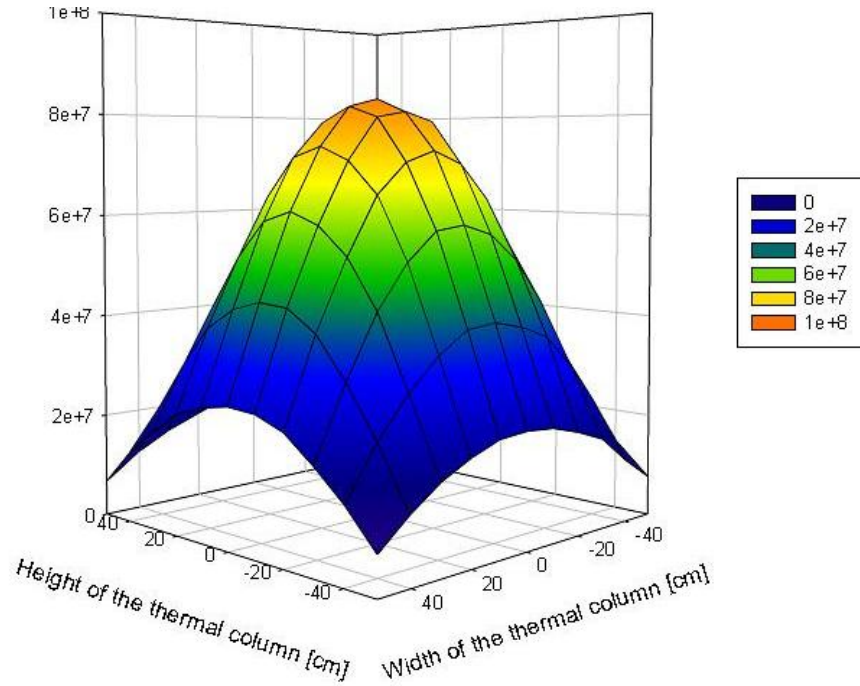
Figure 6.8: MCNP5 thermal flux density ($cm^{-2}.sec^{-1}$) distribution in the thermal column.

Measurement positions	Exp. thermal flux density $(ns/cm^2.s)$	MCNP thermal flux $(ns/cm^2.s)$	Cal./Exp.
(2,2)	1.6932E+07	2.0755E+07	1.226
(2,6)	1.9255E+07	3.7084E+07	1.926
(2,10)	1.5848E+07	2.0693E+07	1.306
(4,3)	4.5127E+07	5.0593E+07	1.121
(4,8)	5.6064E+07	6.0810E+07	1.085
(6,2)	2.9609E+07	4.4650E+07	1.508
(6,6)	8.3050E+07	8.3050E+07	1.000
(6,10)	4.5768E+07	4.4126E+07	0.964
(8,3)	4.4985E+07	5.2957E+07	1.177
(8,9)	4.4196E+07	6.3907E+07	1.446
(10,2)	2.0561E+07	2.2168E+07	1.078
(10,6)	3.2400E+07	4.2623E+07	1.315
(10,10)	1.6723E+07	2.2406E+07	1.340

Table 6.3: Comparison of thermal flux density in the thermal column of the reactor [5].

From the Table 5.3, both i.e. theoretical and experimental results are agreed on the fact that the thermal flux density has a maximum value at its centre and decreases in the radial direction. By the comparison, it is also agreed that flux density in the upper part of the thermal column is smaller than in the lower part of thermal column. This may be due to the fact that all three control rods are mostly kept in upper part of the reactor core and depress the flux density in this part. Both i.e. MCNP and experimental results present the influence of control rods. The possible justification between the theoretical and experimental deviations may become due to the difference in the material composition of the thermal column. As the MCNP model uses nuclear grade graphite of 1.6 $g.cm^{-3}$ while the actual density may vary from 1.6 $g.cm^{-3}$. The differences may also be due to the different structure of the thermal column in the modelling and in the experiments. The MCNP5 results can be improved by the confirmed density of the graphite and modelling of the block structure of the thermal column.

6.3.2 Beam Tube-A

The gold foil activation measurements of thermal flux density distribution in the BT-A is described in section 5.1.2. The comparison of experimental results with the MCNP calculation is given in Figure 6.9 and Table 6.4. The theoretical and experimental results are agreed on the decreasing trend along the length of BT-A. From the Figure 6.9, both MCNP and experimental values on the front face (refers to point no. 0) of the BT-A are much higher than the next results (i.e. on 12 cm, 24 cm etc.). It may be due to the high neutron reflection from the front face of concrete barrel. The possible justification of the deviations between measurements and calculations may be due the difference of material composition of the barite concrete applied to biological shielding of the MCNP model. The standard barite concrete [36] is used in the model while the actual concrete composition still needs its isotopic analysis.

Concrete barrel length (cm)	Exp. thermal flux density $(ns/cm^2 - sec)$	MCNP thermal flux density $(ns/cm^2 - sec)$	Cal./Exp.
0	6,94E+10	6,9407E+10	1.00
12	2,03E+10	1,7214E+10	1.18
24	6,59E+09	3,8118E+09	1.70
36	2,20E+09	1,0964E+09	2.00
48	7,25E+08	1,8629E+08	3.80
60	2,65E+08	1,1407E+08	2.32

Table 6.4: Compaerison of thermal flux density in beam tube A (BT-A).

Diffusion length

The diffusion length is one of the important neutron shielding parameter which depends on the thickness and the energy of the neutron. The diffusion length of thermal neutron in the barite concrete is calculated by using the relation 6.1.

$$\Phi_l = \Phi_o e^{\frac{-l}{d}} \Rightarrow d = \frac{-l}{ln[\frac{\Phi_l}{\Phi_o}]} \qquad (6.1)$$
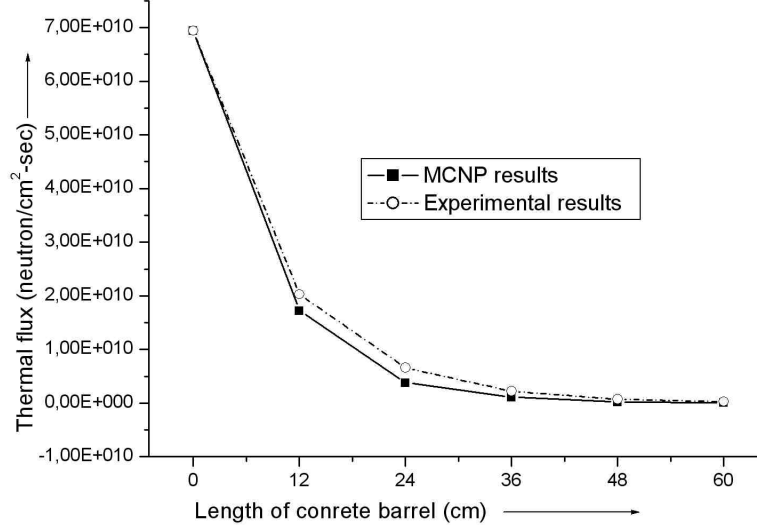
Figure 6.9: Theoratical and experimental thermal flux density distribution in beam tube-A.

Where d is diffusion length, l is the length of the concrete barrel, Φ_l is the flux density at length l and Φ_o shows the flux density at the front face of the barrel. The experimental and theoretical diffusion lengths become 10.77 cm [33] and 9.36 cm respectively with difference of 13%. The possible reason of this deviation between the experiment and the MCNP model may be due to the difference in concrete composition and structure.

Chapter 7

SUMMARY

The TRIGA Mark II research reactor operates since 7th March 1962 at the Atominstitute (ATI) of Vienna University of Technology (VUT). This research reactor is the only nuclear operating facility of Austria to satisfy its research and training demands. Austria, being a OECD member, is playing an active role in nuclear educational and training activities in Europe, particularly through the European Nuclear Education Network (ENEN). Above from national and regional levels, the ATI co-operates with the nearby located International Atomic Energy Agency (IAEA) in international research projects, in Coordinated Research Programs (CRP) and supplying expert services. In support to the IAEA, regular training courses are carried out for safeguard trainees and fellowship places are offered for scientists from developing countries. The staff members carry out the expert missions to research centres in Africa, Asia and South America.

Keeping the importance of reactor operation in view, this neutronics research is performed to analyse the current (burned) core of the ATI reactor of the VUT. The current core is a completely mixed core having three different types of fuels i.e. aluminium clad 20% enriched, stainless steel clad 20% enriched and SS clad 70% enriched (FLIP) FE(s). The completely mixed nature of fuel and complicated irradiation history of the core make the reactor physics calculations challenging. These neutronics calculations are performed by

employing the combination of the two best and well practiced reactor simulation tools which are the MCNP (general Monte Carlo N-particle transport code) for static analysis and ORIGEN2 (Oak Ridge Isotope Generation and depletion code) for dynamic analysis of the reactor core. The PhD thesis is organized into following six chapters.

Chapter 1 introduces the objectives of this research work, research facility used in this study and computational tools employed in these neutronics calculations. Chapter 2 constitutes three sections. The first describes the development of the MCNP model of the very first core configuration of the TRIGA Mark II reactor. To start the reactor operation, the first core was loaded with only 102 type fuel making the initial core a uniform core. The second section explains the validation of the MCNP model by three different local experiments performed on the first core configuration of the reactor. The first experiment was performed in March 1962 to achieve the initial criticality of the core. The second experiment was performed in December 1963 tomeasure the reactivity worths of four FE(s) and one graphite element using the control rods positions. The third experiment was taken from one of the Master Thesis performed on the radial and axial neutron flux density measurement using the gold foil activation method. The third part of this chapter discusses the results in details.

The first criticality experiment verifies the MCNP model that the core achieves its criticality on addition of the 57th FE with a reactivity difference of about 9.3 cents. The percent difference between the theoratical and measured reactivity worths ranges from 4 to 22%. The neutron flux mapping experiment further confirms the model exhibiting good agreement between reactor simulation and the experiment.

Chapter 3 deals with burn up calculations of the reactor history. Since its first operation, the additional three different types of FE(s) were added to keep the reactor into operation. Starting with 57 FE(s), the current core now has 83 FE(s) of three different types. The current core analysis needs to incorporate the new material composition of the burned fuel. Therefore third chapter deals with burn up calculations and its relevant material

composition using the ORIGEN2 code. These reactor physics burn up calculations are confirmed through gamma spectroscopic experiments of the Cs-137 isotope in six 102-type SFE(s). The percent difference between calculations and measurements varies from 0.82 to 12.64. Applying the confirmed ORIGEN2 model, the burn up and its relevant material composition calculations of all 83 FE(s) are calculated to apply the already developed MCNP model of the TRIGA core.

Chapter 4 demonstrates the current core analysis of reactor. For this purpose the confirmed ORIGEN2 model for type 102-fuel is modified for type 104 and FLIP fuel. The modified ORIGEN2 models for three different types of fuels are applied to all 83 FE(s) to calculate the burn up and burned fuel composition of the current core. The burned fuel material composition is applied to already developed MCNP model (fresh fuel) to modify it into the current core model (burned fuel). The current core model employs JEFF3.1cross section library. In this thesis, the current core model refers to the model incorporated with the burned fuel composition at 29th June 2009. The detailed MCNP model of the burned core is verified by three local consistent experiments performed at ATI in June 2009. The criticality experiment confirms the model that the core achieves its criticality with 78 FE(s). The five FE(s) from different ring positions were measured. The percent deviation between MCNP predictions and experimental observations of these five FE(s) ranges from 3 to 19%. The radial and axial neutron flux density distribution experiment validates the model completely.

Chapter 5 presents the perturbation study of the current reactor core employing the verified current core MCNP model. It is frequently of interest to calculate the change in the core multiplication due to small disturbances in the field of reactor physics. These disturbances can be created either by geometry or composition changes of the core. Fortunately if these changes (or perturbations) are very small, one does not have to repeat the reactivity calculations. In this chapter, the small perturbations are created in the Central Irradiation Channel (CIC) of the TRIGA Mark II reactor core to investigate their effects on the core reactivity. Three different kinds of perturbations are considered in this PhD research. The

cylindrical samples of void (air), heavy water (D2O) and Cadmium (Cd) are inserted into the CIR separately and their neutronics behaviour along the axial length of the core is analyzed. The theoretical predictions are confirmed experimentally on the reactor core. The void behaviour in the whole core and its dependence on position and void fraction is also studied in this chapter. Applying the current core model, the void coefficient of reactivity has been calculated as 11 cents per %-void.

Chapter 6 focuses the experimental facilities outside the reactor core. The TRIGA Mark II research reactor is equipped with several irradiation facilities outside the core. For example, four beam tubes (A, B, C and D), thermal column and radiographic collimator are supplying neutrons for education, training and research purposes. To calculate the radiation shielding or other nuclear engineering related parameters outside the reactor core, the MCNP model is extended to the thermal column, radiographic collimator, four beam tubes and biological shielding. The MCNP results are verified in the thermal column and beam tube A region. The percent difference between the simulated and experimental neutron diffusion length of barite concrete is 13%.

The Monte Carlo radiation transport code is basically the steady state behaviour simulating computer program. The aim of the PhD study is to perform static as well as dynamic neutronics analysis of the reactor core. Therefore the combination of two computer programs is employed in this research work. The MCNP5 computer code is applied for static calculation while the ORIGEN2 neutronics code is used for dynamic study of the reactor core. The combination of these two neutronics codes makes it possible to study the static and dynamic parameters of the core simultaneously. In conclusion it has been successfully demonstrated that by using a combination of these two codes, it is possible to calculate complicated reactor cores even after an operation period of more than 48 years. Further the calculations have been validated by a set of experiments, especially by gamma spectrometry of several spent TRIGA fuel elements using a unique fuel scanning tool.

Bibliography

[1] D. M. Fouquet, J. Rizwi, and W. L. Whittemore, "TRIGA research reactors: A pathway to the peaceful applications of nuclear energy," *Nuclear News*, vol. 46, pp. 46–56, 2003.

[2] INIS, "International Nuclear Information System," *The INIS database, http://inisdb.iaea.org*, 2010.

[3] H. Böck and M. Villa, "Practical course on REACTOR PHYSICS AND REACTOR KINETICS," *Atominstitute/Vienna University of Technology*, vol. AIAU 26306, 2009.

[4] H. G. N. Berwanger, *Der Neutronenfluss im Austria 100 kW TRIGA Mark II Reactor*. Atominstitute, Vienna University of Technology, 1964.

[5] R. Khan, S. Karimzzadeh, H. Böck, and M. Villa, "Modeling a TRIGA Mark II Biological Shielding using MCNP5," *Int. Conf. on Nuclear Energy for New Europe 2009/Slovenia*, pp. 101.1–101.8, 2009.

[6] GA, "100-kW TRIGA Mark II Pulsing Reactor Mechanical Maintenance and Operational Manual," *General Atomics, USA*, 1962.

[7] G. Atomics, "Shipment documents from General Atomics," *GA, USA*, 1962-1988.

[8] R. Operator, "Log books of the TRIGA Mark II," *Atominstitute, Vienna University of Technology*, 1962-2009.

[9] G. B. West, R. S. Fe, R. H. Peters, and Encinitas, "Nuclear Reactors," *Genral Atomics Company, Appl. No. 908065*, May 1978.

[10] F. Bensch, H. Böck, and Prochazka, "Sb-Be Pphotoneutronenquellen als Startquellen für Forschungsreaktoren," *Atomkernenergie*, vol. 15, pp. 255–257, 1970.

[11] D. W. Heermann, *Compuetr Simulation Methods in Theoratical Physics*. Springer-Verlag, Germany, 1990.

[12] H. Nifenecker, O. Meplan, and S. David, *Accelerator Driven Subcritical Reactors*. IOP publishing Lt., UK, ISBN 0750307439, 2003.

[13] M. C. Team, *MCNP - A General Monte Carlo N-Particle Transport Code, version 5 1.40*. LA-UR-03-1987, Los Alamos National Laboratory, April 2003.

[14] L. Snoj, *Analysis of Physical Parameters of TRIGA Reactor*. Department of Physics, University of Ljubljana, 2009.

[15] W. M. Stacey, *Nuclear Reactor Physics*. John wiley and sons, INC, 2001.

[16] A. Croff, *A User's Manual for the ORIGEN2 Computer Code*. ORNL/TM-7175, Oak Ridge National Laboratory, Oak Ridge TN, July 1980.

[17] R. Operator, "First log book of the TRIGA Mark II, fisrt criticality experiment," *Atominstitute, Vienna University of Technology*, 1962.

[18] R. Operator, "Second log book of the TRIGA Mark II, Reactivity Distribution Experiment," *Atominstitute, Vienna University of Technology*, 1964.

[19] Y. Jason, "Private email comunication with dr. Jason (Sr. Technical Advisor, GA," *General Atomics Electronic Systems, Inc. TRIGA Division*, 2009-2010.

[20] C. D. Harmon, R. D. Busch, J. F. Briesmeister, and R. A. Forster, "Criticality calculations with MCNP, a primer," *Los Alamos National Laboratory, Nuclear Criticality Safety Group*, vol. LA-12827-M, 1994.

[21] T. Matsumoto and N. Hayakawa, "Benchmark Analysis of Criticality Experiments in the TRIGA Mark II using MCNP," *Nuclear Science and Technology*, vol. 37, pp. 1082–1087, 2000.

[22] Matsson and B. Grapengiesser, "Developments in gamma scanning of irradiated nuclear fuel," *Applied Radiation lsotopes*, vol. 48, pp. 1289–1298, 1997.

[23] M. Ravnik, M. Strebl, H. Böck, A. Trkov, and I. Mele, "Determination of the burn-up of TRIGA fuel element by calculation and reactivity experiments," *Kerntechnik*, vol. 57, p. 291, 1992.

[24] I. Mele, S. Slavic, M. Ravnik, and V. Dimic, "TRIGA data base for ORIGEN2," *11th TRIGA user conference, Heilderberg*, 1990.

[25] A. Persic, M. Ravnik, S.Slavic, and T. Zagar, "TRGLAV, a program package for research reactor calculations," *Josef Stefan Institute, Slovenia*, 2000.

[26] T.-K. Wanga and J.-J. Peir, "An iterative approach for TRIGA fuel burn-up determination using nondestructive gamma-ray spectrometry," *Applied Radiation and Isotopes*, vol. 52, pp. 105–118, 2000.

[27] R. Jeraj, T. Zagar, and M. Ravnik, "Monte carlo simulation of the TRIGA mark II bench mark experiment with burned fuel," *Nuclear technology*, vol. 137, pp. 169–180, 2001.

[28] S. Michalek, J. Hascik, and G. Farkas, "MCNP5 delayed Neutron Fraction Calculation in Training Reactor VR-1," *Electrical Enginering*, vol. 59, pp. 221–224, 2008.

[29] R. Khan, M. Villa, and H. Bck, "Monte calrlo modelling of void coefficient of reactivity experiment," *2010 TRIGA User meeting, Marakesch, Morocco*, 2010.

[30] J. J. Duderstadt and L. J. Hamilton, *Nuclear Reactor Analysis.* John Wiley and Sons, New York, 1976.

[31] R. Khan, T. Hamid, and S. Bakhtyar, "Feedback reactivity coefficients and their coupling," *Nuclear Engineering and Design*, vol. 237, pp. 972–977, 2007.

[32] S. Karimzadeh, *MS Thesis, Behaviour of the Electronic Seals in Mixed Radiation Fields.* Atominstitute/Vienna University of Technology, 2004.

[33] D. Krejci, *Messung der Neutronendiffusionslnge in Schwerbeton.* AIAU 27305, Atominstitute/Vienna University of Technology, 2007.

[34] R. Khan, S. Karimzadeh, H. Böck, and M. V. k, "Neutronics Anylsis of the Current Core of the TRIGA Mark II Reactor, Vienna," *Int. conf. on Research Reactor Fuel Management (RRFM), Marakesch, Morocco*, 2010.

[35] Y. Chen and U. Fischer, "Program system for three-dimensional coupled monte carlo-deterministic shielding analysis with application to the accelerator-based ifmif neutron source," *Nuclear Instruments and Methods in Physics Research*, vol. 551, pp. 387–395, 2005.

[36] R. G. Williams, C. Gesh, and R. Pagh, "Compendium of material composition data for radiation transport modeling," *U.S. Department of Energy under Contract DE-AC05-76RL01830*, vol. PNNL-15870, pp. 12–14, 2006.

1. Appendix

From: "Yi, Jason" <Jason.Yi@ga-esi.com>
     View Contact
To: Rustam Khan <rustamzia@yahoo.com>

Void_Coeff.xls (16KB)

Dear Rustam:
 How are you?
 Happy New Year!
Sorry for the late greeting.
 Could you tell me where the reference void coefficient of -0.002 (dk/k)/% came from?
 The coefficient number looks too high to me.
The typical TRIGA core void coefficient is about -$0.10 ~ -$0.15.
With the typical beta effective value of 0.007 the void coefficient (-$0.10 ~ -$0.15) in terms of dk/k is about -0.0007 ~ -0.001.
 The void coefficient is defined as the reactivity change due to 1% of core water is replaced with void.
The core water volume is normally evaluated by the effective core water volume (using the typical fuel height of 38.1cm X pi*R^2).
Please see the attached excel file. (I included AFRRI core case)
 I normally use the water fraction (in the file) as the water density in the interested area (B-C ring for AFRRI case).
 I hope this will help you.
Please let me know if you have any questions?
Take care,
Jason

Void Coefficient for AFRRI Core

	Radius (cm)		Height (cm)	38,1
Inner core	25,0925			
Fuel	1,87325			
FFCR	1,47955			
TR	1,65862			
R (B-C)	6,0173			

87-3-1		
No	Vol (water+ Fuel)	75363,7871
87	Fuel	36541,4338
3	FFCR	786,0595
1	TR	329,2825
	Vol (water)	37707,0114
	1% Vol (water)	377,0701
	Vol (B-C)	4333,8929
6	Fuel	2520,0989
1	TR	329,2825
	Vol (B-C, Wat)	1484,5115
	Wat Frac (B-C)	0,7460

85-3-1, E23, F9 Water		
No	Vol (water+ Fuel)	75363,7871
85	Fuel	35701,4008
3	FFCR	786,0595
1	TR	329,2825
	Vol (water)	38547,0444
	1% Vol (water)	385,4704
	Vol (B-C)	4333,8929
6	Fuel	2520,0989
1	TR	329,2825
	Vol (B-C, Wat)	1484,5115
	Wat Frac (B-C)	0,7403

85-3-1, E23 Dry Tube, F9 Water		
No	Vol (water+ Fuel)	75363,7871
86	Fuel	36121,4173
3	FFCR	786,0595
1	TR	329,2825
	Vol (water)	38127,0279
	1% Vol (water)	381,2703
	Vol (B-C)	4333,8929
6	Fuel	2520,0989
1	TR	329,2825
	Vol (B-C, Wat)	1484,5115
	Wat Frac (B-C)	0,7432

From: "Yi, Jason" <Jason.Yi@ga-esi.com>
     View Contact
To: Rustam Khan <rustamzia@yahoo.com>

Rustam:

Sorry for the late reply, I was tied up with other projects.

Your new cold critical result with 56 fuel elements looks really good.

When the cold critical result is within 2~3 fuel element (in F-ring) the analysis is normally pretty good and acceptable.

Due to the errors in modeling of the components (such as dimension and mass, etc) and xs data predicting the cold critical case within 2~3 fuel rods are

1. The density of graphite 1.53 g/cc is good for your fuel model (your graphite model is larger than the actual design), but should be 1.75 g/cc for the actual design as mentioned before.

2. When I looked at the your graphite reflector and compared with design value (please see the attached file) your graphite element density should be ~ 1.667g/cc.

 3. With the correction of graphite element density your new calculation could be higher than the 1.0, but it would be fine.

4. By comparing the measured and calculated value you can accomplish the bias and use for your full core analysis.

 I did not have time for the Sm disks check, but you can proceed with full core.

I hope this will help you.

Jason

From: "Yi, Jason" <Jason.Yi@ga-esi.com>
     View Contact
To: Rustam Khan <rustamzia@yahoo.com>
Cc: "boeck@ati.ac.at" <boeck@ati.ac.at>
    Graphite-correction.xls (23KB)

 Rudtam:

I checked your MCNP model briefly, and found few area need to be fixed.

1. The upper and lower graphite plugs (above and below the fuel) dimensions were wrong.

 You should change the graphite density from 1.75 to 1.5308 (g/cc) if you want to keep your graphite dimension.   (see the attached excel file)

This way is the easiest way to check your cold critical run w/o changing your whole model.

 My recommendation is to fix the model after you run the case with 1.5308 (g/cc).

2. Al fittings (upper and lower Al fittings)

This is a little minor case comparing to the #1 but correct way to model is homegenized the Al and water if the model of fittings are larger than the real ones.

3. Do you use ~ 300K cross section data for all materials?

Hopely, changing the graphite density will reduce your cold critical case close to 1.0.

Good Luck.

Jason

From: "Yi, Jason" <Jason.Yi@ga-esi.com>
     View Contact
To: "rustamzia@yahoo.com" <rustamzia@yahoo.com>
Cc: "boeck@ati.ac.at" <boeck@ati.ac.at>

Rustamzia:
I got your email from Dr. Bock, and I briefly checked the fresh fuel isotopic densities for various fuel types in your core.

I noticed the lack of C-12 in your fuel data (Table 1).
If you have your full MCNP input model could you send to me?
I will send you the fuel isotopic number densities as I put together.
The most people made mistakes not only the fuel number densities but also in graphite densities.
Also in the XSDIR lib data files the most people does not have Er x-section data files.
Could you tell me also what kind data files do you use?
Sorry for the late reply.
I will be waiting your response soon.
Jason

		14 inch	15 inch		
		AL Clad		SS Clad	SS Clad
		8.0/20.0	8.5/20.	8.5/20.	8.5/70.
Fuel	Diameter (cm)	3,59664	3,59664	3,6449	3,6449
	Height (cm)	35,56	38,1	38,1	38,1
	Fuel ID (cm)	0	0,635	0,635	0,635
	Vol (cc)	3,6128E+02	3,7502E+02	3,8548E+02	3,8548E+02
Graphite	Diameter (cm)	3,39344	3,39344	3,43662	3,43662
Lower &	Height (cm)	10,033	8,9662	8,6868	8,6868
Upper	Vol (cc)	9,0740E+01	8,1092E+01	8,0577E+01	8,0577E+01
	Density (cc)	1,75	1,75	1,75	1,75

		FLIP Fuel		AL Clad 102 Fuel		SS Clad 104 Fuel	
Nuclide	Atom. Mass	Nuc. Den	Mass (g)	Nuc. Den	Mass (g)	Nuc. Den	Mass (g)
H	1,0079	5,4593E-02	35,22	3,7823E-02	22,87	5,4712E-02	35,30
C	12,011	1,4961E-03	11,50	1,5786E-03	11,38	1,4891E-03	11,45
Zr	91,224	3,5299E-02	2061,24	3,7823E-02	2070,00	3,5684E-02	2083,73
Er-166	165,93	1,0624E-04	11,28		0,00		0,00
Er-167	166,932	7,2950E-05	7,80		0,00		0,00
U-234	234,041	6,5900E-06	0,99	1,9389E-06	0,27	1,9400E-06	0,29
U-235	235,0439	9,0116E-04	135,58	2,5531E-04	36,00	2,5545E-04	38,43
U-236	236,0456	4,2300E-06	0,64	2,8584E-06	0,40	2,8600E-06	0,43
U-238	238,0508	3,7065E-04	56,48	1,0197E-03	145,63	1,0203E-03	155,47
Hf	178,49	2,1179E-06	0,24	2,2694E-06	0,24	2,1410E-06	0,24
Sum		9,2852E-02	2320,73	7,8507E-02	2286,56	9,3168E-02	2325,11
Zr-rod							
Other Er							
Sum							
U wt%			8,35		7,97		8,37
Total U (g)			193,69		182,31		194,63
Er wt%			0,82				
Nat Er wt%			1,45				

Before Hydriding

	w%	wt (g)	w%	wt (g)
U	8,5	193,35165	8	180,98361
C	0,5	11,373626	0,5	11,311475
Zr	91	2070	91,5	2070
Total		2274,7253		2262,2951

CURRICULM VITAÉ

Personal Details

Name:	Rustam Khan
Date of Birth:	08-01-1974
Nationality:	Pakistan
Status:	Married since 25 Oct. 2004
Children:	Two sons (4.5 yrs & 8 months)
Address:	Stadion Allee 2, A-1020, Wien, Austria
Email:	rustamzia@yahoo.com , nrustam@ati.ac.at
Ph. no.	+43-1-58801-14169 (Office), +43-6505380019 (Mob.)

Academic Details:

Certificate	Institute	Year	Main Subjects	Grades (%)
S. S. C.	GHS, Kachi Paind Khan D.I. Khan, Pakistan	1990	Science Subjects	70.8
H. S. S. C.	GDC No.1 D.I.Khan Pakistan	1992	Pre-Engineering	61.9
B. Sc.	Gomal University D.I.Khan, Pakistan	1994	Physics Maths A & B	74.4
M.Sc.(Physics)	Gomal University D.I.Khan, Pakistan	2-12-1997	Nuclear Physics Particle Physics	78.7
M.Sc. (NE)	PIEAS Islamabad, Pakistan	26-09-2002	Reactor Physics Numerical Methods	67.9

Professional Experience:

Employer	Post Title	Duration		Type of work
		From	To	
PAEC	Senior Scientist	Dec. 2004	June 2006	Health Physicist
PAEC	Junior Scientist	Sep. 2002	Nov. 2004	Health Physicist
PIEAS	Fellow	Sep. 2000	Sep. 2002	Course and research work
APS & C	Lecturer	Sep. 1998	Sep. 2000	Teaching at college levels

Teaching Experience at College Level (2 years)

I have been teaching physics at school and college level for two years at Army Public School and College (APS & C, Fort road, D. I. Khan) Pakistan. During this teaching practice, I also taught mathematics as stand-in at APS & C. I was involved in class lectures, training exercises and examinations.

Research Experience at PIEAS (1 year)

During Nuclear engineering at PIEAS, I performed two semesters research project on Pakistan Research Reactor-1 (PARR-1) at PINSTECH. In this work, three reactivity coefficients (fuel temperature, moderator temperature and void coefficient) were calculated using reactor code WIMSD-4. These three coefficients were then coupled by partial differential equations. The solution of these coupled partial differential equations yielded the coupling effects. The results of this research project were published in International Journal of Nuclear Engineering and Design. A computer code was developed to solve coupled partial differential equations to calculate the coupling effects of reactivity coefficients (Master thesis at PIEAS library).

Health Physics Experience (3 years and 8 months)

After completing the M.Sc. nuclear engineering, I worked at PINSTECH as operational health physicist for 3 years and 8 months. During the reactor operation, my responsibilities included the issuance of dosimeters, to maintain the dose records for each worker and decontamination of surfaces. The radiation shielding of radioactive sources were designed at laboratory levels. The confirmation letter, I will be able to get after permission from the PINSTECH.

Doctoral Research Experience (3.5 years)

Monte Carlo simulation of very first core configuration of TRIGA Mark II was completed employing general purpose Monte Carlo N-Particle (MCNP) computer code. This model was verified by three historical experiments performed in 1962. The MCNP model of first core was modified into the current core configuration by incorporating the current material composition of the burned fuel. This material composition was calculated by neutronics code ORIGEN2 and verified by gamma-spectroscopic experiments on six selected spent fuel elements at Atominstitute.

The current core model has been verified by some experiments on the current core. After complete confirmation of the model, neutronics parameters like reactivity coefficients, effective delayed neutron fraction, radial and axial thermal flux distribution in the core have been calculated and confirmed experimentally. I have planned to publish these confirmed results in reputed International journal.

To calculate the nuclear parameters outside the reactor tank, the already developed MCNP model was extended to beam tubes, thermal column, radiographic collimator and external biological shielding. To validate this model, the neutron flux distribution experiment in one of the selected beam tube (BT-B) under progress as a project work of graduate student.

Reactor Experimental Experience

The standards experiments were performed on research reactor as a part of the PhD requirements.

Beyond from the standard PhD requirements, following additional experiments were performed for the validation of Monte Carlo and ORIGEN2 calculations.

1. Reactivity distribution experiments
2. Gamma scanning of six selected spent fuel elements
3. Axial flux distribution of the TRIGA reactor core
4. Critical experiment
5. Measurement of Void coefficient of reactivity

Research projects experience

During the research work at Atominstitute, I have been involved in the research projects of following graduate students. This comprised both the formulation of projects and research support on a daily basis, including guidance on scientific literature, code results, data analysis, physical interpretations, and report writing. I have given significant contributions to the following research projects of graduate students:

Name of Student: Thomas Stummer
E-mail: stummer@ati.ac.at
Project title: MCNP Model of TRIGA Mark II research reactor

Name of Student: Peter Dominik
E-mail: p.dominique@gmx.net
Title: Detection of the activity in containers by external dose rates

Name of Student: Markus Haydn
E-mail: markus.haydn@gmx.at
Title: Accidental Scenarios with Environmental impact of the TRIIGA Mark II, Vienna

Name of Student: Philipp Schauberger
Email: philipp.schauberger@student.tuwien.ac.at

Title:	Radial and Axial Flux Measurement of TRIGA Reactor
Name of Student:	Michael Lechermann
E-mail:	mlechermann@yahoo.com
Title:	Quantifying the Release of Noble gas Isotopes from TRIGA Mark II reactor
Name of Student:	Andreas Drexler
Project title:	Material Composition of Burned FLIP Fuel Element
Email:	andreas.Drexler@gmx.net

The formal supervisor of these research projects was Prof. Helmuth Böck. These students can be reached either through their given e-mail addresses or their formal supervisor.

Reactor simulating software Experience:

I worked with deterministic and stochastic reactor simulating tools. I have good practice of the following reactor codes.

1. Monte Carlo N-Particle (MCNP), version 5, It is general purpose code and can by applied to criticality, radiation shielding and reactor core calculations.
2. ORIGEN2, Generation and Depletion computer code used for burn-up and material composition calculations of an irradiated fuel.
3. WIMSD-4 used for neutronics calculations at cell level.
4. TRIGLAV is used for reactor calculations of mixed cores in a TRIGA Mark II research reactor. The TRIGLAV requires the WIMS-D4 program with the original WIMS cross-section library extended for TRIGA reactor specific nuclides.

Awards

- Distinction in M.Sc. Physics at Gomal University
- Two years fellowship from PIEAS
- PhD scholarship from Austrian government

Scientific research and production

I have written total 16 international publications including articles in international journal, conferences proceedings with referee systems and reports. The reports include documents worked for IAEA, European Union. Details of these publications are given below. Out of these 16 publications, 4 are articles of International Journal and 7 are conference publications with referee system. Out of these seven conference publications, I am first author of four publication and co-author in remaining three publications. In addition to that, I have also compiled two high level technical documents (TECDOC) for IAEA, two reports for European Union. I also prepared one IAEA Brochure on Integrated Safety Assessment of Research Reactors (INSARR) missions.The details and references of these publications have been given below.

International Publications:

Journal:

1. R. Khan, Tehsin Hamid, Sabiha Bakhtyar, "Feedback reactivity coefficients and their coupling", International Journal of Nuclear Engineering and Design, vol.237, Issue 9 May 2007, page 972-977.
2. R. Khan, H. Böck, "Status and Patterns of European Nuclear Education and its Best Practices", European Nuclear Society News, p 1-19, Issue no. 23 winter, Feb. 2009. http://www.euronuclear.org/e-news/e-news-23/status-and-patterns.htm
3. R. Khan, S Karim Zadeh, H. Böck, "TRIGA Fuel Burn-up Calculations and its Confirmation", Nuclear Engineering and Design, vol. 240 (2010) 1043–1049, May2010.
4. R. Khan, H. Böck, M. Villa, "Status and Patterns of Nuclear Education in Anti-nuclear Environment Austria", International journal of Nuclear Knowledge management (IJNKM), status: in press, sop131, vol. 4, N3, 2010.

Conference:

5. T. Stummar, R. Khan, H. Böck, M. Villa, "Monte Carlo Core calculation for mixed TRIGA HEU/LEU core", International conf. on Research Reactor Fuel Management RRFM 2008, ISBN 978-92-95064-04-1, Session V, 2-5 March 2008, Hamburg Germany.
http://www.euronuclear.org/meetings/rrfm2008/transactions/rrfm2008-session5.pdf
6. R. Khan, S. Karim Zadeh, H. Böck, M. Villa, "TRIGA Fuel Burn-up Calculations supported by Gamma Scanning", International conf. on Research Reactor Fuel Management RRFM 2009, ISBN 978-92-95064-07-2, Session IV, 22-25 March, Vienna, Austria.
http://www.euronuclear.org/meetings/rrfm2009/transactions/rrfm09-transactions-session-4.pdf
7. R. Khan , S. Karimzadeh, H. Böck, M.Villa, "Modeling a TRIGA Mark II Biological Shield using MCNP5", proceedings of the International conf. on Nuclear Energy for new Europe, 14-17 Sep. 2009, Bled, Slovenia.
http://www.djs.si/bled2009/restricted/Bled2009/htm/home.htm
8. H. Böck, M. Haydn, R. Khan, M. Lechermann, P.R.J. Saey, G. Steinhauser, M. Villa, "Fission Gas Release from Research Reactors" International Workshop on Siignatures of Medical and Industrial Isotope Production", 1-3 July 2009, Italy.
9. M. Villa, T. Stummer, R. Khan, H. Böck ,"Possibility of a Partial HEU-LEU TRIGA Fuel Shipment" International conf. on Research Reactor Fuel Management RRFM 2007, session VII, 12-14 March 2007, Lyon, France.
http://www.euronuclear.org/meetings/rrfm2007/transactions/rrfm2007-transactions-session-7.pdf
10. R. Khan, S. Karim Zadeh, H. Böck, M. Villa, "Neutronics Analysis of the Current Core of the TRIGA Mark II Reactor Vienna", International conf. on Research Reactor Fuel Management RRFM 2010, Rabat, Morocco. (Status: accepted)
11. R. Khan, H. Böck, "Fuel Temperature and Void Coefficient of Reactivity for TRIGA Fuel" International conf. on Research Reactor Fuel Management RRFM 2010, Rabat, Morocco. (Status: accepted)

Reports:

12. IAEA TECDOC "Role of Universities in Preserving and Managing Nuclear Knowledge", Vienna, Dec. 10-14, 2007. (under publication)
13. IAEA TECDOC, Post Irradiation Techniques of two Technical Meetings, 2006 Argentina and 2007 Norway. IAEA TECDOC CD Series No. 1635 IAEA-TECDOC-CD-1635, ISBN 978-92-0-162709-4.
14. IAEA Brochure on Integrated Safety Assessment of Research Reactors (INSARR) missions, Ref. no. 09CT04873
15. R. Khan, Helmuth Böck, M. Villa, "Nuclear Knowledge Management in Europe", FP6-036414, ENEN project.
16. R. Khan "Translational Access Preparation", MTR+I3 project for European Union, under contract number FI6O-656-036440, submitted in 2009.
17. Helmuth Böck, R. Khan " Maintain and Improve Nuclear Education", ATIR1002, Atominstitute, Vienna University of Technology, April 2010.

Conferences/ Meetings Participation:

1. International Conference on Research Reactor Fuel Management (RRFM) 2008, Hamburg Germany.
2. International Conference on Research reactor Fuel Management (RRFM) 2009, Vienna, Austria.
3. Technical Meeting on the "Role of Universities in Preserving and Managing Nuclear Knowledge" 10-14 Dec. 2007, Vienna, Austria.
4. Consultancy Meeting on "The Development of a detailed Proposal for a Coordinated Research Project (CRP) on Innovative Methods in Research Reactor Physics", 10-12 March 2008 IAEA headquarters, Vienna, Austria.
5. "Technical Meeting on the Status and Trends in Nuclear Education" 4-8 May 2009, IAEA headquarters, Vienna, Austria.
6. Consultancy meeting on "Evaluation of the Integrated Safety Assessment of Research reactors (INSARR) mission results", CS-09CT04873, 8-12 June 2009, IAEA headquarters, Vienna, Austria.
7. Technical Meeting on the Development of Curricula in Nuclear Science and Technology", 7 -11 December 2009, IAEA's Headquarters, Vienna, Austria.